predictive mineral discovery
COOPERATIVE RESEARCH CENTRE

pmd*CRC

Final Report

Camp- to Deposit-Scale Alteration Footprints in the Kalgoorlie-Kambalda Area

Project Y3

2002-2004

P. Neumayr, J. L. Walshe & S. Hagemann (editors)

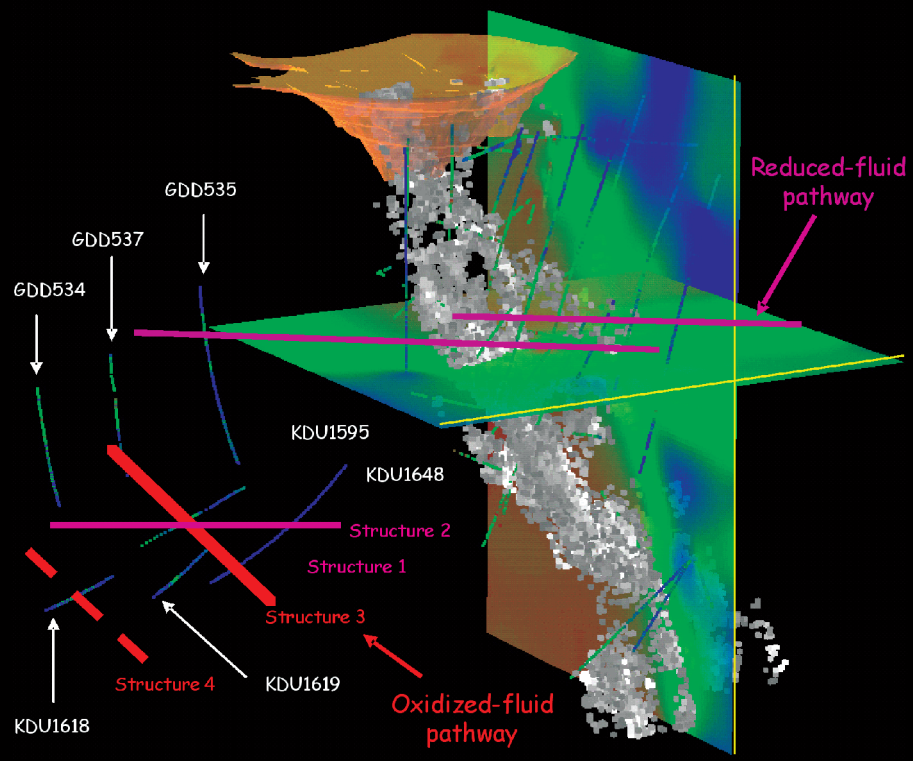

Fig. 1: Model of reduced and oxidized fluid pathways in the Kanowna Belle - Velvet area.

CSIRO · AMIRA INTERNATIONAL · Australian Government Geoscience Australia · MONASH University · The University of Melbourne · JCU James Cook University · The University of Western Australia

Project Y3:

Camp- to Deposit-Scale Alteration Footprints in the Kalgoorlie-Kambalda Area

Final Report (2002 to 2004)

June 2005

Role	Name	Affiliation
Team Leader	A/Prof Steffen Hagemann	UWA
Chief Scientist	Dr Peter Neumayr	UWA
Team Members	Dr John Walshe	CSIRO/MERIWA
	Dr Bill Stone	UWA (finished 8/2003)
	Dr Klaus Petersen	UWA (started 2004)
Embedded Researchers	Leo Horn	St Ives Gold Mining Company Pty. Ltd. (Gold Fields Ltd.)
	Glen Masterman	MERIWA/Placer Dome Asia Pacific/Uni Melb
	Susan Drieberg	MERIWA/Placer Dome Asia Pacific/Uni Melb
	Peter Frikken	MERIWA/St Ives Gold Mining Co (Gold Fields Ltd)/Uni Melb
	Carl Young	MERIWA/Placer Dome Asia Pacific/Uni Melb
	Anthony Roache	MERIWA/St Ives Gold Mining Co (Gold Fields Ltd)/Uni Melb
PhD Candidates	Louis Gauthier	UWA
	Joanna Hodge	UWA
	Mherdad Heydari	UWA
Honours Students	Daniel Howe (2002)	UWA
	Sian Nichols (2003)	UWA
	Kate Moran (2003)	UWA

Introduction and Organization of Final Report

The ***pmd****CRC* Yilgarn 3 project was set up in 2001 with the following aims:

1. Develop a generic model to predict the alteration and geochemical signatures of hydrothermal alteration events, including the gold event(s).
2. Develop mineralogical, geochemical and geophysical criteria to characterize, predict and localize Au-transporting and barren hydrothermal systems.
3. Model Au (metal) transport and deposition to distinguish and predict barren and mineralized hydrothermal fluid systems.

As a working area, the Kalgoorlie-Kambalda corridor (Fig. 2) was chosen because of its significant gold and nickel endowment, accessibility of open-pit and underground mines and diamond core, significant amount of structural work completed by GSWA and other researchers, and substantial support of sponsors such as St Ives Gold Mining Company Pty. Ltd. (Gold Fields Ltd), Barrick, and Placer Dome Asia Pacific.

The aims of this project changed at the start of 2004 when there was a shift in emphasis within the CRC from the original aims of the project to five strategic questions:

(Q1) Geodynamic Setting of the System,

(Q2) Structural Architecture,

(Q3) Fluids Reservoirs,

(Q4) Fluid Pathways, and

(Q5) Gold Transport and Deposition.

The following final report for the ***pmd****CRC* Yilgarn 3 project reflects this shift in emphasis. The report concentrates on the Kalgoorlie-Kambalda area but also incorporates results from MERIWA 358 (Scale-integrated, architectural and geodynamic controls on alteration and geochemistry of gold systems in the Eastern Goldfields Province, Yilgarn Craton; Project Leader Dr John Walshe) investigations on the Kanowna Belle and Wallaby gold deposits, as well as the ***pmd****CRC* Y2 project (Terrain-scale architecture; Team Leader Dr Richard Blewett).

It is important to emphasize that the PhD students involved—Louis Gauthier, Joanna Hodge, and Mehrdad Heydari—have only worked on the project since 2002. Therefore, their contributions, namely the individual reports on their research in Part 2 of this report, are only a summary of preliminary results.

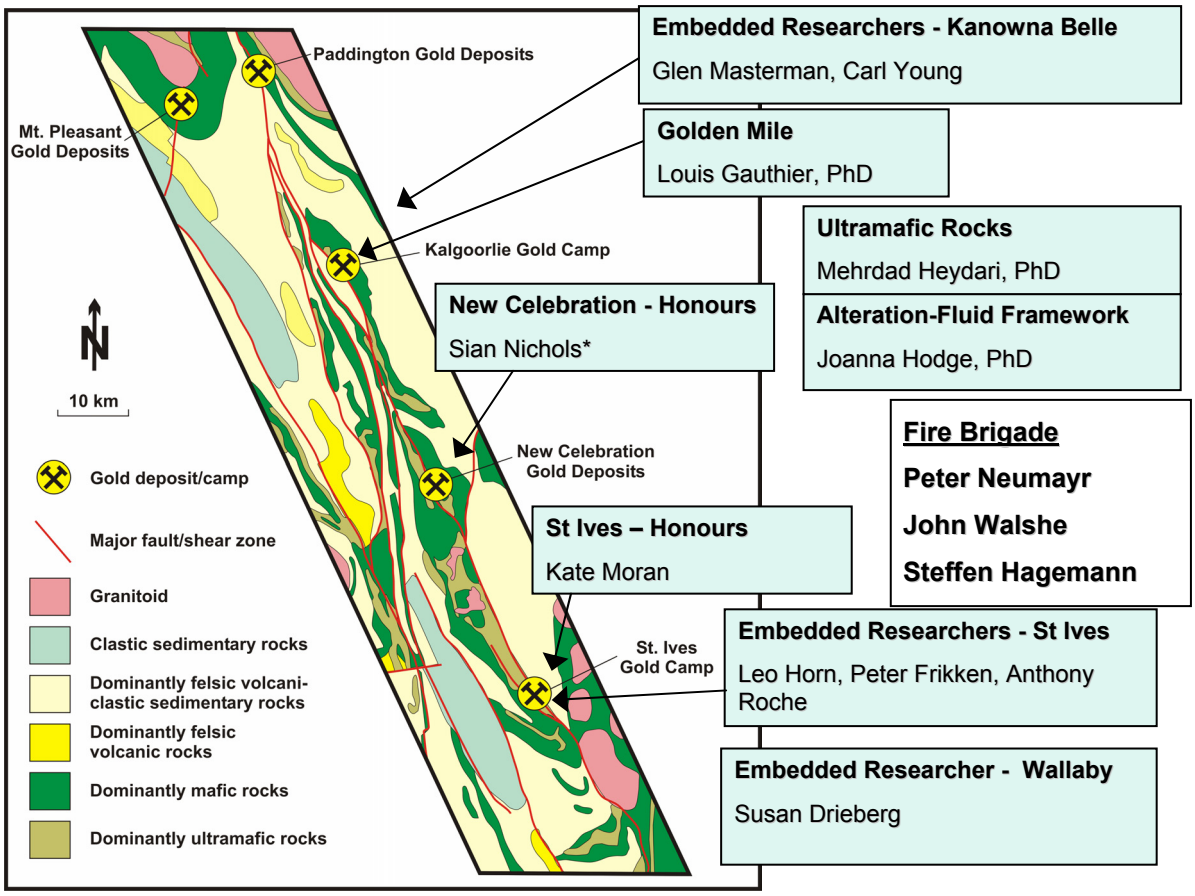

Fig. 2: Working areas and researchers of the Y3/M358 project in the Kalgoorlile-Kambalda Corridor.

The final report is organized into three parts:

Part 1 provides an Executive Summary, a Synthesis of the main research findings, and a section on the Exploration Significance of the research results. The Synthesis is a statement of progress on the five questions and includes summaries of preliminary results for individual research projects. The section is intended as a first draft of the "answer" to the five questions. The "answer" will be amplified in subsequent reports summarizing the results of ***pmd****CRC* YNEW and MERIWA 358 projects.

Part 2 includes Reports on individual research projects. Most of these reports are preliminary in nature due to the limited time these projects have been worked on. It is planned, in the future, to convert these reports into scientific papers to be published in national and international journals.

Part 3 includes Appendices which are organized based on working areas from the north (i.e., the Golden Mile deposit) to the south (the Kambalda gold deposits).

Table of Contents

Introduction and Organization of Final Report 1
Executive Summary 7
Part 1 Synthesis: Progress on the Five Questions 9
Geodynamic and Architectural Setting (Q1 and Q2 Terrane to District Scale) 9
Introduction to the Fluids in the System (Q3) 12
Introduction 12
Ambient Fluid 14
Magmatic Fluids 15
Spatial Association 15
Relative Temporal Association 16
Nature of the Magmatic Fluid 16
Mantle/Deep Crustal Fluids 17
Sulphur Isotopes & Sulphur Reservoirs 20
Fluid Inclusion and Paragenetic Constraints on Fluids in the System 21
Fluid Pathways/Fluid Flow/Mechanisms/Timing (Q2, Q3, Q4 Deposit to Camp-Scale) 24
Camp- to Deposit-Scale Architecture and Hydrothermal Alteration 24
St. Ives Camp 24
Camp-Scale Architecture 24
Alteration Types and Relative Timing 27
Camp-Scale Alteration Zonation 28
Deposit-Scale Alteration Zonation 32
Location of Gold Mineralization 36
Golden Mile 38
New Celebration 40
Kanowna Belle 41
Camp-Scale Architecture 41
Lithological Architecture: Geochemical Definition of Kanowna Belle Lithologies 43
Deposit-Scale Architecture, Flowpaths and Mixing Boxes in the Kanowna Belle System 49
Relative Timing 49
Relationship of Mineralization to Architecture 49

Alteration/Geochemical Characteristics of Reduced and Oxidized Fluid Pathways 54
Definition of Flowpaths and Mixing Boxes 59
Camp-Scale Alteration Zonation 61
Phengite – Muscovite Transition 61
Regional Extent of Muscovite/Paragonite Alteration 63
Wallaby 63
Introduction 63
Camp-Scale Architecture 65
Camp-Scale Chemistry 67
Deposit-Scale Architecture 68
Deposit-Scale Chemistry 68
Relative Timing/Paragenesis/Genetic Model 69
Integration of Common Camp-Scale Geological and Chemical Components 70
Introduction 70
Camp-Scale Litho-Stratigraphic Controls 70
Comparative Camp-scale Alteration and Geochemical Gradients 71
Redox – Sulphur Activity Gradients 73
pH Gradients 74
Sulphide and Gold Precipitation on the Chemical Gradients 77
Sulphur Isotopic Constraints on the Redox States of Fluids at Deposit to District-Scale 79
Gold Transport and Deposition (Q5) 84
Introduction 84
Isotopic and Mineral Constraints on Fluid Chemistry 85
Fluid Inclusion Constraints on Fluid Chemistry 85
St. Ives Camp 85
New Celebration 86
Exploration Significance 86
Introduction 86
Structural implications for exploration 87
Find the chemical gradients 89
What are the main geological features to assist with targeting 89

How Do We Read the Chemical Gradients in the Rock 90
Grade versus Tonnage Controls 91
Grade controls 91
Tonnage Controls 95
Summary 95
References 96
Part 2: Deposit- and Camp-Scale Results 99
Report 1: Structural and hydrothermal alteration evidence for early and late stages of gold mineralization at the New celebration gold deposits in Western Australia 99
Report 2: The New Celebration gold deposits: characteristics and evolution of hydrothermal fluids 99
Report 3: Architecture and timing of gold mineralization at the Golden Mile gold deposit, Kalgoorlie, Western Australia 99
Report 4: Hydrothermal alteration footprints and gold mineralization in the St. Ives gold camp 99
Report 5: The hydrothermal architecture of the St Ives gold deposits 99
Report 6: Alteration of the Kambalda Komatiite Formation in the Hannan lake area near Kalgoorlie, Western Australia 99
Part 3: Appendices 100
Appendix 1: Project Proposal, Research Approach and Personal 100
Appendix 2: Data base including data from St. Ives, Golden Mile, New Celebration and Hanons Lake 100
Appendix 3a: Additional reports, St. Ives Gold camp 100
Appendix3b : Additional reports, Kanowna Belle 100
Appendix 4: Annual reports 100
Appendix 5: Powerpoint presentations 100

Executive Summary

This report summarizes the results of the ***pmd****CRC* Y3 project from 2002 until end of 2004. The project team was tasked to determine camp- to deposit-scale hydrothermal alteration footprints to identify possible vectors which can assist exploration. The project initially focused on the St. Ives gold camp with additional studies on the Golden Mile and selected areas in the Kalgoorlie-Kambalda corridor. Additional resources were provided by St. Ives Gold Company Pty Ltd and Placer Dome to support researchers on-site at St. Ives, Kanowna Belle and Wallaby. These resources are managed through MERIWA project M358 and selected results of this project, as well as information from the ***pmd****CRC* Y2 project, are integrated into this report.

Most of the study was conducted in the Kalgoorlie-Kambalda corridor which forms the southern part of the "Golden Corridor." Three dimensional seismic interpretations reveal that a significant N-S trending subsurface anticlinorium, with an undulation about an E-W axis, underlies the Kalgoorlie-Kambalda region. Significant faults dip both east and west away from the antiform. Consequently, gold deposits occur in the footwall of the master faults.

Three main fluid reservoirs (ambient fluids, magmatic fluids, mantle/deep crustal fluids) are identified based on stable isotope and fluid inclusion evidence. Near surface environments potentially show the influx of surface-derived, meteoric fluids, but their relationship to gold mineralization is unclear. Importantly, fluid types are likely to be identified in specific trends in the stable isotope plots rather than by a unique stable isotope composition. In order to form large-tonnage, high-grade gold deposits it is postulated that both fluid-flow and contrasting thermochemical conditions (gradients) have to be sustained at the site of ore deposition. The latter is best achieved by having contrasting fluid types in the system (e.g., mantle/deep crustal and magmatic fluids). Hydrothermal alteration assemblages on a camp-scale monitor fluid flow and fluid type; therefore, zones of thermochemical gradients (i.e. sites best suited for gold precipitation) can be interpreted from alteration patterns. Importantly, if multiple fluids of contrasting chemistry were present in the system, evidence should be found at all scales from camp- to micro-scale. Fluid inclusion studies at St. Ives give evidence of rapidly changing fluid conditions with fluctuations from saline H_2O-rich fluids prior to gold precipitation to CO_2-rich fluids during gold precipitation to extremely saline H_2O fluids post gold. Distinct fluctuations from CH_4-rich, to H_2O-CO_2 fluids back to CH_4-rich fluids have also been identified at New Celebration, further emphasizing the importance of different hydrothermal fluids in the system.

At the Golden Mile, Fimiston style gold mineralization is bracketed by feldspar porphyry dykes, which overprint both limbs of the Kalgoorlie fold pair. These feldspar porphyry dykes both pre-date and cross cut mineralization. Importantly, dykes and mineralization are overprinted by the regional NNW-trending foliation.

At New Celebration, two gold events are recognized. An early event hosted in porphyry dykes is interpreted to be synchronous with D_{3NC} deformation and contains gold-bearing and gold-absent tellurides. The late gold event formed within a brittle fracture network at the margins of M2 porphyries and consists of free gold and gold in pyrite.

The most critical data sets for exploration are camp-scale hydrothermal alteration distribution maps which allow interpretation of the spatial distribution of fluid chemistry and identification of zones of rapidly changing fluid chemistry (i.e. sites best suited for gold precipitation). These maps have been developed for the St. Ives camp, Kanowna Belle and Wallaby deposits. In the St. Ives camp, oxidized magnetite-pyrite±hematite assemblages are spatially associated with major gold deposits such as Victory-Defiance and Revenge. The domains of oxidized assemblages are focused on gravity lows which indicate abundant porphyry intrusions at depth. During gold precipitation, the oxidation state of the hydrothermal fluid increased from magnetite stable to hematite stable. Domains of reduced assemblages (pyrrhotite-pyrite) occur flanking the oxidized domains. Most importantly, high grade gold intersections (>100 ppm) and also most of the known ore bodies occur at the domain boundary, but within the oxidized domain.

The Kanowna Belle gold deposit and surrounds also exhibit distinct alteration patterns in whole-rock multielement geochemistry and PIMA data sets. A V-bearing phengitic mica domain (oxidized) is characterized by high AlOH SWIR wavelengths and occurs at the Kanowna Belle deposit. It borders a Ba-rich muscovite domain (reduced) characterized by low AlOH SWIR wavelengths. Gold occurs in the oxidized domain in close proximity to the domain boundary with the reduced domain. In addition, a regional scale reduced-acidic domain characterized by paragonite, pyrite and carbonate can be distinguished which could potentially indicate pH gradients. Back calculation of multielement whole-rock geochemical data sets into modal mineralogy allow identification of reduced and oxidized domains and mapping of these domain in three dimensions.

In the district surrounding the Wallaby deposit, the broad areas of low AlOH wavelength mica imply widespread acidic conditions. The coexistence of chloritoid with short wavelength mica in these areas is consistent with reduced-acidic conditions. The Wallaby deposit occurs within a domain of longer AlOH wavelength mica, at the boundary between the reduced-acidic domain and the more oxidized-neutral domain.

The spatial distribution of sulphur isotopes in all three locations indicate that negative S-isotopes correlate well with the oxidized domains, whereas zero to positive S-isotopes correlate well with the reduced domains. Zones where S-isotopes switch from negative to positive host the gold deposits, further emphasizing the importance of chemical gradients. Based on the S-isotope data sets, it appears that the absolute state of oxidation is not critical for gold precipitation. However, it is critical to have evidence of both oxidized and reduced fluids in the system—i.e. zones of maximum geochemical gradient.

For exploration it is essential to determine the structural architecture and the spatial distribution of fluid chemistry. The combination of this information in 3D provides the best guide to mineralization. Whilst traditional structural geology and geophysical data sets provide information on the architecture of the system, new data sets have to be collected to understand the chemical architecture. At St.Ives, traditional mineral mapping from drill core provides information on the chemical zonation, but at Kanowna Belle and Wallaby, multielement whole-rock geochemical data sets and PIMA data sets provide the best guide. The key to localizing mineralization is to find suitable structural positions which show evidence of hydrothermal fluids of strongly different chemical composition. Zones with strong redox, pH and S gradients are best suited to host mineralization.

Part 1 Synthesis: Progress on the Five Questions

(This synthesis incorporates preliminary results from **pmd***CRC Y3, Y1 and MERIWA 358 projects.)

Neumayr, P., Walshe, J., Hagemann, S., Petersen, K., Gauthier, L., Nichols, S., Hodge, J., Horn, L., Heydari, M., Blewett, R., Connors, K., Halley, S., Masterman, G., Drieberg, S., Frikken, P., Roache, T., Young, C., Moran, K., Howe, D., Mikucki, E., Deyell, C., and Cooke, D.

Geodynamic and Architectural Setting (Q1 and Q2 Terrane to District Scale)

The Boorara and Kambalda Domains of the Kalgoorlie Terrane are the most richly endowed regions of the Yilgarn Craton (Fig. 3). They contain the world-class Au deposits such as the Golden Mile, Kanowna Belle, and the Kambalda deposits. A 'Golden Corridor' exists from Kambalda to Wiluna (and possibly as far north as Plutonic), along the axis of the Kalgoorlie Terrane. This section outlines the architecture of this Golden Corridor, from the south (where, due to data density, it is best defined) to the north.

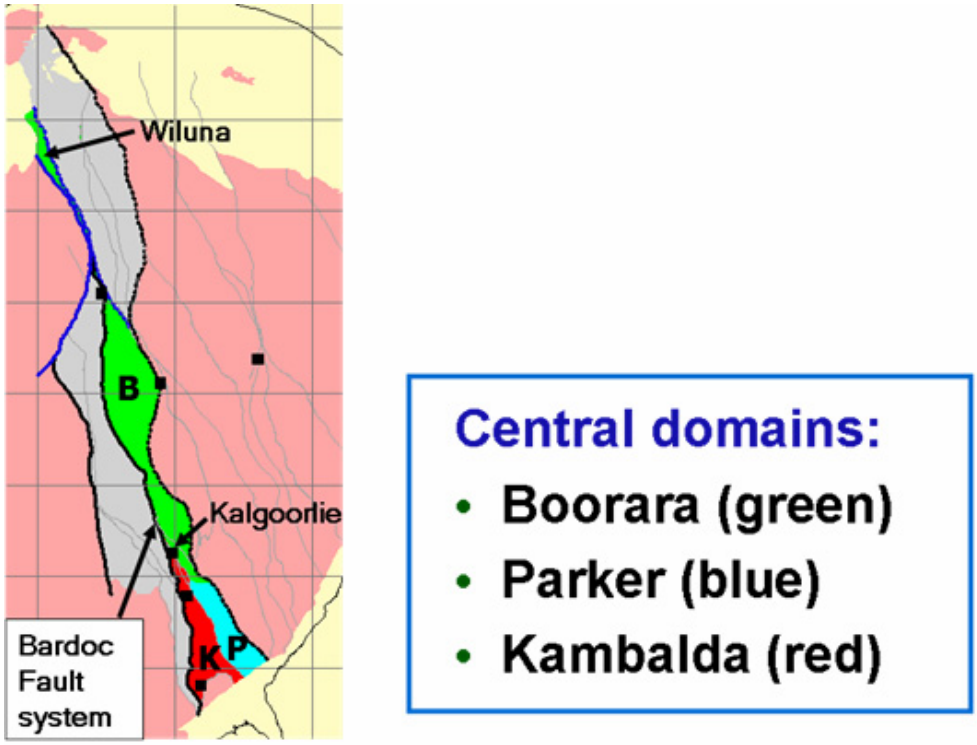

Fig. 3: Image showing the domains to the east of the Bardoc Fault System within the Eastern Yilgarn Craton.

In the south, this mineralized zone lies on a NNW trend bounded on its western side by the Bardoc Fault System (Fig. 3). Seismic reflection data across the Eastern Yilgarn Craton reveal that the majority of faults are east-dipping and west-verging, consistent with the geometries generally associated with a fold-and-thrust belt. Within the Kalgoorlie region though, faults dip both east and west with prominent faults such as the Bardoc Fault System occurring as a west-dipping structure.

Interpretation of the subsurface geometries generated during the construction of the 3D map of the Kalgoorlie-Kambalda region revealed that a significant anticlinorium occurs in a corridor stretching from Kambalda to Kalgoorlie and extending northwards (Fig. 4). This structure is a broadly N-S trending antiform with an undulation about an E-W axis. The interference of the N-S and E-W fold structures results in a series of elongate domical structures along a N-S corridor. To the east of this antiform is the reinterpreted Lefroy Fault, which through recent seismic reflection data (conducted by St. Ives Gold Mining Company Pty. Ltd.), has been reinterpreted from a west-dipping structure to an east-dipping structure.

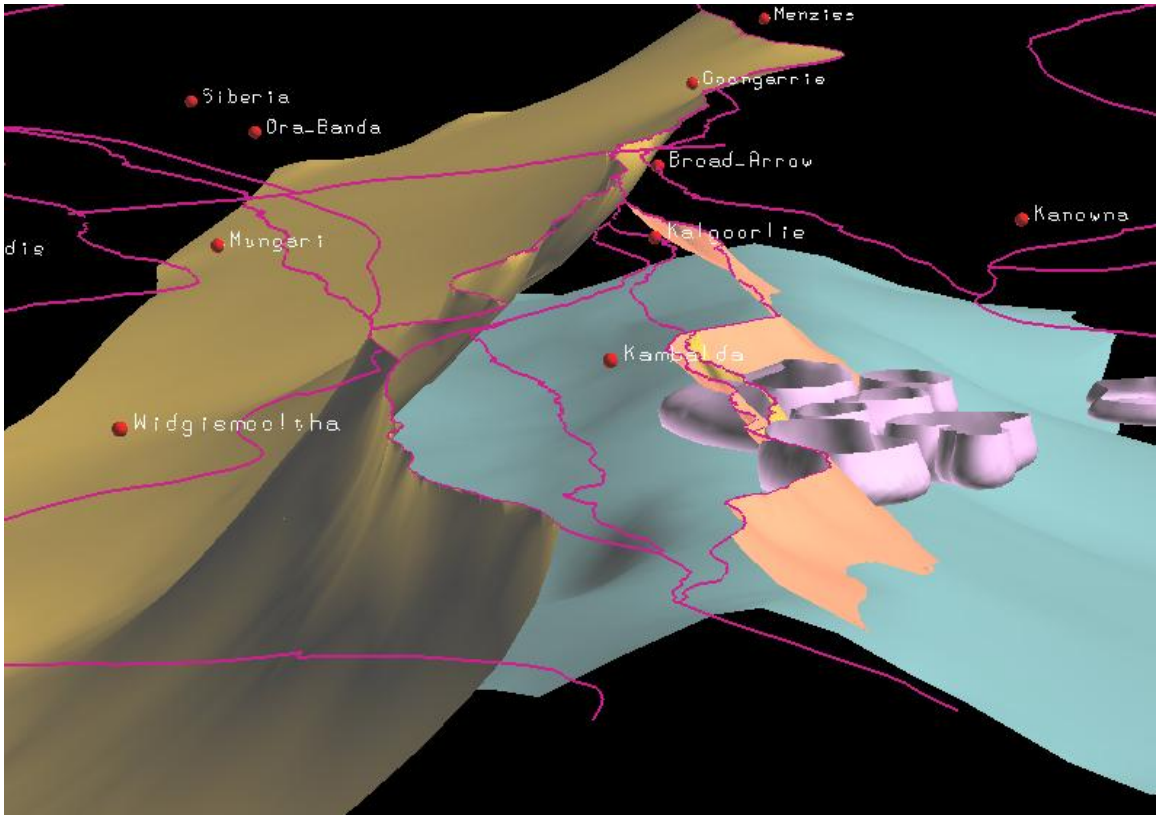

Fig. 4: Screen capture from Gocad of the southern section of the Golden Corridor looking north showing the anticlinorium beneath the Kalgoorlie-Kambalda region. Bardoc Fault (gold); Lefroy Fault (orange); LASH/antiform (blue); Granites (pink).

Overall the region is an antiform with major faults dipping in opposing directions away from its apex (Fig. 5). This places the major Au deposits in the footwall of these master faults and in two locations in subsidiary faults sub-parallel to the master faults. At the Golden Mile,

mineralization occurs within the steeply west-dipping Golden Mile Fault (sub-parallel to the Bardoc Fault System), which could be interpreted as a minor fault with genetic links to the Bardoc Fault System. At Kambalda the east-dipping Playa Shear appears to be a related to the east-dipping Lefroy Fault.

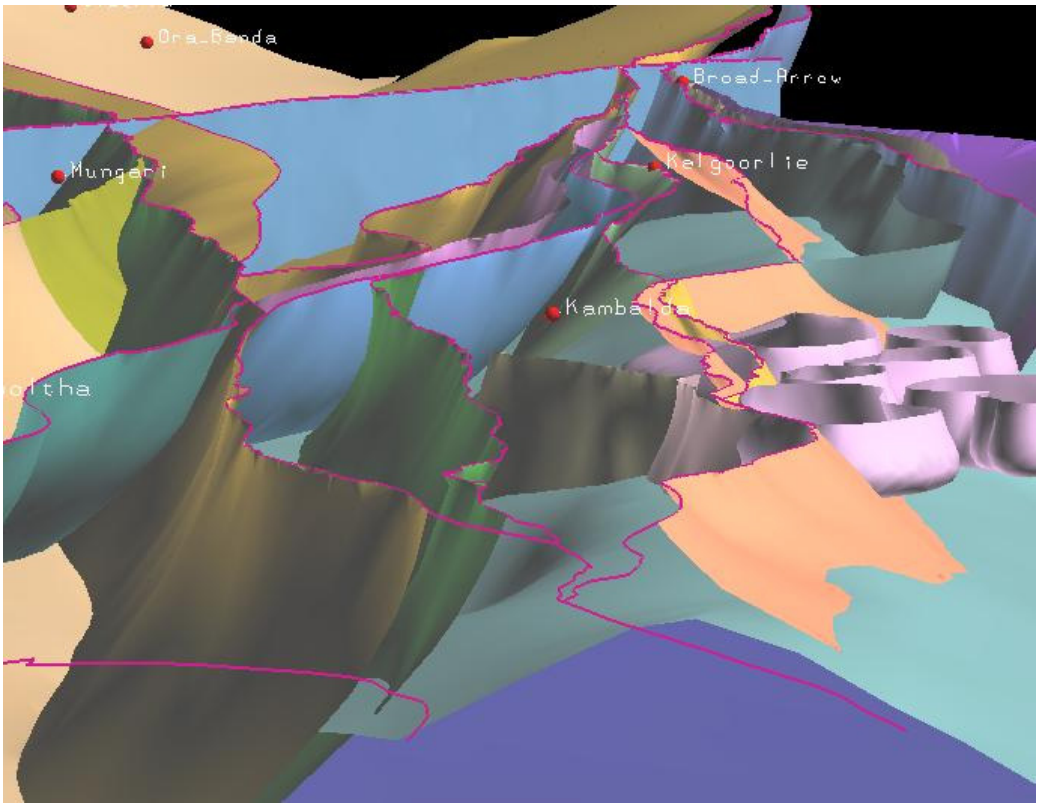

Fig. 5: Screen capture from Gocad looking north, showing the Kalgoorlie-Kambalda section of the Golden Corridor and additional minor faults.

Regionally, the Bardoc Fault System continues north until it intersects the reinterpreted northern Ida Fault at depth and the Waroonga Fault System (Fig. 6). At this location it is difficult to separate the faults because they both dip west and appear to merge. If the Bardoc Fault System continued and merged with this structure it would place the Au deposits at Wiluna in the same structural position as the Golden Mile and Kambalda (with respect to the dip of master fault and the associated anticlinorial axis).

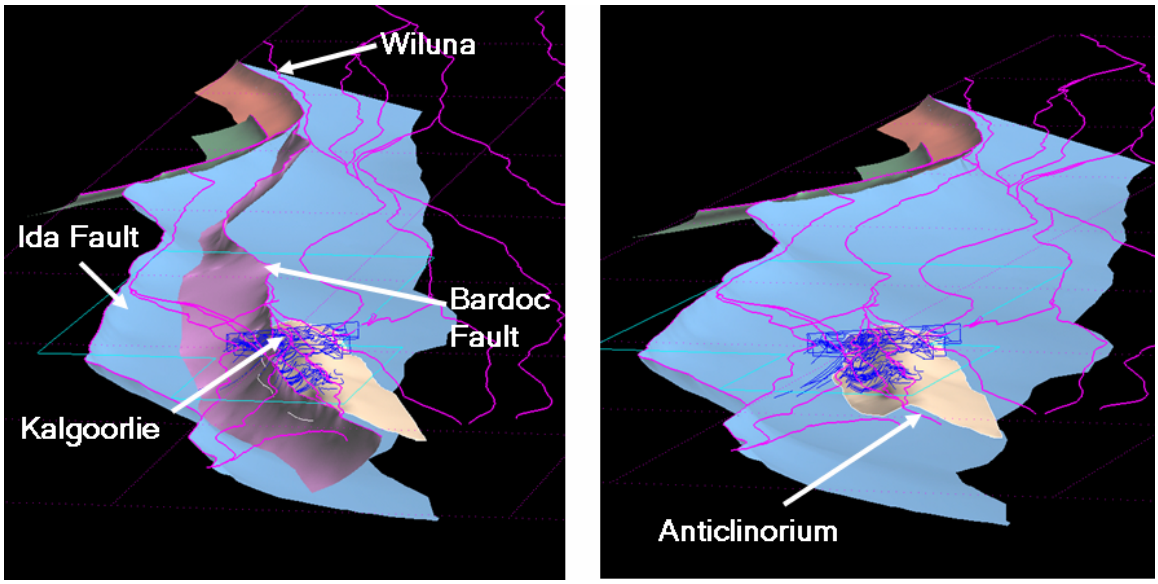

Fig. 6: Screen capture from Gocad looking north, showing the reinterpretation of the northern Ida Fault, the Bardoc Fault System and the anticlinorium beneath Kalgoorlie-Kambalda (the Golden Coridor).

Introduction to the Fluids in the System (Q3)

Introduction

It is necessary to consider at least three classes of fluids (Fig. 7) in the gold systems of the Eastern Yilgarn in order to account for the geochemical constraints (mineralogical, fluid inclusion and stable isotope data sets), the spatial associations of gold deposits and camps with significant architectural elements of the system (trans-crustal structures, intrusive complexes, district-scale structural culminations) and temporal correlations with the geodynamic and magmatic history of the terrane.

The three classes of fluids are:

1. An ambient fluid, representing fluids of diverse origins (basinal brines, metamorphic fluids) that are rock-equilibrated.
2. Magmatic fluids, either brines or volatile-rich fluids, that retain some geochemical properties that reflect equilibration with silicate melts at some time/place in their history. Such fluids may be considered
   - ortho-magmatic, in the sense that the chemical potentials of a significant number of fluid components retain values reflecting a history of melt-fluid equilibration, or
   - para-magmatic, i.e. the chemical potentials of a significant number of components in the fluid reflect a history of sub-solidus fluid-rock reaction and/or fluid mixing.

3. Mantle/deep crustal fluids that were potentially introduced into the mid- and upper-crust via the trans-crustal architecture.

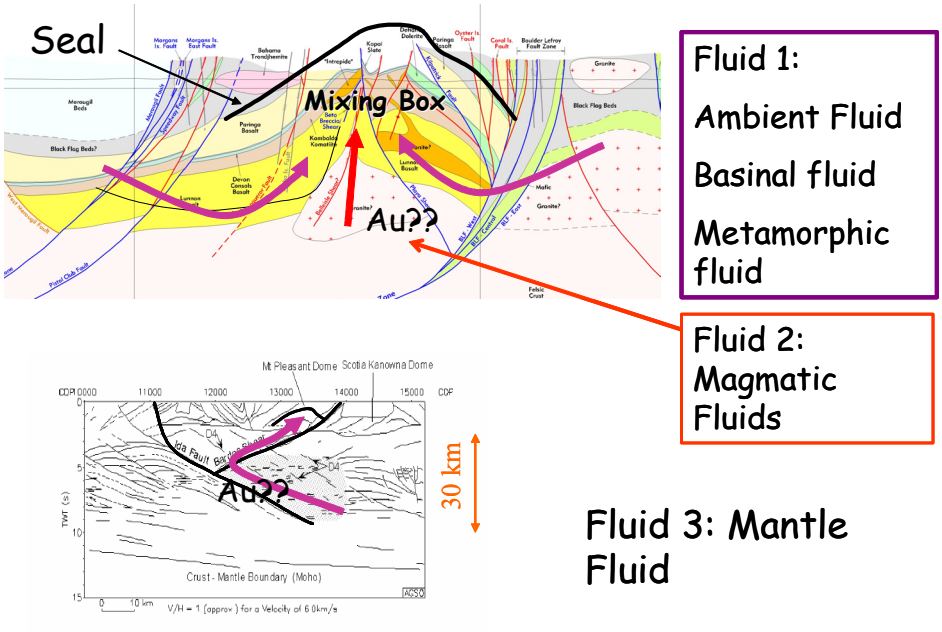

Fig. 7: Illustration of the three classes of fluids involved in the formation of Archean gold deposits of the Eastern Goldfields. The St Ives section (after Karen Connors) is used to illustrate district-scale relationships to magmatic centres. The flow paths drawn on the "Y-front" crustal-scale architecture are illustrative only.

Potentially, near-surface derived fluids (meteoric fluids, Hagemann et al., 1994) may have been important in some parts of the Au systems. Epizonal Achaean lode gold deposits in Western Australia (Wiluna, Racetrack), Canada (Renco) and Zimbabwe (Commoner) are interpreted to represent shallow level equivalents to the mesozonal deposits in the same terrain. The presence of low-temperature (150º to 325º C), low salinity aqueous fluid inclusions, low inferred depth of orebody emplacement of <5km, and high δD_{fluid} (-6‰ ± 9 ‰ relative to SMOW) and low $\delta^{18}O_{fluid}$ (4.4 ‰ ± 2.3 ‰ relative to SMOW) values of gold-related hydrothermal alteration minerals such as quartz, chlorite, and sericite have been interpreted by Hagemann et al. (1994) as evidence for surface water influx into epizonal Achaean lode-gold deposits. The geochemical evidence for local influx of surface fluids into the hydrothermal system is further corroborated by:

1. predominantly brittle shear zones that host orebodies
2. breccia hosted lodes
3. low temperature gangue and ore minerals such as silver sulphosalts, stibnite, and precursor chalcedony, and
4. vertical metal zonation of these orebodies.

The exact chemistry of the surface fluids, and mechanism of interaction of this fluid with the ascending deep-sourced fluids, including possible disturbances in both radiogenic and C/O

isotope signals that may reflect the input of Proterozoic or younger fluids into the systems, is presently the subject of on-going research.

Large-tonnage, high-grade deposits result from sustaining both fluid flow and contrasting thermo-chemical conditions at the site of mineral deposition. The thermo-chemical gradients reflect the histories of fluids in the mineralizing system. Most, if not all, of the major gold camps in the Eastern Goldfields Province contain deposits with reduced (pyrite, pyrrhotite, arsenopyrite) and/or oxidized (hematite, magnetite, anhydrite) sulphide-oxide assemblages (see below, Neumayr et al., 2003). Arguably the two most important fluid classes that provided the chemical contrasts, particularly redox contrasts, were fluids related to mid to upper crustal magma chambers and fluids from deep crustal/mantle reservoirs (Walshe et al., 2003).

Ambient Fluid

The most commonly observed fluid type in fluid inclusion studies of Achaean gold deposits is a H_2O - CO_2 ± NaCl fluid (Ho et al., 1990) The fluid is inferred to have been moderately oxidizing with CO_2 and H_2S the dominant C and S species, respectively (Mikucki, 1998). The C and O isotope characteristics of carbonate within and around deposits provide some significant clues to its history (Fig. 8). In a number of major deposits and camps (e.g., Kalgoorlie, Kanowna Belle, St Ives) and also prospects (e.g., Gidji, north of Kalgoorlie) $\delta^{13}C$ and $\delta^{18}O$ isotope data yield a broad band of values on $\delta^{13}C$ and $\delta^{18}O$ plots consistent with a theoretical cooling trend for a rock-buffered "ambient" fluid.

A variation of temperature of formation of the carbonate of several hundreds of degrees (450-150 ° C) is inferred. The temperatures of carbonate formation are broadly compatible with other constraints on temperature. The calculated starting $\delta^{18}O$ composition of the H_2O - CO_2 fluid is 6 ‰ consistent with the fluid being rock-equilibrated. The inferred $\delta^{13}C$ of CO_2 in the fluid is close to zero, suggesting that the ultimate origin of much of the CO_2 in the greenstones was seawater incorporated into the greenstones during sea-floor metamorphism or during DE/D1 deformation.

The more negative $\delta^{13}C$ values at low $\delta^{18}O$ values on Figure 8 (illustrated by the St Ives data) could either be a different CO_2 reservoir or more likely a high temperature, CH_4-rich fluid (see later discussion).

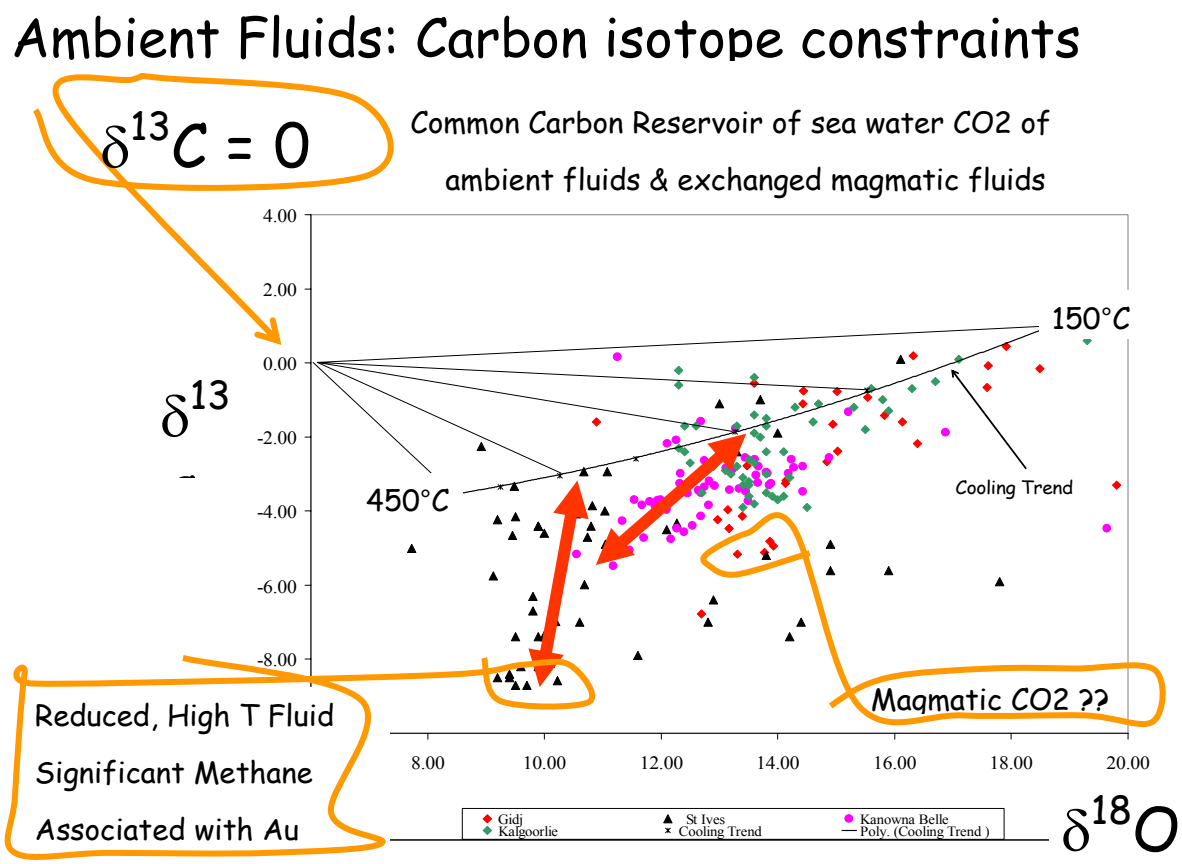

Fig. 8: Figure illustrates the variation in C and O isotopes in carbonate for St Ives (Victory – Defiance); Kanowna Belle and environs; Kalgoorlie and the Gidji prospect. Data from historical sources and the current study. The broad band of data around the theoretical cooling trend from 450° to 150°C (drawn assuming $\delta^{18}O$ of fluid is 6 ‰ and $\delta^{13}C$ of CO_2 in the fluid is 0 ‰) is taken to reflect rock-buffered "ambient" fluid conditions with the CO_2 ultimately derived from Precambrian seawater. The more negative $\delta^{13}C$ values at low $\delta^{18}O$ values (illustrated by the St Ives data) could either be a different CO_2 reservoir or more likely a high temperature, CH_4-rich fluid. The latter interpretation is consistent with fluid inclusion data. An approximate position is shown on the figure for magmatic CO_2. The origin of very positive $\delta^{18}O$ values (up to 30 ‰ is not known; possibly a Proterozoic overprint).

Magmatic Fluids

There is a spatial and temporal association of oxidized alteration assemblages within and subjacent to major gold deposits in the eastern Goldfields Province with 2665-2650 Ma mafic and syenitic intrusions described by Smithies and Champion (1999). These associations provide compelling arguments that oxidized fluids involved in the formation of many of the major deposits were magmatic fluids or fluids driven by magmatic intrusions. The main lines of evidence linking lode gold formation to magmatic-hydrothermal processes are detailed below.

Spatial Association

A spatial association occurs at the district scale of magnetite±hematite-bearing alteration assemblages with intrusive complexes. In the St Ives Gold Camp the mineralogical

associations are being documented in some detail (Figure 9; see also report by Neumayr et al. in Part 2 of this volume). More generally, these associations may be inferred from the geophysical data sets with gravity lows defining the intrusive complex in mafic/ultramafic host sequences and magnetic highs defining the associated hydrothermal magnetite.

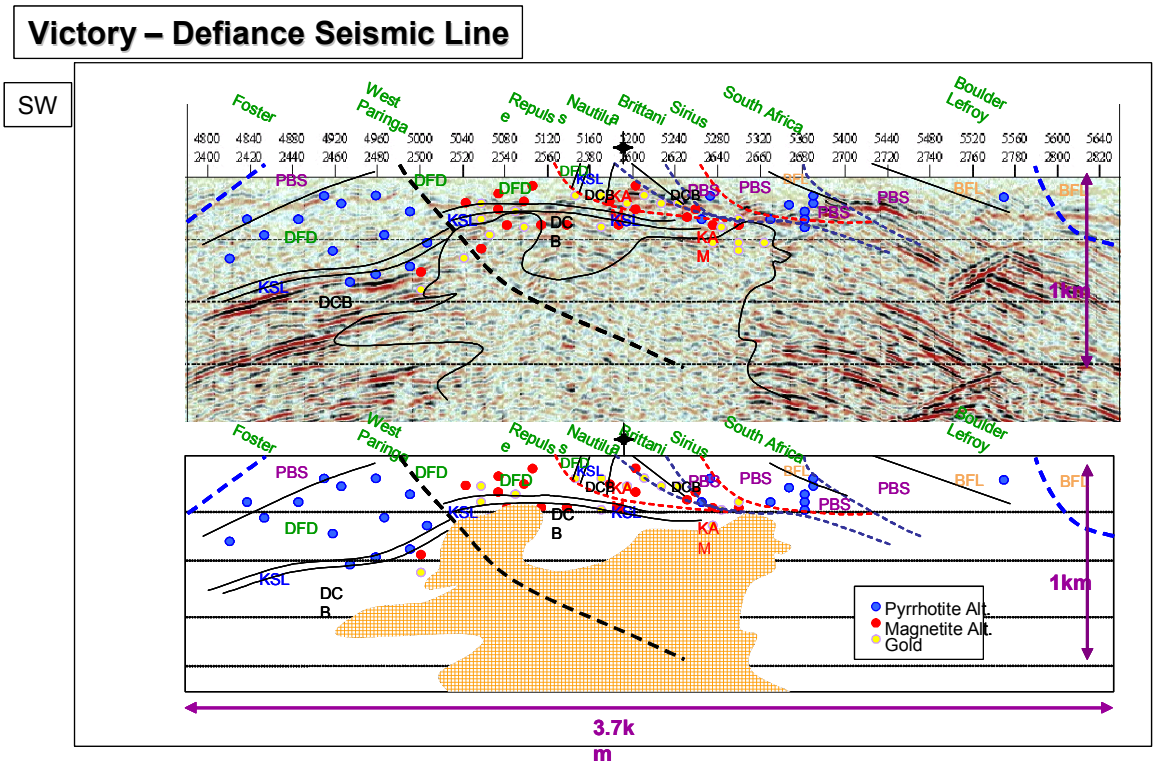

Fig. 9: Interpreted Victory-Defiance seismic section acoss the St Ives Camp showing the distribution of pyrrhotite, magnetite and gold with respect to the interpreted intrusive complex (after Ned Stolz, Karen Connors and Leo Horn).

Relative Temporal Association

A relative temporal association of oxidized alteration assemblages with gold occurs in many of the major deposits of the Kalgoorlie - Kambalda region. Much of the secondary magnetite spatially associated with the gold predates the gold-sulphide-plagioclase-carbonate assemblages (Neumayr et al; this volume) but some magnetite and hematite is stable with pyrite and gold (Ren et al., 1994, this study). The temporal association is clearly apparent in the largest deposit in the Eastern Goldfields Province, the Golden Mile (Clout, 1989) where hematite, roscoelite, anhydrite and tellurides occur with gold and sulphides that have a negative sulphur isotope signature. The trace element association of Mo and W, as well as V and Te, is taken as further evidence of an association of gold with magmatic fluids.

Nature of the Magmatic Fluid

Base-metal sulphides and salt-rich fluid inclusions are relatively rare in gold deposits of the Eastern Goldfields Province compared with relatively common evidence of oxidation, either spatially or temporally related to many major gold deposits. Hence the dominant ortho-magmatic fluid (used in the sense of a fluid that retains evidence of having equilibrated with

a magma) was vapour rather than brine at the time of gold deposition. Arguably the ortho-magmatic fluid was CO_2-rich with a component of SO_2 as well as volatile species of Te, V and Li, the evidence for these last components coming particularly from mineralogical associations in the Golden Mile.

Cooke and McPhail (2001) argue that the telluride content of gold deposits is a magmatic contribution. Two fluids are required to form gold tellurides because of their very low solubility. Tellurium was most likely transported by oxidized magmatic volatiles and the telluride rich ores of the Golden Mile formed by condensation of these magmatic vapours into Au-rich fluids within the Golden Mile Dolerite. The telluride-roscoelite-sulphate mineralogical association of the Golden Mile is a characteristic shared with deposits of the circum-Pacific (Porgera, Cripple Creek, Emperor) that are genetically linked with magmatic-hydrothermal processes.

Mantle/Deep Crustal Fluids

There is mineralogical, fluid inclusion and stable isotope evidence for high temperature, reduced, CH_4-rich fluids present at the time of gold deposition in most camps. Pyrrhotite-pyrite±arsenopyrite is the typical "reduced" sulphide assemblage. In the Junction deposit, St Ives Gold Camp, CH_4-rich fluids are paragenetically linked to gold deposition and preferentially occur on the margins of quartz veins (Polito, 1999). In the Mount Charlotte deposit, Kalgoorlie they occur in the pyrrhotite-rich assemblage formed at highest temperatures (Mernagh, 1996).

Trends to both lower $\delta^{13}C$ and $\delta^{18}O$ values for hydrothermal carbonate in these deposits (e.g., Victory-Defiance deposit, St Ives; Fig. 8) clearly transgress the cooling trends on $\delta^{13}C$ vs $\delta^{18}O$ plots, implying the significant methane contribution was associated with a high temperature fluid. Variations in $\delta^{13}C$ values up to 12.7 ‰ (Golding, 1984, and references therein) observed in the St Ives Gold Camp and Mount Charlotte district, Kalgoorlie may be indicative of high degrees of reduction of CO_2 or carbonate to CH_4. However, attempts to replicate these uncommonly positive signals reported by Golding (1984) have not been successful to date.

Insights into the origin of the high temperature, reduced fluids may be obtained from gold deposits formed within the Earth's crust at amphibolite to lower granulite facies metamorphic grade. Researchers from the mid 1980s (e.g., Groves, 1993) have emphasized the range of metamorphic conditions and depths over which Archaean lode gold deposits formed. In deposits formed at 500-700 ºC the CO_2/CH_4 ratio ranges from less than 0.01 to 100 (Ridley and Hagemann, 1999) consistent with the range in CO_2/CH_4 inferred from mineral assemblages, providing the maximum stability field for loellingite is assumed (Fig. 10). From the phase calculations, the most reduced fluids at 500-700 ºC are inferred to have been anhydrous and composed dominantly of H_2 - CH_4 - H_2S. The crustal dimension of the redox gradient requires a reductant at depth in the gold mineralizing system.

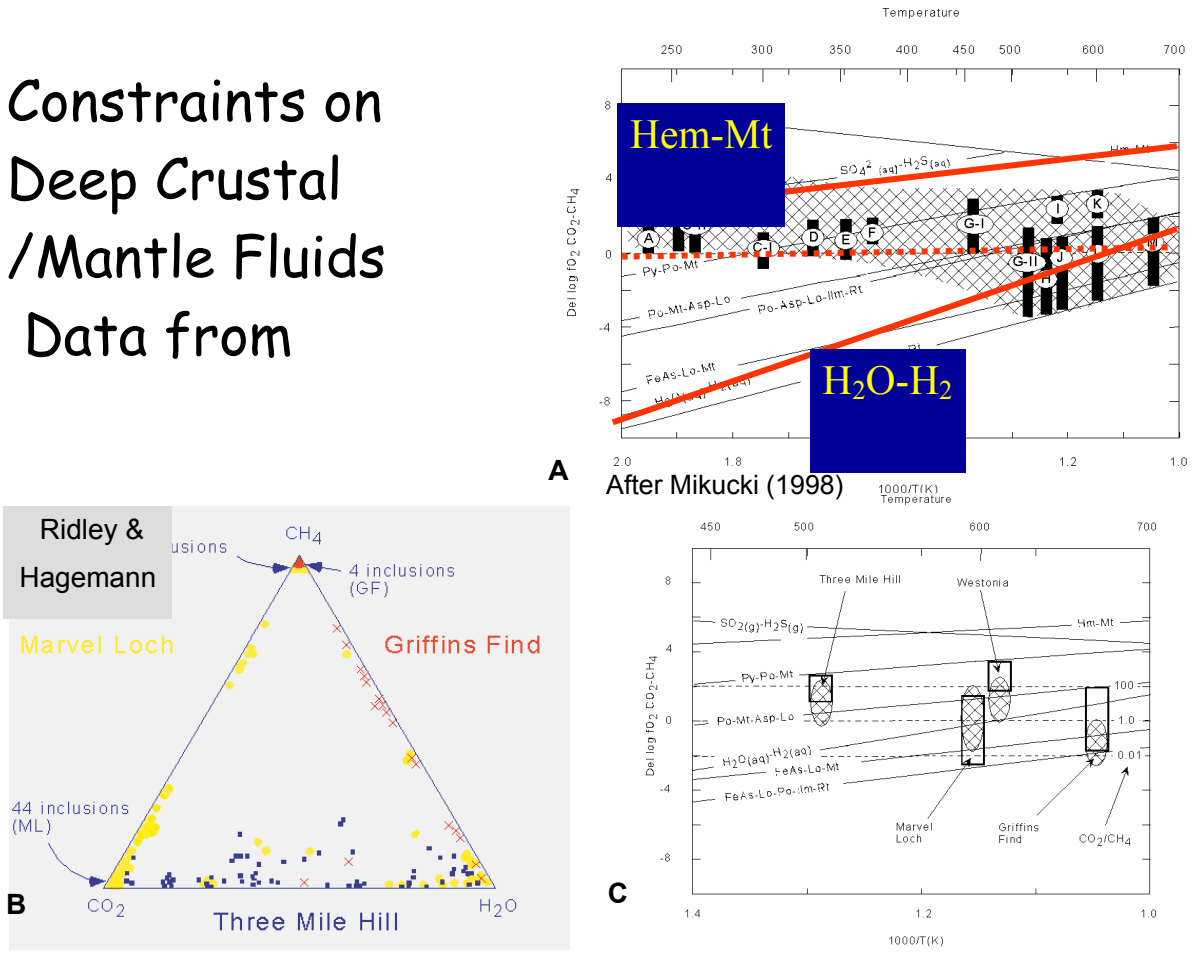

Fig. 10: Fluid inclusion and mineralogical constraints on deep crusta mantle fluids from gold deposits in amphibolite - granulite facies rocks.

A: Redox state of Archean lode-gold deposits relative to that of the CO_2(g)-CH_4(g) buffer as a function of temperature at two kilobars (modified from Mikucki, 1998). Del log fO_2 measures the displacement from the CO_2(g)-CH_4(g) buffer. The lower redox limit, which is based on maximum stability of the assemblages pyrrhotite, arsenopyrite, ilmenite and pyrrhotite, loellingite and ilmenite, extends into the anhydrous fluid domain of the diagram with H_2 and CH_4 the dominant species in the fluid. Thermodynamic data for reactions involving loellingite, pyrrhotite, rutile or ilmenite from Barton and Skinner (1979).

Deposit References given in Mikucki (1998) A: Racetrack, B: Golden Mile, C: Lady Bountiful, D: Wiluna, E: Mount Charlotte, F: Hunt, G-I: Norseman, north and central deposits, G-II: Norseman, southern deposits, H: Main Hill, I: Zakanaker, J: Nevoria, K: Westonia, L: Marvel Loch, M: Griffin's Find.

B:Composition of fluid inclusions with respect to H_2O-CO_2-CH_4 from the Three Mile Hill deposit, Coolgardie Goldfield and the Marvel Loch and Griffins Find deposits, Southern Cross Goldfield (from Ridley and Hagemann, 1999). Water contents determined by phase ratios and CO_2/CH_4 by micro-thermometry or laser-Raman spectroscopy.

C: Redox state of lode-gold deposits formed at amphibolite to granulite facies metamorphic conditions relative to that of the CO_2(g)-CH_4(g) buffer (after Mikucki, 1998) comparing estimates from mineralogical redox buffers (boxes) with CO_2/CH_4 estimates from mixed aqueous–carbonic fluids (Ridley and Hagemann, 1999; Hagemann and Cassidy, 2000).

It is suggested that mantle degassing of H_2 was key to the production of high temperature, reduced, anhydrous fluids (Walshe et al., 2004a; 2004b). Conceivably, these hydrogenous fluids may have been generated during subduction cycles through extreme hydration of the mantle wedge, yielding serpentine ± chlorite with reduction of CO_2 to CH_4, in the absence of melting (Fig. 11). Alternatively the hydrogen may be sourced from the deep mantle or even the core of the Earth. It is clear that the interior of the Earth (particularly the core) is anomalously rich in H_2 (Williams and Henley, 2001). First order observations about the temporal and spatial distribution of giant deposits through Earth history hints that the core was the most likely source of H_2. Arguably, episodic release of hydrogen from the core to the mantle, crust, hydrosphere and atmosphere provides a plausible alternate explanation for many redox-related phenomena through Earth history: anoxia in the Earth's oceans, mass extinction events, oil and gas generation, diamond growth, base and precious metal transport and/or deposition within the crust (Fig. 12). Episodic, large-scale release of H_2 may have occurred via anhydrous plumes or sheets sourced from the core-mantle boundary. Such large scale features within the mantle are known, e.g., a sheet-like hydrous plume straddles a 2000 km length of the present coastline of the US-Atlantic margin, dipping westwards into the mantle down to at least 660 km depth.

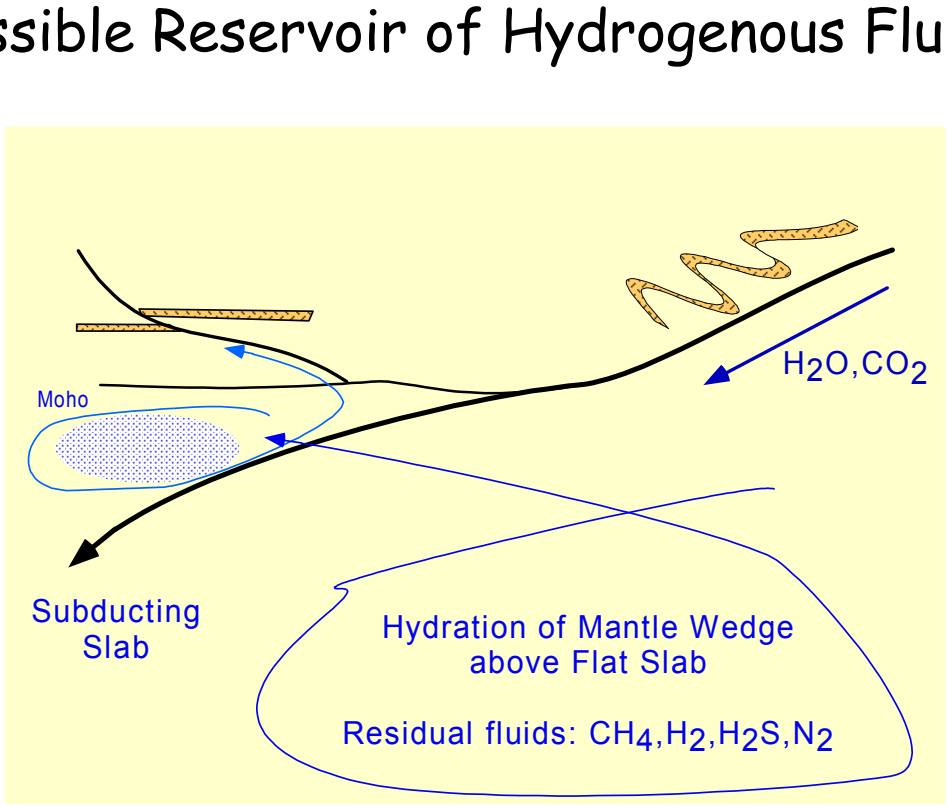

Fig. 11: Possible location of a reservoir of hydrogenous fluid in a flat slab setting. Hydrogenous fluids result from extreme hydration of the mantle wedge in the absence of melting.

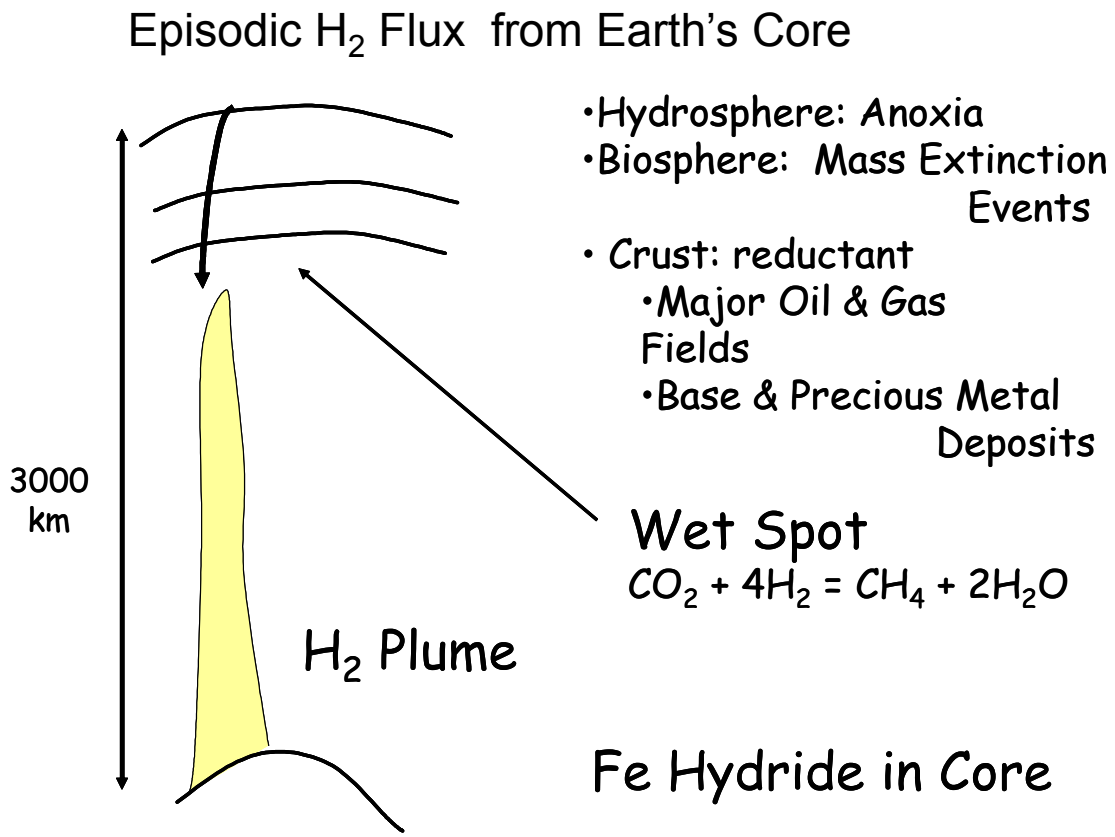

Fig. 12: Hydrogenous plume from the core-mantle boundary. Episodic release of hydrogen from the core to the mantle, crust, hydrosphere and atmosphere provides a plausible alternate explanation for many redox-related phenomena through Earth history. The length scale of 3000km to the Earth's core is consistent with the length scale of many major metallogenic provinces.

Sulphur Isotopes & Sulphur Reservoirs

The available data suggest that the sulphur isotopic composition of the ambient fluid was close to zero. Sampling of background sulphides is difficult because of the size of the hydrothermal systems and the lack of outcropping sulphides. However, historical data sets of sulphides from igneous rock, nickel deposits and sedimentary rocks well outside of gold systems point to a sulphur isotope range from 0 ‰ to +3 ‰. Data obtained in this study from the St Ives and Laverton Camps for interflow sediments (Kapai Slate), Black Flag Beds, Merougil Beds and Wallaby Conglomerate yielded values between 0 and 2.8 ‰ giving an average of 1.3 ‰ for 11 samples (Fig. 13).

Samples in sediments distal from known deposits/camps or early/diagentic sulfides

St Ives camp

Area	Sample #	DDH	Metres	Description	del 34S(per mil)	Source of info
Victory - Defiance area	LD65020600	LD 6502	60.0	carbonaceous K.S. with abundant py	1.80	this study
Victory - Defiance area	LD65020616	LD 6502	61.60	carbonaceous K.S. with abundant py	0.70	this study
Victory - Defiance area				Kapai slate, North Orchin (sub grade)	1.70	Western mining report 1987
Foster South Area				Kapai Slate	2.40	Western mining report 1987
5km south of Foster South Area				Blag Flag Beds Pyritc VSW?	0.30	Western mining report 1987
East Tramsways				Kapai Seds	0.70	Western mining report 1987
Merougil Beds				Merougil pyritic sandstone	0.50	Western mining report 1987
Wallaby and Granny Smith						
	GSD3593510	GSD 359	351.0	From seds north of Granny Smith	1.40	this study
	GSD3593675	GSD 359	367.50	From seds north of Granny Smith	1.80	this study
	LCAD0021625	LCAD 002	162.50	Distal sulfides	2.80	this study
Harmony: Chip samples						
	02CTRC016B	02 CTRC 016	79-80	py-bearing shales	0.0	this study
				Average Value	1.28	

Fig. 13: Sulphur isotopic compositions of sulphides from sediments distal to known deposits/camps or early/diagenetic sulphides.

There is no direct information on the sulphur isotopic composition of either magmatic sulphide or sulphate sensu stricto, i.e. sulphide or sulphate species that equilibrated with a silicate melt. However, $\delta^{34}S$ values of sulphate within the Golden Mile (Clout, 1989) provide a proxy for magmatic sulphur dioxide or sulphate derived from subsolidus disproportionation of sulphur dioxide to sulphate and H_2S.

The postulated deep fluid, sourced from the lower crust or mantle, can be anticipated to have a sulphur isotopic composition close to zero, indistinguishable from the sulphur isotope signal of the ambient fluid, so it would appear that magmatic sulphate is the only likely source of heavy sulphur in the gold mineralizing system. Given the size of the alteration systems, this heavy component may be widely dispersed and may be a component in apparent "background" sulphides. The "true" background signal may actually be very close to zero rather than slightly positive.

Fluid Inclusion and Paragenetic Constraints on Fluids in the System

The chemical composition of fluids as analyzed in fluid inclusions in any host mineral is the product of the chemistry of the fluid and the reactions which take place during mineral precipitation (e.g., fluid-rock interaction, fluid mixing, and phase separation) in fluid reservoirs, along pathways and at sites of mineral deposition. Consequently, the observed fluid composition in fluid inclusions does not necessarily directly reflect the composition of fluid reservoirs or the composition of source regions in the system regardless of where the fluids are analyzed in the system. However, if fluid inclusions are analyzed in a variety of settings in the same pathway and if processes and reactions which take place along the pathway are understood, fluid end member compositions (in the reservoir) can be inferred. At the very least, grossly differing fluid compositions in different settings indicate that fluids from different reservoirs infiltrated the deposit, provided that phase separation can be excluded as depositional mechanism.

Fluid inclusions in a range of settings and host minerals have been analyzed in the New Celebration gold deposit and in the Revenge and Conqueror gold deposits of the St. Ives gold camp with the view to determine the compositional diversity of fluids in the system and their chemical evolution. The diversity is inferred from observation of fluid inclusions in different alteration assemblages and host minerals of different relative timing as well as in different fluid pathways of similar timing.

In the St. Ives gold camp, at least three stages of hydrothermal fluid flow are distinguished:

1. Early fluid stage with epidote-calcite-magnetite-chalcopyrite alteration.
2. Intermediate fluid stage with gold-related plagioclase-dolomite/ankerite-pyrite-hematite±magnetite alteration and contemporaneous(?) pyrrhotite-bearing alteration in different fluid conduits. Biotite and chlorite occur in proximal alteration assemblages and PIMA studies indicate white mica is also a significant proximal alteration phase.
3. Late fluid stage resulting in abundant quartz-carbonate veins which overprint alteration related to the first two stages.

The three fluid stages are characterized by different hydrothermal fluid compositions. The early stage contains only aqueous fluids with a low salinity (<7.4 wt% NaCl equiv.) with high homogenization temperatures (>250º C) indicating the influx of hot fluids. The origin of the fluid is difficult to determine using chemical compositions only, but given that the epidote alteration is typically proximal to intermediate porphyries and abundant magnetite and chalcopyrite is part of the mineral assemblage, a magmatic-hydrothermal origin of the fluid is plausible.

The intermediate, gold-related cycle is chemically quite complex and will be described in more detail below. The hydrothermal fluid changed rapidly from saline (< 23 wt% NaCl equiv.) aqueous fluids to CO_2-H_2O and H_2O-CO_2 fluids of low salinity (<5.15 wt% NaCl equiv.). Importantly, the influx of CO_2 is difficult to explain through phase separation processes and is best interpreted as the influx of a new CO_2-rich fluid. The lower salinity of the mixed CO_2-H_2O fluids compared to the earlier aqueous fluids during this cycle means also that the new fluid contained some H_2O but with less salinity than the earlier aqueous fluids. The overall greater fluid inclusion sizes compared to the paragenetically older aqueous fluid inclusions indicate also a more rapid mineral growth during this stage.

The late fluid stage trapped within abundant quartz-carbonate veins that overprinted gold-related alteration contains mostly H_2O±CO_2 fluids with daughter minerals (e.g., halite, carbonate) indicating high salinities up to 37 wt% NaCl equiv. These fluid inclusions were probably trapped at very low temperatures indicated by quite low homogenization temperatures.

Overall, the fluid evolution indicates that hydrothermal fluid compositions changed between different fluid stages, but also fluctuated rapidly during the intermediate, gold-related stage. The changing fluid chemistry is mainly due to the influx of CO_2-rich, low salinity aqueous fluids coincident with gold precipitation.

At New Celebration, fluid compositions as determined from fluid inclusions are also quite diverse both spatially and temporally. In the Porphyry-, Mylonite and Fracture-style mineralization four main fluid inclusion assemblages are identified:

1. H_2O-NaCl±KCl inclusions with two sub-populations: low- to moderate-salinity (0-12 equiv. wt% NaCl), and high-salinity (18-22 equiv. wt% NaCl),
2. H_2O-CO_2-NaCl±CH_4±solids inclusions with a sub-population which appeared aqueous but that contained between 0 and 2.2 molal CO_2,
3. CO_2±CH_4±N_2 inclusions, and
4. CH_4±CO_2 inclusions.

The earliest fluid inclusion assemblage in the Porphyry-style mineralization is primary CH_4±CO_2 inclusions. This assemblage predates all other fluid inclusion assemblages, including those associated with the Mylonite- and Fracture-style mineralization. The latter comprises predominantly H_2O-CO_2-NaCl inclusion assemblages, but H_2O-NaCl and CO_2 inclusions are also observed. The fluid inclusion assemblages associated with mineralization are themselves crosscut by low-salinity H_2O-NaCl inclusions in all mineralization styles. Paragenetically late high-salinity aqueous inclusions occur in the Fracture-style mineralization. The paragenetically last inclusion assemblage in Porphyry-style mineralization comprises secondary CH_4 inclusions.

Therefore, the fluid inclusion evidence indicates the fluid chemistry at New Celebration changed significantly during the main stage of gold precipitation. The fluid was dominated by CH_4 both pre- and post-mineralization; however, the fluid was predominantly H_2O-CO_2-NaCl syn-mineralization.

At the current stage of research for this study, detailed fluid inclusion investigations have been completed only for the Revenge, Conqueror, and New Celebration gold deposits. However, each study has revealed significant fluctuations in fluid chemistry directly related both spatially and temporally to gold mineralization.

Fluid Pathways/Fluid Flow/Mechanisms/Timing (Q2, Q3, Q4 Deposit to Camp-Scale)

Camp- to Deposit-Scale Architecture and Hydrothermal Alteration

St. Ives Camp

Camp-Scale Architecture

The stratigraphic sequence for the St. Ives camp (Fig. 14) shows the effects of four phases of post-volcanic compressional deformation (D1-D4) and a number of deformation schemes have been proposed. More recent interpretations of the structural history have recognised the importance of several episodes of extensional deformation and basin formation in the development of the early fault architecture, which in turn has had a significant influence on the later history of compressional deformation.

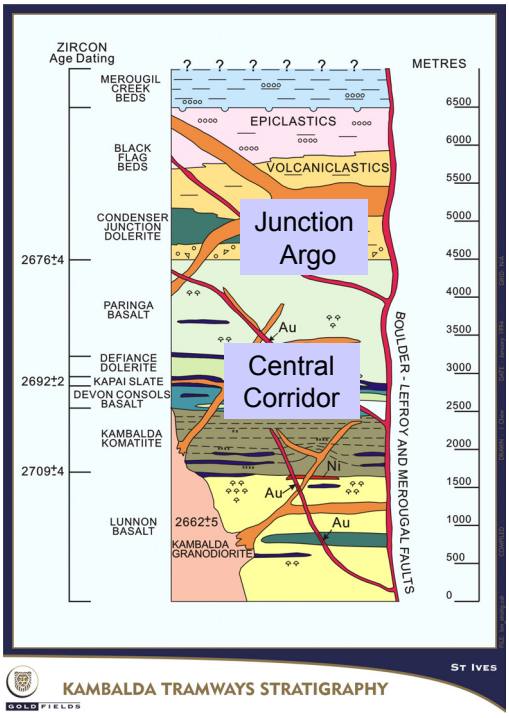

Fig. 14: St Ives gold camp stratigraphy

De1 mafic-ultramafic volcanism - The tectonostratigraphic history of the Eastern Goldfields Province starts with a period of mafic - ultramafic volcanism (De1) from 2720-2690 Ma (Barley et al., 2002). The stratigraphic units in the St Ives area which formed during this period include: 1) Lunnon basalt, 2) Kambalda komatiite (2709±4 Ma U-Pb zircon SHRIMP, Claoue-Long et al., 1988), 3) Devon Consols basalt (2693±30 Ma U-Pb zircon SHRIMP, Compston et al., 1986), 4) Kapai slate (2692±4 Ma U-Pb zircon SHRIMP,

Claoue-Long et al., 1988), 5) Defiance dolerite, and 6) Paringa basalt (2690±5 Ma U-Pb zircon SHRIMP, Clout, 1991). Together these units form the Kalgoorlie Group. The faults which originated during this deformation event are interpreted to include many of the major NNW trending structures which have previously been interpreted as D3 in age. Significant across-structure stratigraphy variations indicate that these structures may have been involved in basin development during this event.

De2 felsic magmatism - The second major depositional event (De2) occurred from ca. 2690 to 2660 Ma (Barley et al., 2002), involving a NNW-SSE extension direction (based on extensional fabrics in ca. 2680 Ma granitoid domes; e.g., Williams and Whitaker, 1993) and was associated with felsic magmatism, sedimentation and local mafic magmatism (e.g., Condenser-Defiance-Junction Dolerite; 2680±8 Ma). This event resulted in deposition of the extensive Black Flag beds. The basins related to this stage of extension generally deepen to the south therefore implying SE side down displacement (Nick Hayward, WMC pers comm. 2001). Interpretation of seismic data in the St Ives area suggests that the Boulder Lefroy fault dips east and formed as an extensional fault during deposition of the Black Flag sequence.

D1 N-S thrusting - D1 thrust faulting at ca. 2657 Ma involved ~N-S compression and inverted the basins developed during De2. This event resulted in the development of ~E-W trending thrust faults and recumbent folds such as the Foster, Tramways and Republican thrusts (Fig. 15).

D2a ~ENE-WSW shortening - Early NNW trending D2a folds are truncated by the late basins (De3 sedimentation) in both the Pig Well (Blewett et al., in press) and Kurrawang areas. This implies that a stage of ~ENE-WSW shortening had initiated prior to the extensional event related to deposition of the late basins.

De3 late basin sedimentation and felsic magmatism - A third major depositional event occurred post ~2655 Ma, based on the youngest zircons found in any of the late basins (Krapez et al., 2000), however the age of these basins vary across the Eastern Goldfields Province (Blewett et al., in press). Age dating in the St Ives area suggests that widespread felsic to intermediate porphyries and the Kambalda granodiorite ((2662±4 Ma: U-Pb zircon SHRIMP, Compston et al., 1986) were emplaced during or just prior to this event. Porphyries have been dated at 2660±6 Ma and 2658±4 Ma (U-Pb zircon SHRIMP, Nguyen, 1997) and 2680±12 Ma (U-Pb zircon, Clark, 1987). The extension direction during this event is interpreted as ~NE-SW by using the dominant ~NW-SE trend of the porphyries in most of the St Ives camp. The fluvial rocks of late basins such as the Merougil Beds are interpreted to have been deposited in elongate, localized basins (Fig. 15).

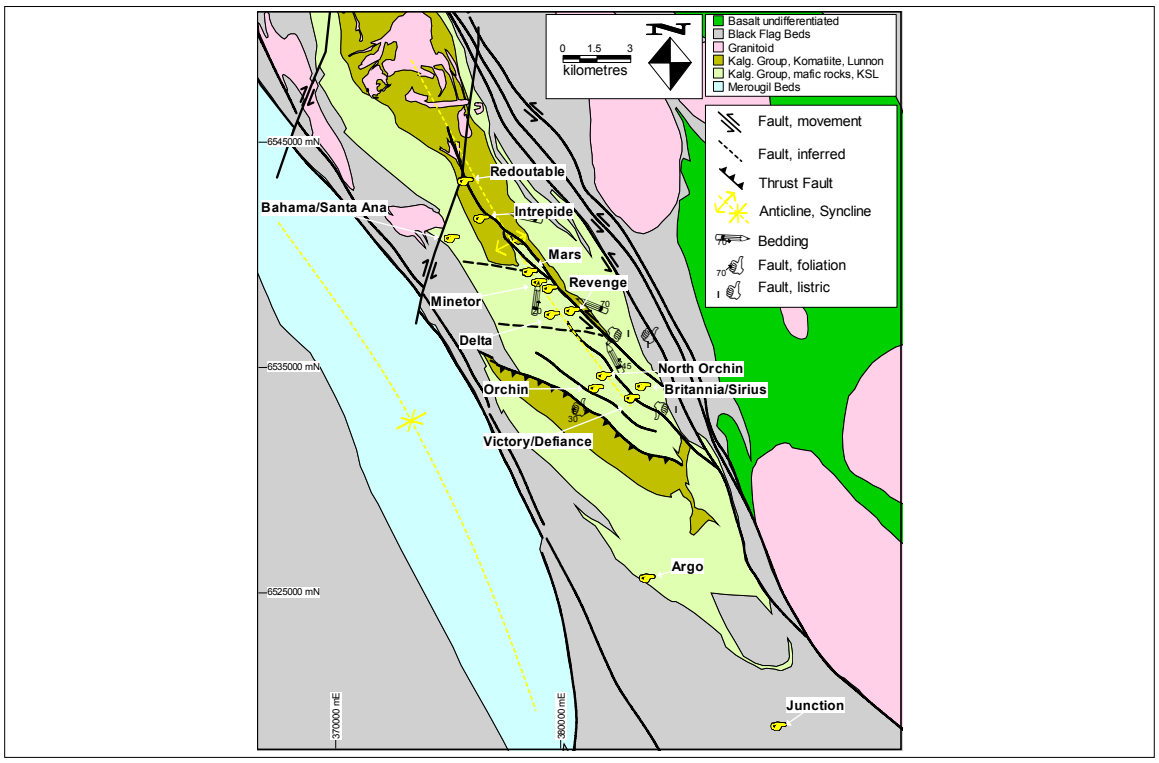

Fig. 15: Geological map of the St. Ives gold camp. The camp is bounded by the first-order Lefroy fault zone and the Merougil fault. The stratigraphy comprises mafic and ultramafic rocks of the Kalgoorlie group, felsic volcanic and volcaniclastic rocks of the Black Flag Beds and sedimentary rocks of the Merougil group.

D2b main stage of ENE-WSW shortening - D2b ENE-WSW shortening is interpreted to have occurred late syn- to post-granite intrusion (Archibald, 1985; Nguyen, 1997) at ca. 2650 Ma or later. D2b involved generation of open upright folds such as the Kambalda Dome (Fig. 15) and the development of the main upright cleavage (S2 foliation) and M2 greenschist-facies metamorphism, possibly synchronous with the main phase of granitoid intrusion.

D2x NW-SE shortening - Recently workers from Geoscience Australia have documented evidence for a period of ~NW-SE shortening which occurred after D2 and prior to the D3 event (Blewett, pers. comm. 2004). At St. Ives, some "D1" thrusts appear to cut D2 folds and are not folded by this event as previously interpreted. The D1 Republican thrust cuts a NW trending fault which in turn cuts the major Boulder Lefroy fault. At present it is uncertain whether D1 thrusts have simply been reactivated during the D2x NW-SE shortening event, or whether these faults may have originated at this time.

D3 ESE-WNW shortening - This represents a return to the broadly ~E-W shortening direction of D2. The ESE-WNW shortening direction for the St Ives area is confirmed by sinistral reverse movement on numerous N-trending faults. D3 deformation resulted in the tightening of D2 folds and local development of new folds overprinting D2 structures, as well as reactivation of pre-existing faults and development of new faults, largely as subsidiary structures to the pre-existing N- to NW-trending faults (Fig. 15). The timing of

the change from ENE to ESE shortening is not well constrained, but is considered likely to have occurred around 2645 Ma (or later).

The later stages of D3 ESE-WNW shortening, which coincided with gold mineralization at St Ives, must have predated 2632 Ma, the age of a post-tectonic granite cutting the Ida Fault (Bateman, 2001). This age represents a minimum age for any major deformation including D4. Age dating at St Ives suggests that the Victory and Revenge gold mineralization formed during the final stages of D3 deformation.

D4 shortening - D4 deformation is generally interpreted as NE-SW shortening which resulted in reactivation of various faults and development of brittle NE and NW faults (Fig. 15, Nguyen, 1997). In general, this event does not appear to be very significant. However, it may be associated with the final stages of mineralization. At St Ives, the Redoubtable deposit has been interpreted as synchronous with D4 deformation given that it is associated with the Alpha Island fault which has been considered to be D4 in age. However, observations during this study suggest that the fault may be older.

Alteration Types and Relative Timing

Based on diamond drill core logging, at least four alteration cycles can be distinguished (Fig. 16):

- Early epidote-magnetite-carbonate alteration,
- Carbonate alteration (camp-scale),
- Intermediate magnetite, pyrrhotite, biotite, chlorite and plagioclase-carbonate-pyrite-magnetite-hematite alteration, and
- Late quartz veins.

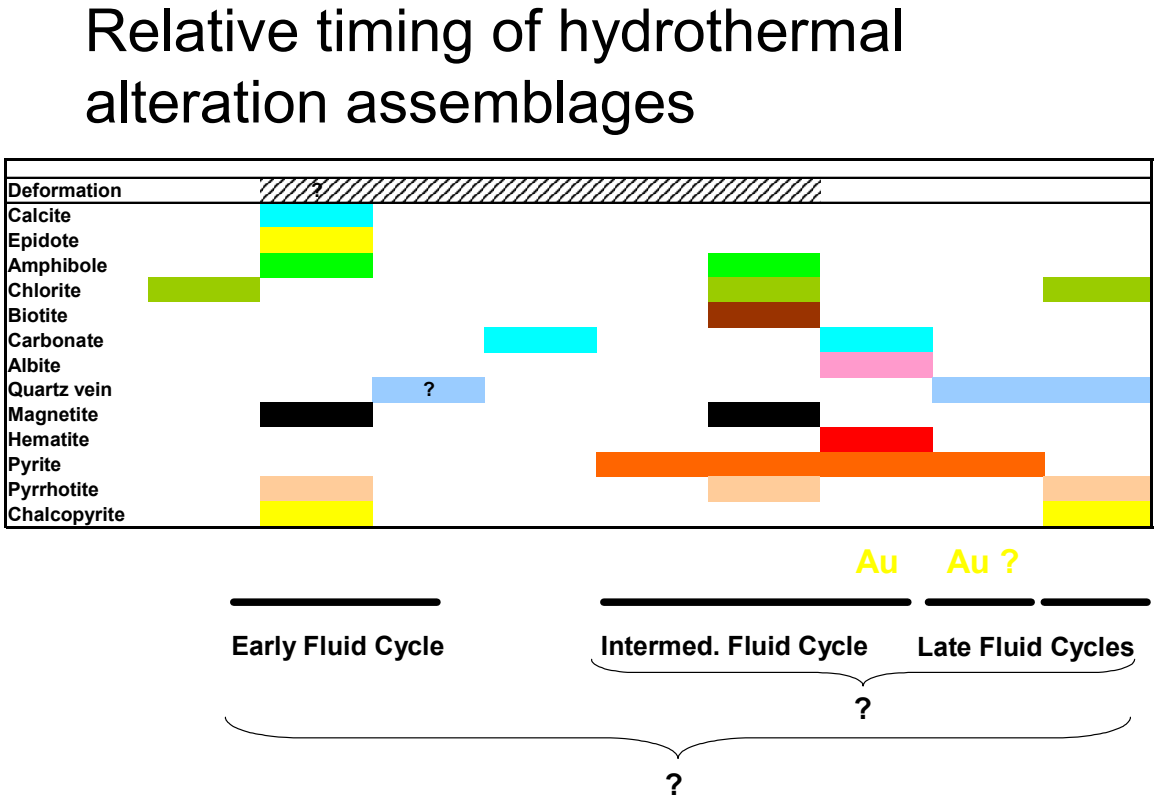

Fig. 16: Paragentic evolution diagram for hydrothermal alteration in the St. Ives gold camp. Note that three different fluid cycles are distinguished. At present, Au mineralization is confirmed for the intermediate fluid cycle with visible gold inclusions in pyrite. It is unclear whether the late fluid cycle also contains gold mineralization. This question is currently being tested with microanalysis.

Camp-Scale Alteration Zonation

The distribution of gold-associated sulphide and oxide minerals indicate a zonation with respect to ore-fluid chemistry within the St. Ives gold camp. Oxide and sulphide assemblages are correlated to reduced and oxidized conditions using fO_2-a$\sum$S diagrams at 400º C and 2 kbars. Deposits in the southwest of the camp, such as Argo and Junction, contain arsenopyrite-pyrrhotite and pyrrhotite-pyrite assemblages, respectively. These assemblages indicate dominant relatively reduced hydrothermal fluids. The deposits in the Central Corridor of the St. Ives gold camp are characterized by pyrite-magnetite and pyrite-hematite assemblages that indicate dominant relatively oxidized hydrothermal fluids.

In the Central Corridor, two main domains with respect to the redox conditions of the hydrothermal alteration are distinguished during the intermediate fluid cycle (Fig. 17, Neumayr et al., 2003): (1) oxidized (pyrite-magnetite, pyrite-hematite assemblages) centered around gravity lows in the Victory-Defiance and Revenge areas, and (2) reduced (pyrrhotite-pyrite, pyrrhotite assemblages) broadly flanking the oxidized domains. A similar pattern emerges also for the early alteration cycle with epidote-pyrite-chalcopyrite-magnetite (oxidized?) assemblages focused into the core of the Central Corridor and epidote-pyrrhotite-chalcopyrite-magnetite (reduced?) assemblages flanking the Central Corridor

(Fig. 18). However, drill information for distal (to Central Corridor) assemblages during the early alteration cycle is too sparse to have enough confidence in the pattern. Therefore, the discussion focuses on the intermediate alteration cycle.

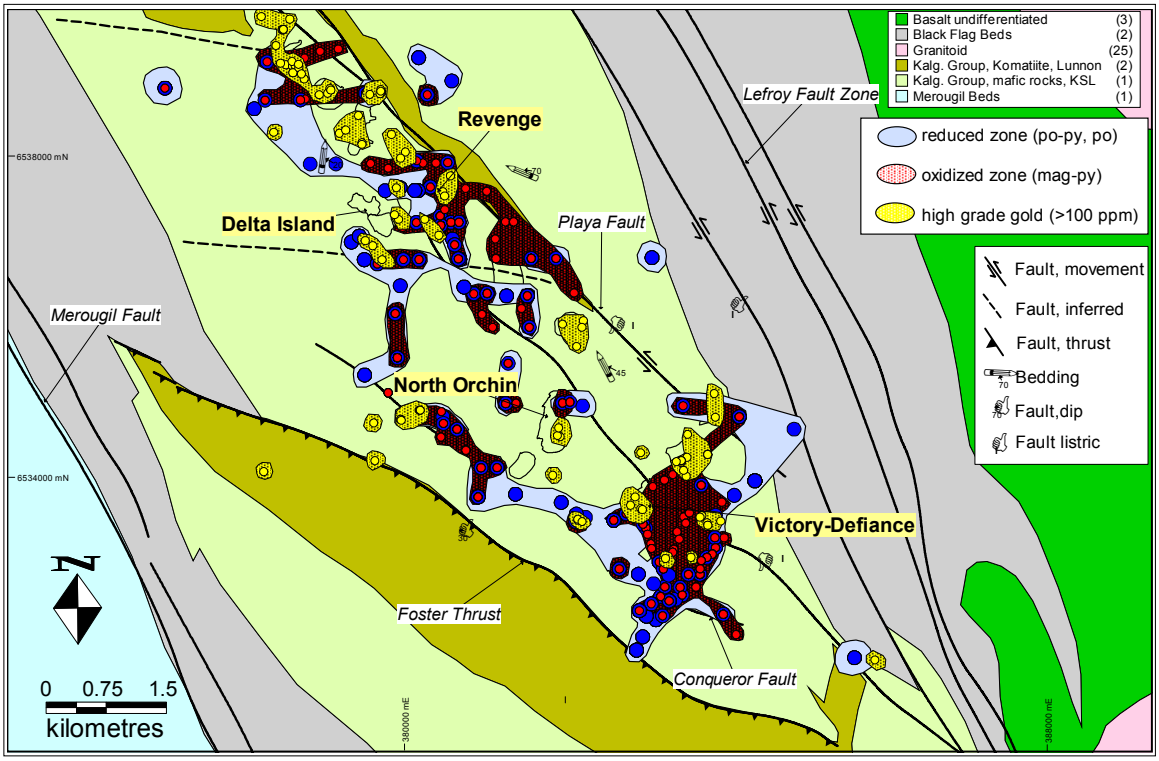

Fig. 17: Distribution of main sulphide/oxide mineral assemblages in mafic rocks in the Central Corridor of the St. Ives gold camp. High-grade (>100 ppm) gold intersections are located in zones where reduced and oxidized mineral assemblages overlap.

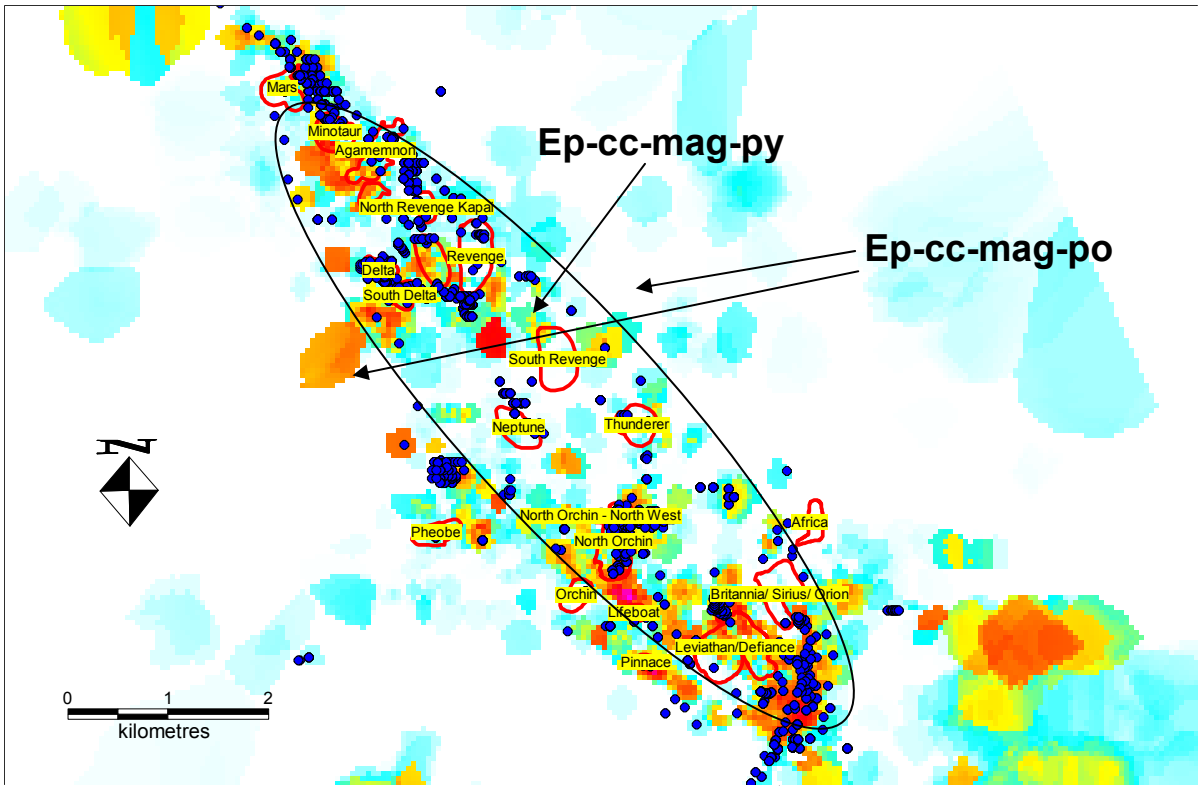

Fig. 18: The early fluid cycle is characterized by bands of epidote-calcite-magnetite-pyrite which replaced alteration/metamorphic amphibole adjacent to intermediate porphyry intrusions in the Central Corridor. The bands of epidote are overprinted by calcite-quartz magnetite veins and quartz-calcite veins. This alteration type is not associated with gold mineralization, but shows a distinct Te and Bi enrichment in whole-rock geochemical analyses indicating the presence of Bi-tellurides. Importantly, it appears that there is a spatial link to zones which contain subsequent gold mineralization. However, gold-associated hydrothermal alteration clearly overprints the epidote-bearing assemblage. The epidote-calcite-magnetite-pyrite assemblage is focused into the central parts at a camp scale proximal to the most abundant porphyry intrusions, whereas in distal parts the assemblage consists of epidote-calcite-magnetite-pyrrhotite (the yellow field indicates approximately the distribution of the epidote-calcite-magnetite-pyrite assemblage and the arrows indicate where the epidote-calcite-magnetite-pyrrhotite assemblage was confirmed in diamond drill core).

Domain mapping (using mainly mafic and metasedimentary rocks) for the intermediate alteration cycle indicates a distinct distribution pattern (Fig. 17). Oxidized assemblages are focused around the Victory-Defiance deposits (Victory-Defiance, Britannia, Sirius, Orchin, and North Orchin) and to the southeast of, and intermittent within, the Greater Revenge area. Further, oxidized domains with magnetite-pyrite assemblages are aligned along some major structures, such as the NW-trending, NE-dipping Playa fault. The oxidized domain around the Victory-Defiance deposits is focused on a distinct low in the detailed gravity data (Fig. 19) which extends for several kilometers and is interpreted to represent abundant magmatic intrusions at a depth of about 500-1000 m below present surface. Based on the spatial association of oxidized domains (magnetite and magnetite-pyrite) and the centre of porphyry intrusions, a genetic link has been inferred.

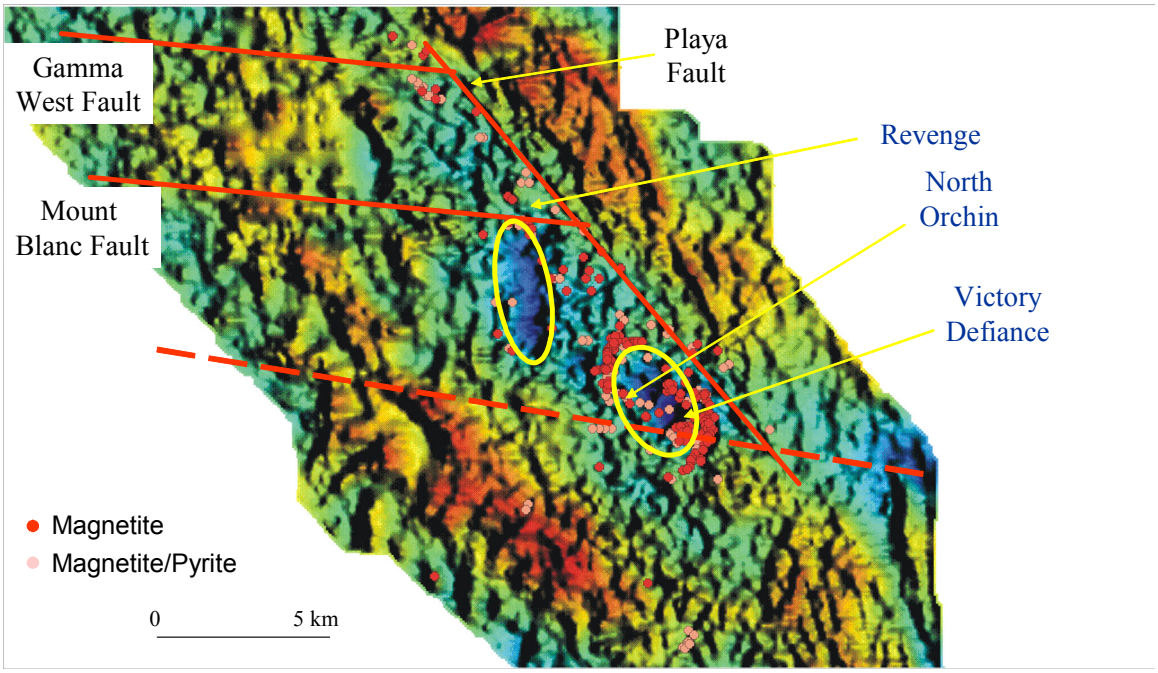

Detailed gravity data: SIG

Camp-scale redox variations

Fig. 19: Detailed gravity image of the Central Corridor of the St. Ives gold camp. Two distinct gravity lows occur in the Victory-Defiance area and SW of the Revenge gold deposits. The gravity lows are interpreted to reflect abundant porphyry intrusions at depths of 500-1000m below present surface. In the Victory area, abundant porphyry stocks are confirmed by seismic images and diamond drill core information. Magnetite alteration in interflow sedimentary rocks is focussed at the gravity lows in the Victory area.

Domains with reduced alteration assemblages (pyrrhotite-pyrite) flank those with oxidized assemblages to the NE and SW of the Victory-Defiance and Greater Revenge deposits and also occur intermittent between oxidized domains in the Greater Revenge deposits. Due to sparse drilling information outside main mineralized zones, it is difficult to confirm the structural conduits for reduced fluids. However, to the SW of Conqueror, reduced assemblages are clearly focused in shallowly SW-dipping faults. Reduced assemblages cluster in particular in a broad band to the S of the Revenge deposits. This band coincides with interpreted early, E-W trending faults. However, as only limited drilling intersects these faults, it is unknown at present whether these faults had a control on the distribution of reduced assemblages.

Further support for reduced and oxidized domains within the St. Ives camp is provided by the distribution of stable isotopes, in particular S isotopes. The $\delta^{34}S$ isotope data range from -7.9 ‰ to 2 ‰ in the Victory-Defiance area (Fig. 20). Extremely negative numbers are focused to the centre of the oxidized domain, whereas the switch to positive numbers occurs along the domain boundary. The extremely negative $\delta^{34}S$ numbers are interpreted to result from oxidation induced by the influx of oxidized fluids. The general background $\delta^{34}S$ value is around 0 ‰ to 3 ‰ (see earlier section on fluids in the system-Q3).

S – isotope zonation

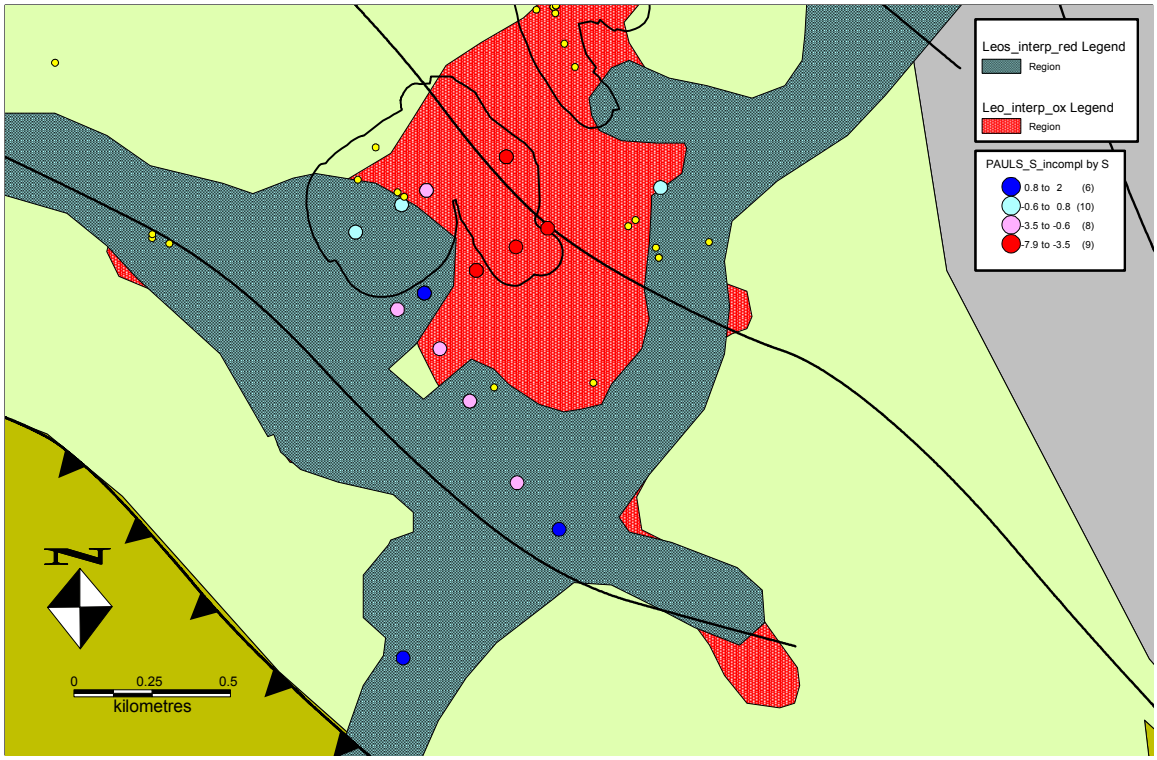

Fig. 20: Map of the Victory-Defiance deposits and surrounds showing the distribution of oxidized and reduced domains based on sulphide-oxide mineral mapping. The $\delta^{34}S$ values are shown in coloured dots. Note that negative sulphur isotope values are mostly restricted to oxidized domains and positive sulphur isotope values are located in the reduced domain.

Deposit-Scale Alteration Zonation

At a deposit- to ore shoot-scale, gold related alteration is zoned (intermediate alteration cycle) from distal chlorite-carbonate to intermediate biotite-carbonate to proximal albite-carbonate-pyrite-gold. Importantly, hydrothermal magnetite halos rim the proximal alteration assemblage (Fig. 21) and typically occur in the distal and intermediate zones.

Mineral textures indicate that magnetite pre-dates gold-related pyrite, but also forms during the early stages of pyrite growth as indicated by magnetite inclusions in the core of ore-stage pyrite (Fig. 22). Rims of the ore-stage pyrite contain only hematite inclusions, and magnetite in the core of the pyrite locally contains thin rims of hematite. This is interpreted to reflect an increase in the redox state of the hydrothermal fluid during gold precipitation.

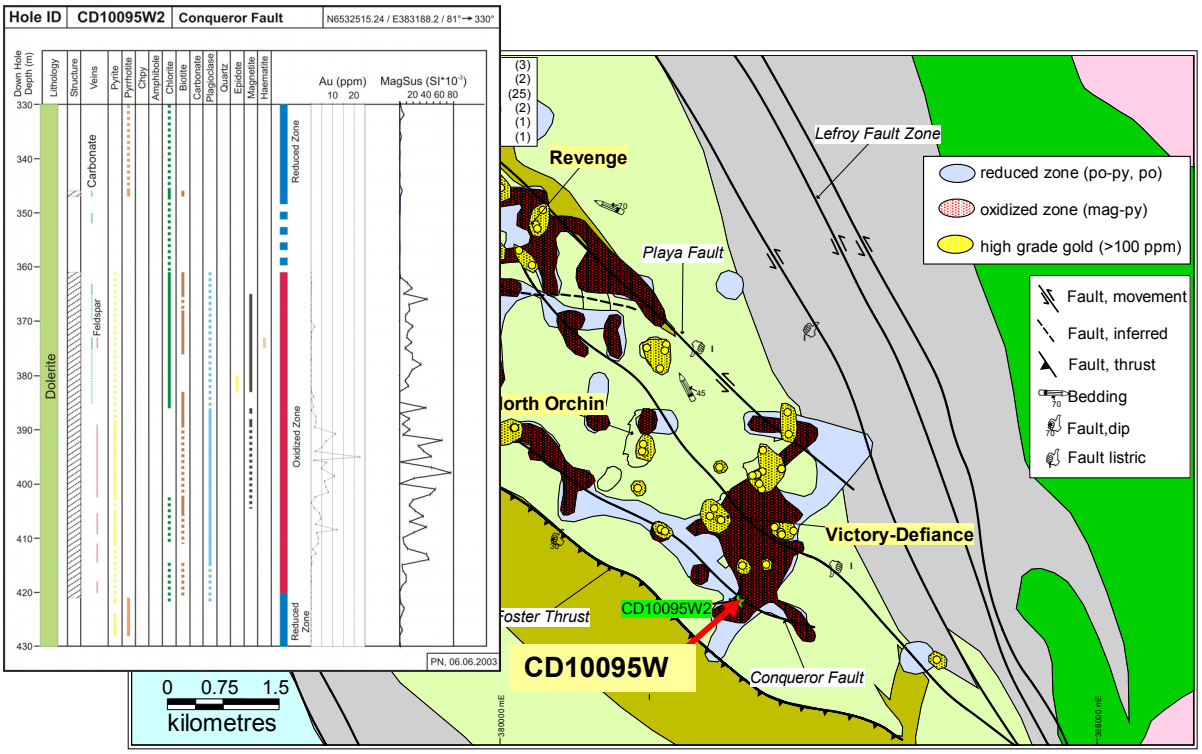

Fig. 21: Graphical log of diamond drill core CD10095W2 which intersects the Conqueror Fault in the Central Corridor of the St. Ives gold camp. The diamond drill core is sited at the camp-scale boundary between oxidized and reduced domains. Note that gold mineralization is enveloped by a halo of hydrothermal magnetite. Reduced mineral assemblages (pyrrhotite-pyrite) occur distal to the gold lode, the oxidized magnetite-pyrite assemblage and the shear zone hosting gold mineralization. This indicates that the domain boundary between oxidized and reduced zones is quite complex in detail, possibly with oxidized fluids travelling along structures into the camp scale reduced domain. This relationship is further confirmed by textures depicted in subsequent figures. Gold mineralization is hosted in the centre of the oxidized magnetite-pyrite domain in this diamond drill core.

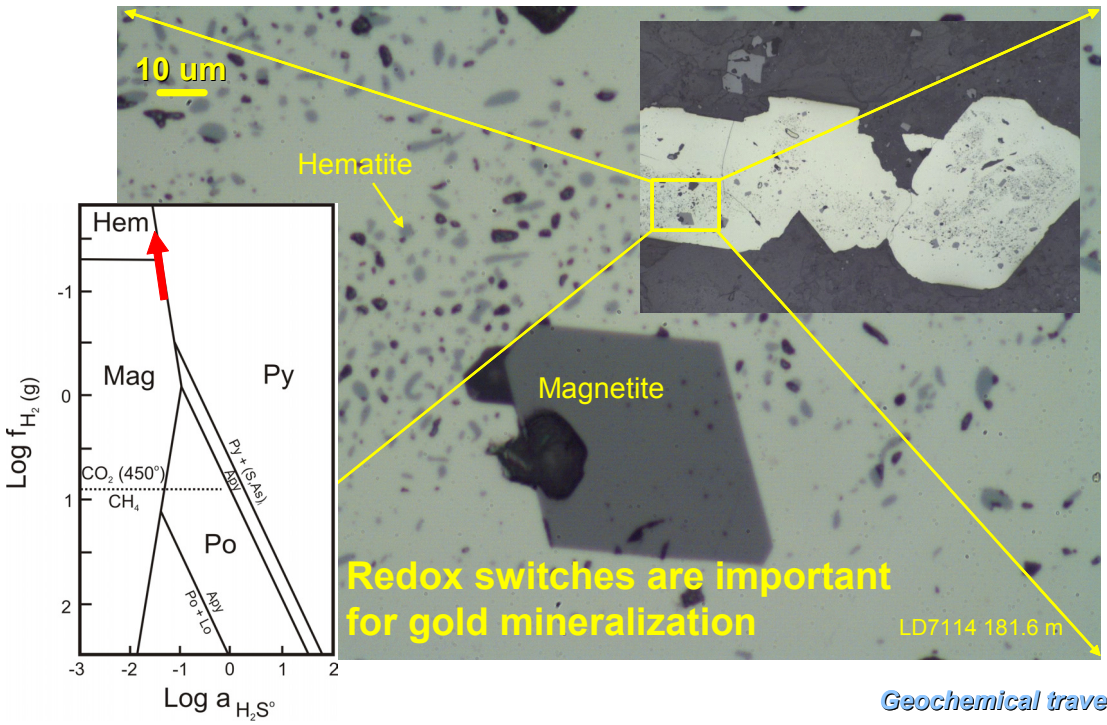

Fig. 22: Photomicrograph of ore-stage pyrite at Revenge showing magnetite inclusions in the core of the pyrite and hematite inclusions in the rim of the pyrite. This indicates a redox switch during the growth of the pyrite grain.

Important clues for the architecture of reduced and oxidized fluid conduits are derived from the Conqueror area (Figs. 23 through 26). Here, following the camp-scale boundary between the pyrrhotite±pyrite and magnetite-pyrite domains, magnetite-pyrite formed proximal to gold mineralization within a steeply-dipping foliation. Pyrrhotite±pyrite occurs in a shallowly SW dipping deformation zone (e.g., diamond drill core CD10632), and pyrite is only locally present. Where minor pyrite occurs, gold grades are just above background (less than 1 g/t and greater than 0.1 g/t). Drill core about 100 m into the magnetite-pyrite zone (e.g., diamond drill core CD10628) shows the development of both alteration styles (reduced pyrrhotite±pyrite and more oxidized magnetite-pyrite). The reduced alteration occurs in a shallowly dipping fabric, whereas the oxidized assemblage is restricted to a steeply dipping fabric. High gold grades (>10 g/t) occur where both fabrics are developed and form S-C fabrics. It is interpreted that reduced fluids migrated along shallowly dipping deformation zones in the Conqueror area, whereas oxidized fluids used steeply dipping fluid conduits. The intersection of the two structures appears to have resulted in high-grade gold mineralization. These observations are based on diamond drill core observations only and are currently being tested through examination of underground exposures.

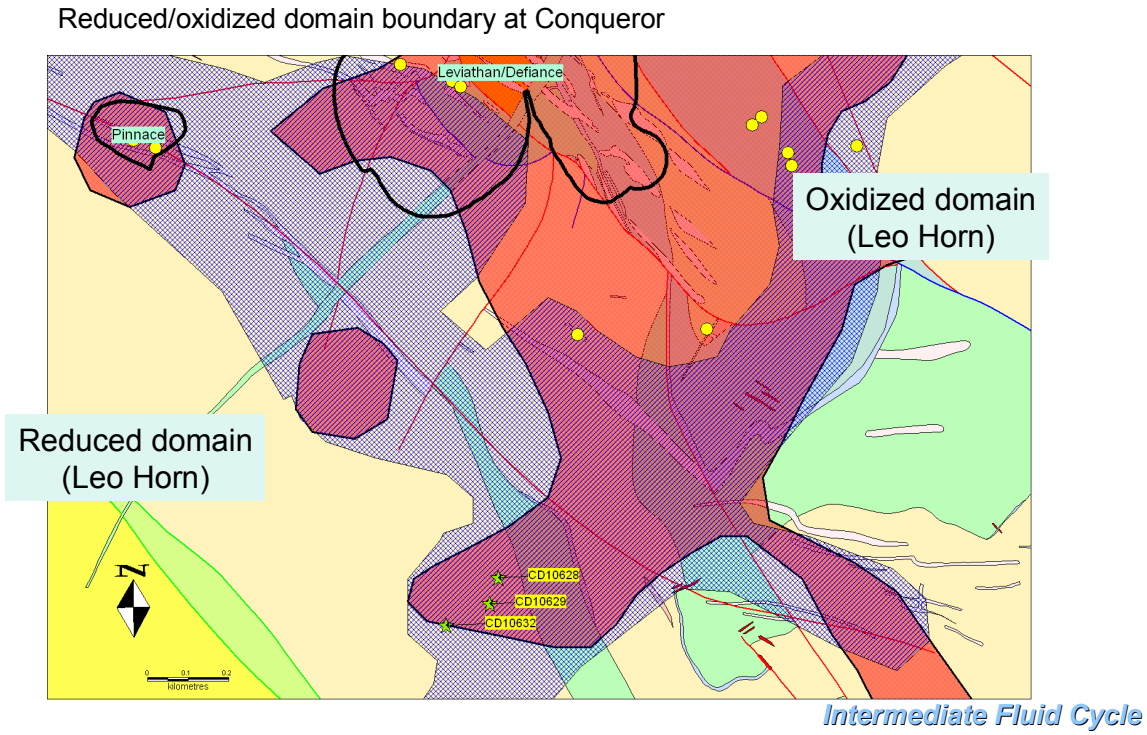

Fig. 23: Location of diamond drill corse CD10628, CD10629 and CD10632 with respect to oxidized and reduced fluid domains at Conqueror as determined by Leo Horn using redox alteration mapping of historic drill core data.

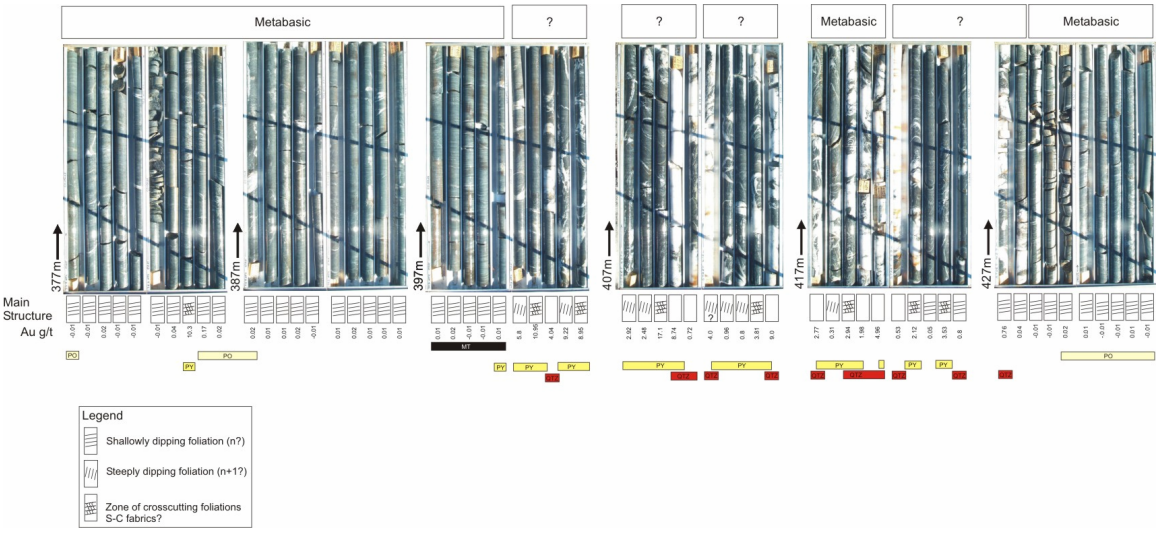

Fig. 24: Photographs of diamond drill core CD10628 annotated with gold grades. Note that the shallow dipping foliation contains pyrrhotite alteration (reduced fluid), but is barren of gold. The steep foliation hosts fine-grained pyrite, but hosts only subgrades of gold. Sections with both foliations and locally developed S-C fabrics contain abundant pyrite and high gold grades. Zones with abundant quartz veins have lower gold grades than foliated wallrock zones.

Handsample CD10628

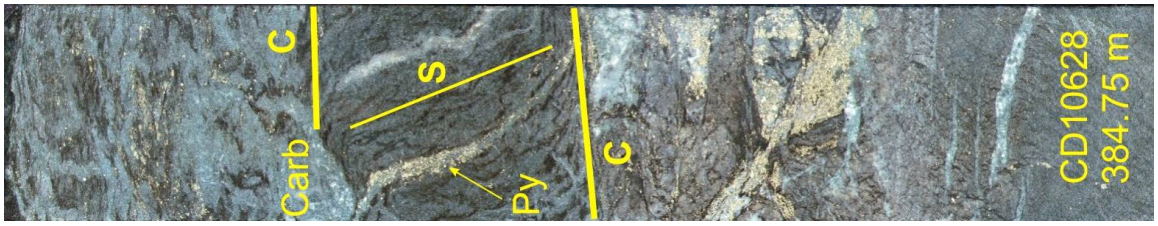

Fig. 25: Handsample of diamond drill core CD10628 at 384.75 m. Note that there are two foliations are developed: a steep (subparallel to subvertical drill core) and a shallowly dipping foliation which show typical S-C fabrics. Pyrite is focused into the steep structure, but occurs locally also in the shallow foliation. The one meter composite assay that included this sample analyzed 10.3 g/t gold. This sample is the only pyrite-bearing sample within the metre and the only part of the core which shows two foliations. Adjacent zones are barren.

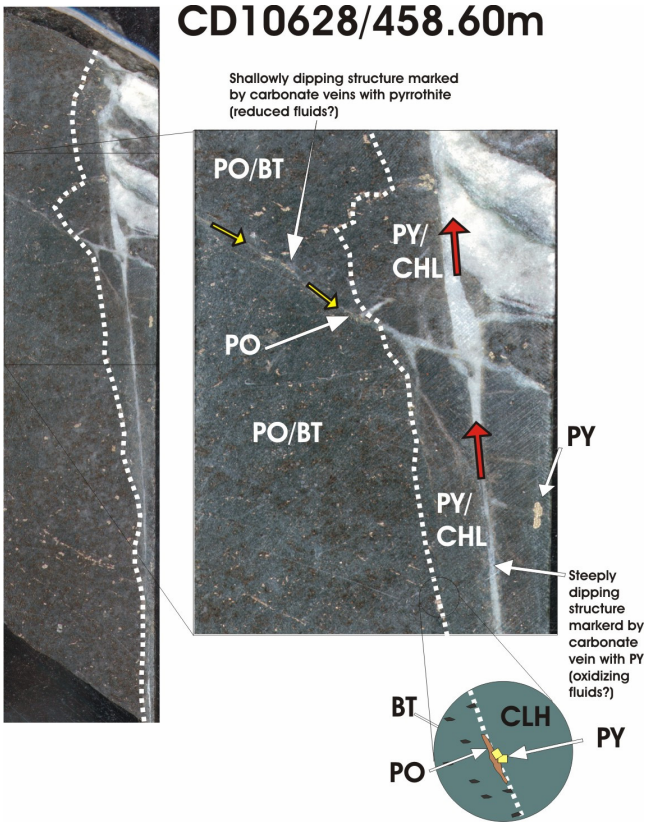

Fig. 26: Handsample of diamond drill core CD10628 at 458.60 m showing the intersection of steep fractures and shallow fractures. The two fracture sets have different hydrothermal alteration. The shallow set contains pyrrhotite and locally chorite and is cross cut by the steep set which contains abundant pyrite at points of intersection with the shallow fracture set.

Location of Gold Mineralization

At a camp scale, high-grade (>100 g/t) gold intersections and gold lodes occur close to the boundary between oxidized and reduced mineralogical and S-isotope domains (Figs 17, 20, 27). This relationship is particularly well developed in the Victory-Defiance area. The high-grade intersections are typically located within 200m of the domain boundary in the oxidized domain. Given the uncertainty in the 3D construction of both the structural and alteration architecture, a much closer spaced drilling grid or detailed underground exposure is needed to better constrain the location of gold mineralization with respect to the domain boundary. Importantly, 3D reconstructions of economic gold mineralization demonstrate that the bulk of gold mineralization is located at the boundary between reduced and oxidized domains, indicating that both high grade mineralization and bulk tonnage are spatially controlled by the switch from oxidized to reduced alteration domains.

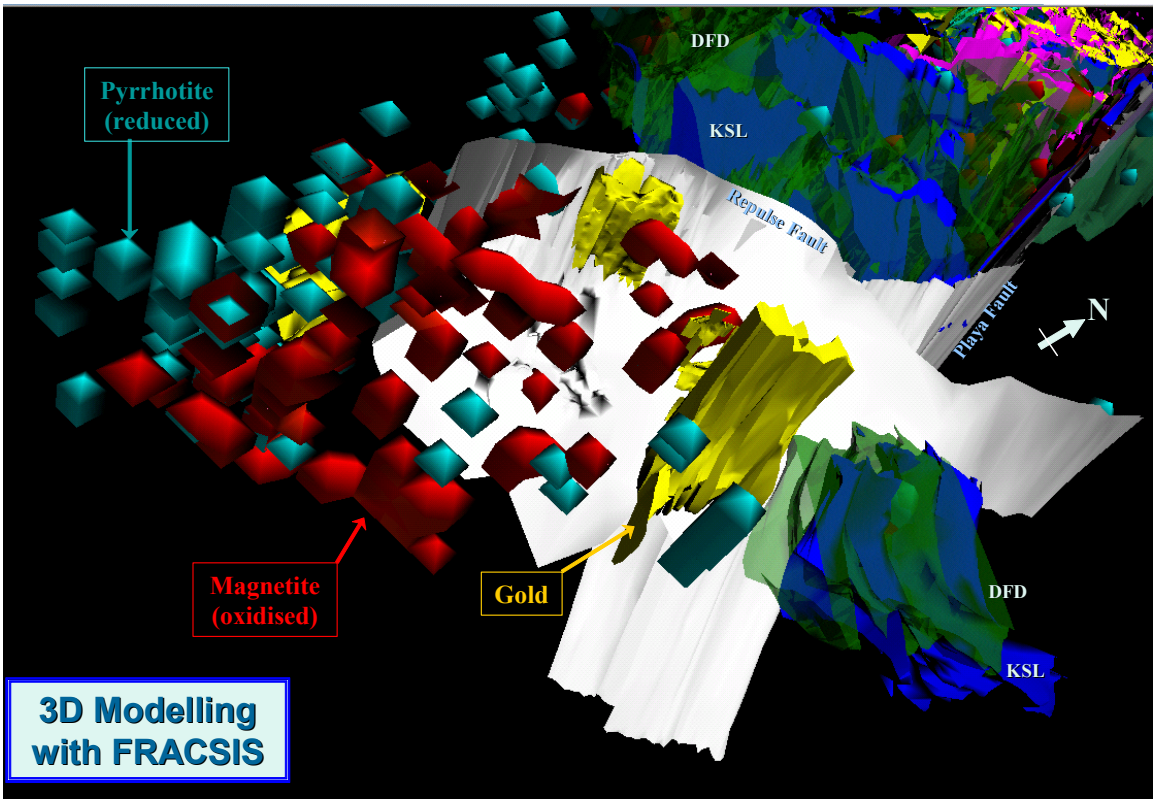

Fig. 27: Screenshot of 3D model of the geology of the Victory-Defiance area in the St. Ives cold camp (view to NW). The 3D modeling was made possible by translating downhole alteration data (pyrrhotite = blue; magnetite = red) into XYZ points using the survey data. A 20m iso-surface was constructed around each point to increase visibility and wire-frames for faults and orebodies were added. The 3D model for the Kapai slate (KSL) and Defiance dolerite (DFD) were also added to show the Kambalda antiform. The model shows that magnetite (oxidized assemblage) is focused in the Victory-Defiance area while pyrrhotite (reduced assemblage) flanks the oxidized domain. Gold orebodies occur preferentially at the interface between oxidized and reduced domains.

Golden Mile

Surface and underground mapping combined with geochemistry and compilation of previous work has led to an improved understanding of the structural framework of the Golden Mile deposit. The relative timing of multiple hydrothermal events, including the Fimiston gold and telluride mineralization event, is constrained relative to deformation events and the intrusion of multiple sets of dykes.

Abrupt changes in thickness, composition and in the internal magmatic layering of the Golden Mile Dolerite and Paringa Basalt indicate the presence of early syn-volcanic faults, which have an important control on the architecture of the Golden Mile. The upright Kalgoorlie anticlinal axis overprints a major synvolcanic growth fault, which forms the original eastern margin of the Golden Mile Dolerite.

Geochemistry confirms the equivalence of the Golden Mile and Aberdare dolerites across the late stage Adelaide Fault, and establishes the regional continuity of the NNW trending, upright, and shallow south plunging Kalgoorlie syncline-anticline pair, which dominates the structural architecture of the Golden Mile (Fig. 28). The Lake View South syncline, occurring in the southern part of the Golden Mile and in continuity with the Kalgoorlie anticline, is truncated by the Golden Mile Fault (GMF) indicating that the initiation of the GMF postdates the development of the Kalgoorlie syncline-anticline pair. The presence of the Lake View South syncline east of the GMF does not support the interpretation of the GMF as a thrust and the Kalgoorlie anticline as an overturned hangingwall anticline. A regionally extensive steeply west dipping NNW foliation overprints the Kalgoorlie syncline-anticline pair. This fabric is axial planar to the Boomerang anticline which folds the GMF and Kalgoorlie syncline-anticline pair.

A swarm of feldspar porphyry dykes transects both limbs of the Kalgoorlie fold pair and is in turn overprinted by the regional NNW trending foliation. The feldspar porphyry dykes are also overprinted by Fimiston style gold mineralization consisting of narrow, vertically and laterally extensive lodes (>1200m vertical and >1000m along strike) of carbonate-quartz-pyrite breccias, quartz veins and carbonate-quartz-pyrite disseminations. The feldspar porphyry dykes and the Fimiston lodes are spatially associated and share common orientations (Main N140°/80°W, Caunter N115°/65°W and Cross Lode N050°/85° N-S). Hornblende porphyry dykes, also sharing the same orientations, cross cut the feldspar porphyry dykes and the Fimiston lodes and are also overprinted by the regional NNW trending foliation. This NW regional foliation is preferentially developed within weak layers such as mudstone beds and strongly sericite-rich Fimiston lode selvedges. The constant orientation of the NW-trending foliation in lode selvedges across a wide range of lode orientations, including the NE-trending Cross Lodes and the shallow-dipping Caunter lodes, provides clear evidence that the foliation overprints the lode selvedges rather than being related to shearing synchronous with lode formation. The NW regional foliation is associated with localised small-scale folds and faulting of Fimiston veins, which is consistent with NE-SW shortening.

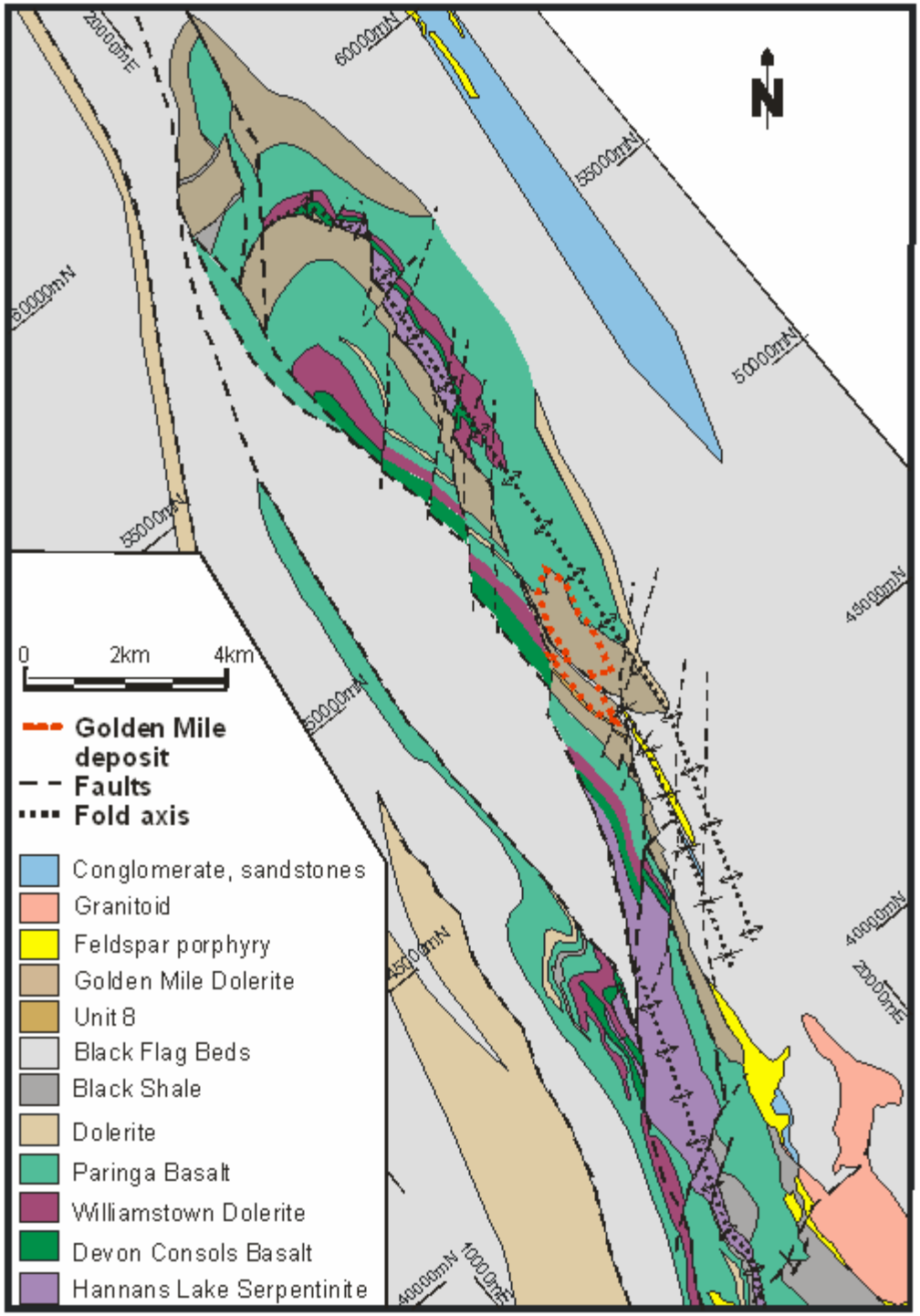

Fig. 28: Geological and structural map of the Golden Mile.

Some steeply E-dipping NNW-trending faults occurring in the footwall of the GMF display pre-lode reverse slip and post-lode dextral slip as indicated by the larger offset on the stratigraphy than on the Fimiston lodes. In addition, some feldspar porphyry dykes are emplaced within these faults. A conjugate network of shallow dipping, reverse faults, generally post-dates these steep faults. Quartz-carbonate veins and breccias are locally

associated with the late steeply dipping and shallow dipping fault sets. Where these veins cut the Fimiston lodes, they contain fragments of Fimiston lodes showing random orientation of the foliation in alteration selvedges. This indicates that these veins and some of the shallow dipping reverse faults and steeply E-dipping reverse-dextral faults postdate the regional NNW-trending foliation.

This study establishes the Fimiston stage gold mineralization as an upright array of narrow lodes that funnel upwards within the Golden Mile Dolerite and overprint both limbs of the early upright Kalgoorlie fold pair. The lodes are in turn, transected by hornblende porphyry dykes, overprinted by the regional trending NNW steeply dipping regional foliation, and dissected by steep reverse and dextral faults. Mt Charlotte-type coarse-grained quartz-carbonate and scheelite veins cross cut Fimiston lodes and are associated with a late set of fractures post dating the regional NW trending foliation.

New Celebration

Four deformation events are recorded at the New Celebration deposits. (1) D_{2NC} is represented by vertical stratigraphic contacts and the expression of upright folds formed on a regional scale in the New Celebration area. (2) D_{3NC} deformation is expressed as a well-developed NNW-trending, steeply WSW-dipping penetrative shear foliation (S_{3NC}), which is representative of the regional D_3 Boulder fault zone. Lineations formed during D_{3NC} deformation include: (a) moderate to steep, SSE- to SSW-plunging L_{3mNC} mineral elongation lineations, (b) moderate NW-plunging L_{3iNC} intersection lineations between S- and C-foliation planes, and (c) moderate to steep, SSE- to SSW-plunging L_{3sNC} slickenline lineations. Moderate to steep SSW-plunging quartz L_{3mNC} elongation lineations, in conjunction with the orientation of S-C fabrics, constrain the sense of movement on the shear zone as sinistral oblique-slip, west-block-down to the SSE. The S_{3NC} foliation is also developed in thin (1 to 5m width) M_1 plagioclase-rich porphyry dykes thus indicating their formation pre- to syn-D_{3NC} deformation. The M_1 porphyry dykes are subsequently overprinted by the intrusion of second generation M_2 quartz-feldspar porphyry dykes, preferentially along the mafic-ultramafic rock contact. The lack of internal ductile deformation fabrics and a predominance of brittle structures (e.g., fractures) in M_2 porphyry dykes indicate their emplacement into a brittle deformation environment. (3) D_{4NC} deformation resulted in NNE-trending, WNW-dipping faults, quartz-carbonate vein sets and widely-spaced S_{4NC} foliation. Sub-horizontal L_{4sNC} slickenline lineations on D_{4NC} faults planes indicate strike-slip movement during D_{4NC} (no kinematic indicators observed). (4) D_{4+nNC} deformation is represented by W-dipping curviplanar faults. Based on the markedly different orientations of D_{4+nNC} faults to D_{4NC} structures, curviplanar faults are interpreted to represent post-D_{4NC} deformation, although no cross cutting relationships are observed with D_{4NC} structures.

Two gold events are recognised at the New Celebration deposits. A paragenetically early gold event hosted in porphyry dykes (quartz-biotite-sericite-ankerite schists) is interpreted to be synchronous with the D_{3NC} deformation. Pyrite aligned parallel to the S_{3NC} foliation planes contains minute inclusions of gold (<100 microns). Gold occurs in equilibrium with sericite-ankerite-biotite and is also associated with telluride minerals such as calerverite ($AuTe_2$), petzite (Ag_3AuTe_2), hessite (Ag_2Te), altaite (PbTe), melonite ($NiTe_2$) and a bismuth telluride. A paragenetically late gold event hosted within brittle fracture networks

formed at the margins of the M_2 quartz-feldspar porphyry and adjacent high-magnesium basalt is interpreted to be synchronous to the D_{4NC} deformation event. In M_2 porphyry dykes free gold and inclusions of gold in pyrite occur in equilibrium with sericite-ankerite-quartz+chlorite, whereas gold hosted in the high-magnesium basalt occurs in equilibrium with ankerite-sericite-quartz. No telluride species are observed associated with this gold mineralization event.

The structurally controlled New Celebration gold deposits provide evidence for two stages of gold mineralization during D_{3NC} and D_{4NC} deformation events. Early gold mineralization, emplaced in a ductile environment, was controlled by strain heterogeneity between M_1 porphyry dykes and D_3 ductile shear zones. Late gold mineralization, formed in a brittle environment, was controlled by the M_2 porphyry dykes and their contact with mafic and ultramafic rocks. Although geochronological data is presently not available, the contrast between ductile and brittle ore textures may suggest substantial uplift between the two gold stages. Significant amounts of telluride minerals in equilibrium with gold in the Early gold event may point to a component of magmatic hydrothermal fluids circulating through the D_{3NC} shear zones.

Kanowna Belle

Camp-Scale Architecture

Kanowna Belle is located in the Boorara Domain subdivision of the Kalgoorlie Terrane, Eastern Goldfields Province, Western Australia. Mineralization is hosted in a sequence of conglomeratic and felsic volcaniclastic rocks (2668 Ma), which have been intruded by a porphyritic granodiorite (Kanowna Belle Porphyry; 2655 Ma) and minor felsic intrusives (Fig. 29). An intense zone of structural disruption divides the deposit into hangingwall and footwall structural domains and has a close spatial association with mineralization (Figs. 29 & 30).

Initial deformation that controlled deposit architecture occurred in response to northerly directed thrusting during N-S shortening. This produced a mylonitic fabric (Fitzroy mylonite), variation in the strike of lithology in the footwall and hangingwall, and was instrumental for localising subsequent emplacement of the tabular Kanowna Belle Porphyry. A short tectonic hiatus is inferred during emplacement of the Kanowna Belle Porphyry, followed by resumption of N-S shortening, resulting in the formation of an extensive zone of brittle-ductile deformation characterized by fault splays that bound zones of intense foliation, all of which have accommodated steeply-directed reverse movement. This zone is termed the Fitzroy Shear Zone. Formation of the Fitzroy mylonite and Fitzroy Shear Zone are interpreted to have occurred during regional D_1.

A switch in far-field stress axes to an approximate ENE-WSW orientation caused sinistral reactivation of the Fitzroy Shear Zone. This imparted sigmoidal geometries to pre-existing Fitzroy Shear Zone structures and produced a shallow lineation on pre-existing structures in response to subhorizontally directed shearing. Emplacement of mineralization is interpreted to have been contemporaneous with sinistral reactivation of the Fitzroy Shear Zone (~2650 Ma). Gold mineralization is hosted by carbonate breccias, carbonate vein stockworks, quartz-carbonate veins, siliceous breccias, sulphide-quartz-carbonate veinlets (stringers), and sheeted vein arrays. A synchronously developed steep NW-SE trending foliation has locally

controlled emplacement of mineralization. Fitzroy Shear Zone reactivation, cleavage formation and emplacement of mineralization are all interpreted to have occurred synchronous with the regional D_2 deformation event.

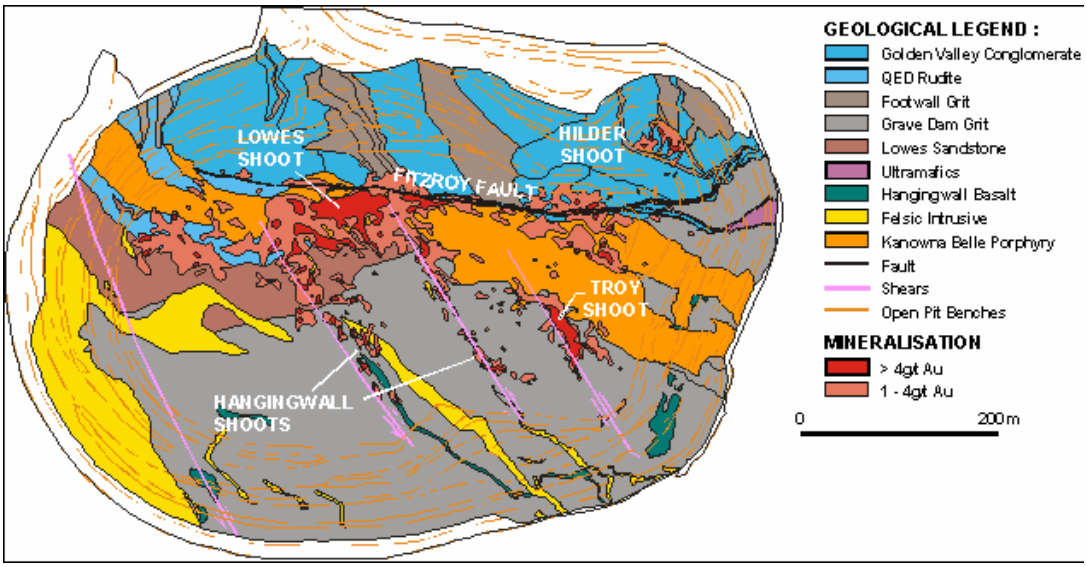

Fig. 29: Geology of the Kanowna Belle open pit (map is orientated in KB mine grid; mine grid north=330° true north).

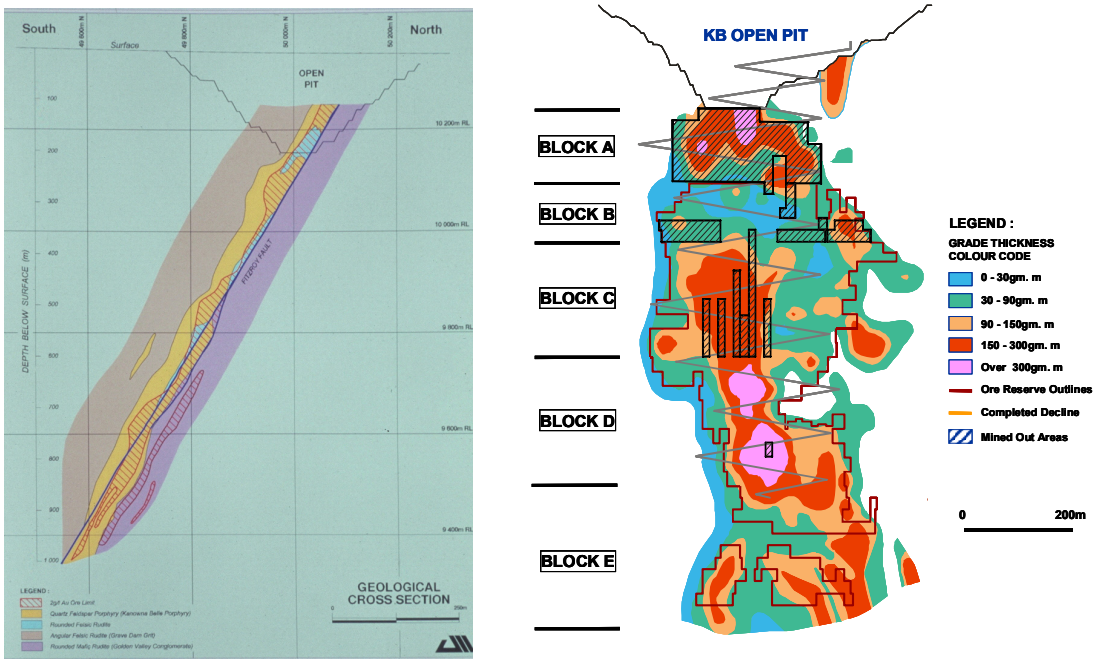

Fig. 30: Kanowna Belle NW-SE cross section (looking west) and long section (looking NW in the plane of the Fitzroy Shear Zone).

Lithological Architecture: Geochemical Definition of Kanowna Belle Lithologies

A number of geochemical discriminate plots (Figs. 31 through 39) are proving useful in defining lithologies in the Kanowna Belle district, understanding the evolution of the porphyries, and providing the background lithological constraints for alteration studies.

As shown in Figs. 31 and 32, Sc is as useful proxy for Fe so that Sc versus Th and Sc versus Ce plots discriminate the mafic and felsic lithologies.

The Kanowna Belle porphyries show variable degrees of enrichment in light rare earth elements (LREEs) – up to 100 -110 ppm Ce (Fig. 33) and are also in enriched in Th up to 8-10 ppm. Higher scattered values on the discriminate plots may reflect mobility of these elements during hydrothermal alteration.

The point density contours of Figure 34 highlight a number of subgroups within the felsic porphyries, based on Sc, Ce and Th contents. The Kanowna Belle porphyries may also be subdivided into high and low P sub-groups (Fig. 35). The low-P subgroup is dominant. The high-P subgroup is enriched in Y, Yb, Zr, Hf, Ta, Nb, Ti and depleted in Th, relative to the low-P subgroup. The high-P subgroup correlates with the porphyries elevated in Sc (8- 10 ppm) relative to Ce and Th, depicted in Figure 34.

The importance of elevated levels of transition elements: V, Cr, Ni, Co, as well as Fe and Sc in the Kanowna Belle deposit and the low- and high-P porphyry subgroups have yet to be clarified.

Least altered samples of the high-P porphyry subgroup appear to have slightly elevated V, Cr, Ni and Co compared with least altered samples of the low-P porphyry subgroup. Porphyries enriched in first transition elements occur in the hangingwall of the Kanowna Belle porphyry and to the west of the Kanowna Belle deposit in the Velvet area, particularly along structural/lithological contacts. Similar element enrichments of the transition elements occur within the grits above the hangingwall contact of the Kanowna Belle porphyry in GDD 310. Extensive alteration also occurs in these locations.

In GDD535 in the Velvet area, a 175 metre interval of quartz porphyry is distinctly Cr and Ni enriched (100 to 200 ppm) compared with other porphyries in GDD535 (Figs. 36 & 37) and equivalent LREE enriched and/or high-P porphyries in the Kanowna Belle – Velvet area. More variable and higher Cr values in the quartz porphyry (200 to 300 ppm) are coincident with zones of alteration and mineralization as indicated by As, Au, S and V abundances (Fig. 38) and reflect at least local (within lithology) remobilization of the Cr. The linear covariance of Ce with P (Fig. 37) is suggestive of mobilization of LREEs at least locally also.

One of the difficulties in assessing the mobility of the first transition elements is that of defining the composition of the protoliths. The linear variation of V with Sc (Fig. 39) defines the lithological variation of V and provides a means of assessing the extent of V enrichment during alteration.

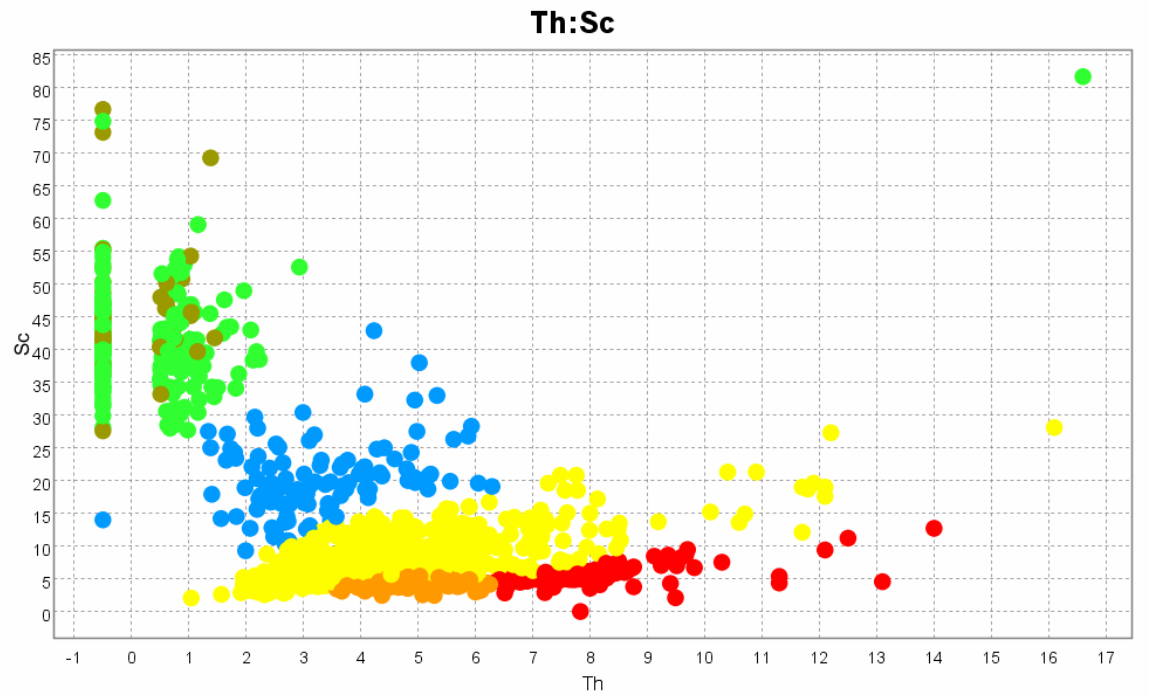

Fig. 31: Plot of Sc versus Th for the mafic and felsic rocks in the Kanowna Belle district. Sc correlates with Fe (mafic indicator) and Th with Si (felsic indicator) and the plot shows a good discrimination from basalts => conglomerates => grits and rudites => late porphyries. Sc and Th are two consistently immobile elements so the plot is useful for correlating between altered and unaltered rocks. (GAS plot by Scott Halley)

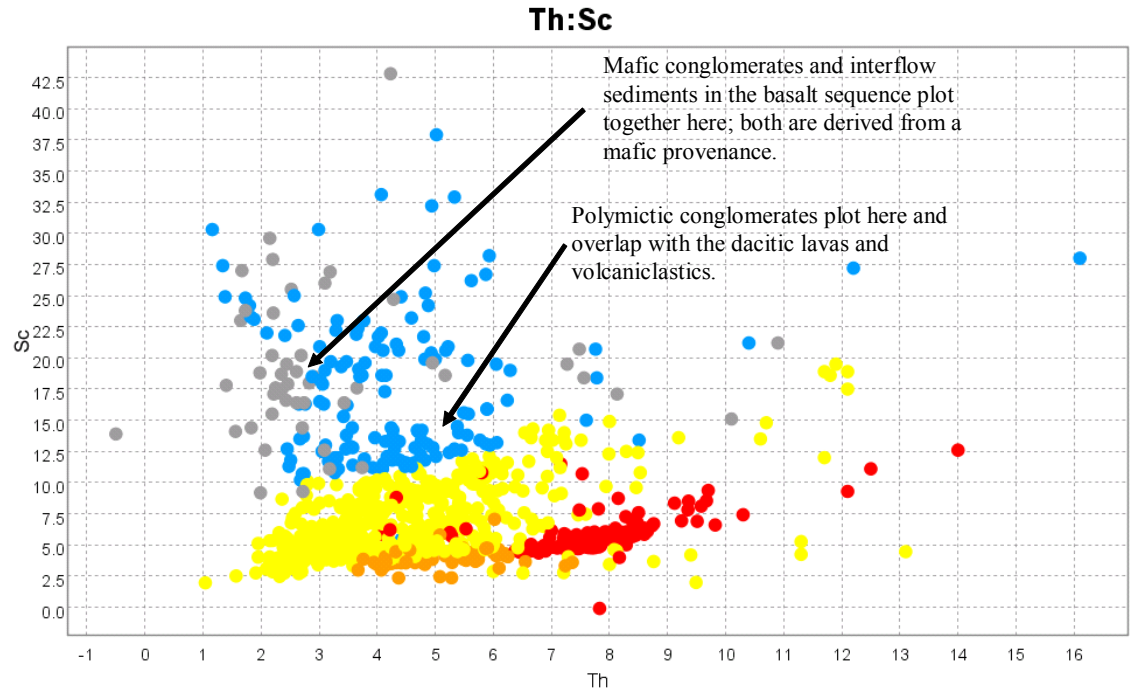

Fig. 32: Plot of Sc versus Th illustrating relationships between volcanic rocks and related sediments. Mafic conglomerates and interflow sediments in the basalt sequence plot together indicating both are derived from a mafic provenance. Polymictic conglomerates overlap with the dacitic lavas and volcaniclastics. (GAS plot by Scott Halley)

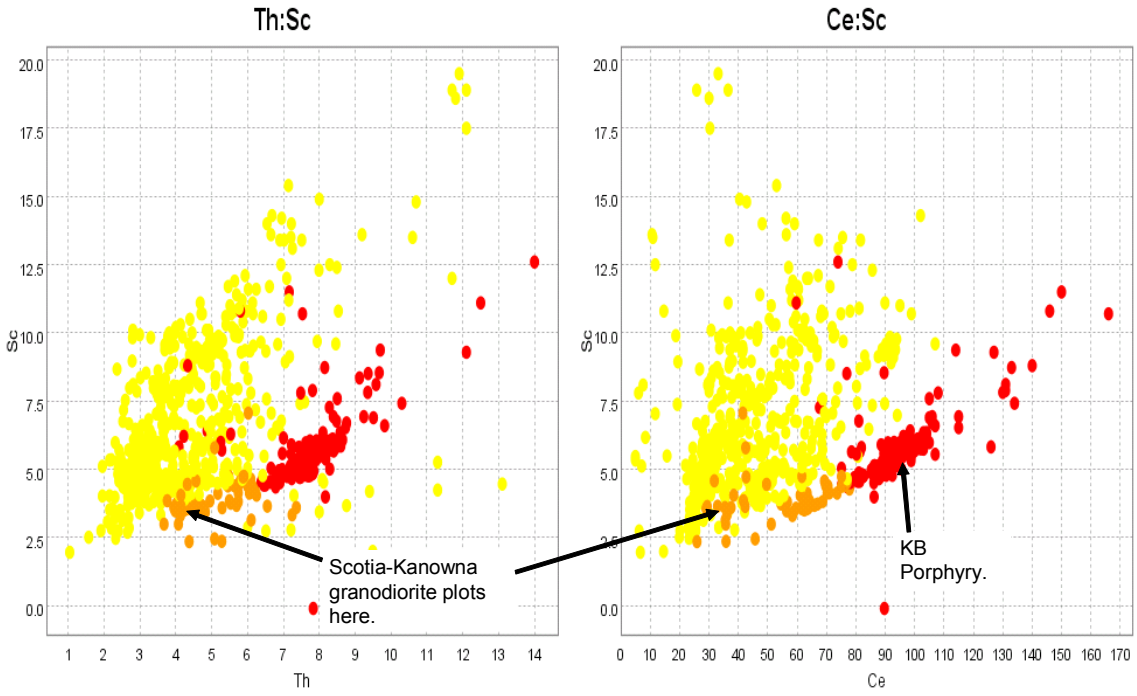

Fig. 33: Plots of Sc versus Th and Ce for the felsic rocks illustrating two distinctly different groups (red and orange clusters) of porphyries at Kanowna Belle. The porphyries that host Lowes Shoot mineralization are predominantly in the red group. The orange group is also part of this trend. Most of the points in red and orange groups are very tightly clustered on Sc:Th and Sc:Ce plots. Data from the Scotia-Kanowna pluton fall at the lower end of this trend. (GAS plot by Scott Halley)

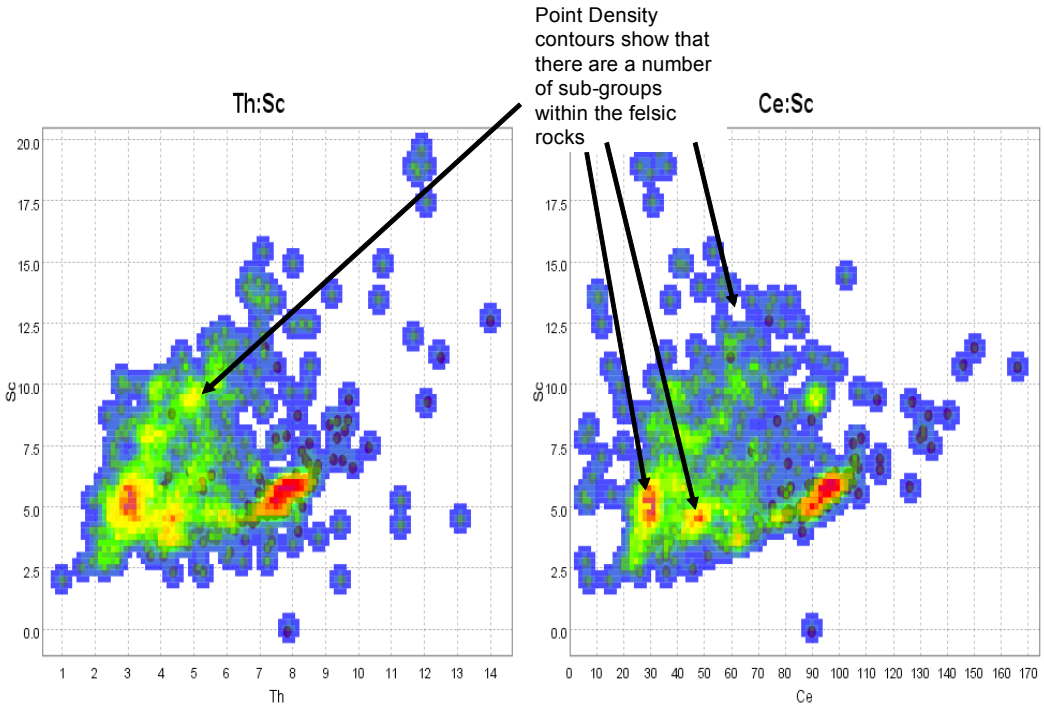

Fig. 34: Plots of Sc versus Th and Ce for the felsic rocks in the Kanowna Belle district. The point density contours highlight a number of subgroups within the felsic rocks. The cluster at 8-10 ppm Sc and 4-5 ppm Th corresponds with the high-P porphyry subgroup defined in Figure 35. (GAS plot by Scott Halley)

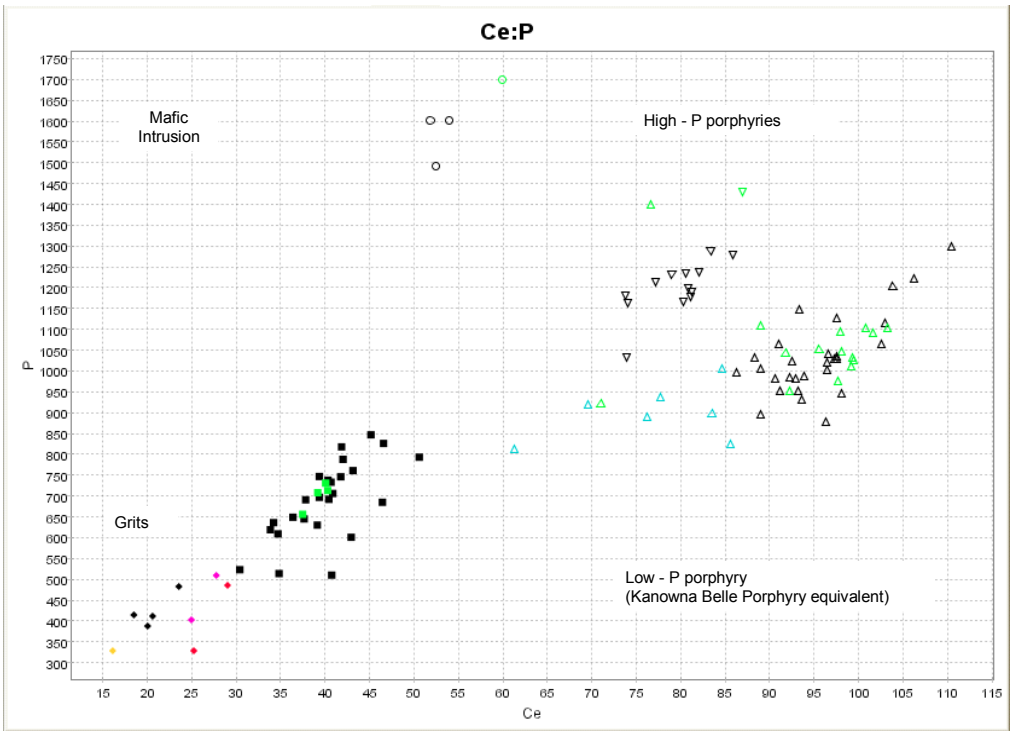

Fig. 35: Plot of P versus Ce illustrating the high and low P porphyries in the Kanowna Belle environs (inverted and upright black-outlined triangles are the least altered and most altered samples, respectively). Data from KDU 1648; 500 m west of Kanowna Belle.

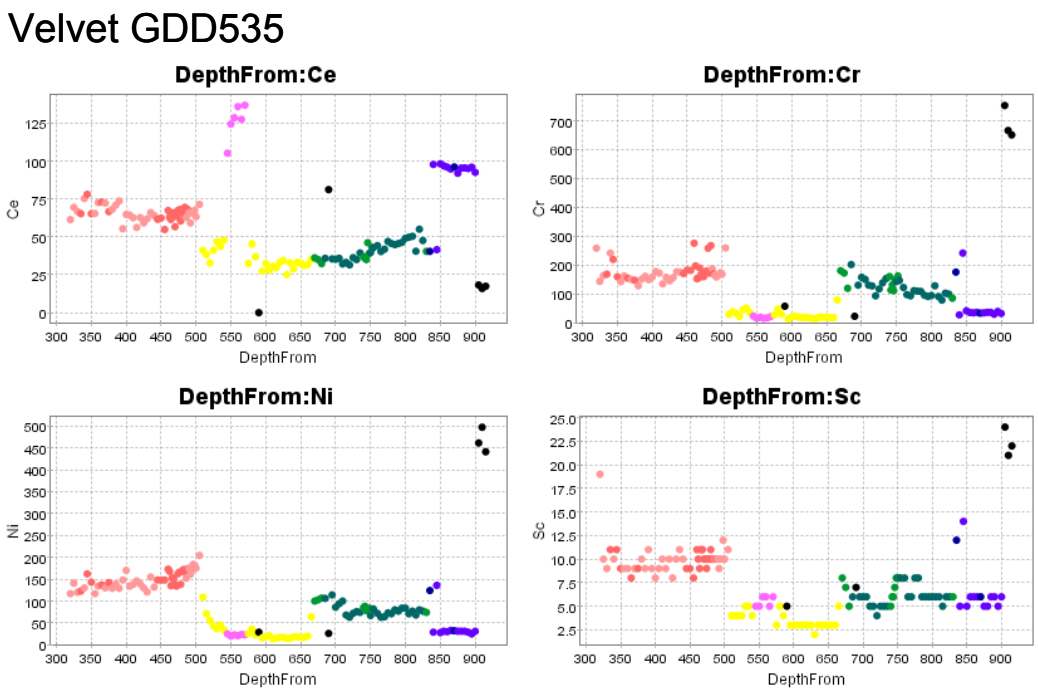

Fig. 36: The downhole distribution of rock units in GDD535 (west of Kanowna Belle). Pink: porphyry 1; Yellow: grits; Green: polymict conglomerates with volcanic clasts; Blue: porphyry 2; and Purple: porphyry 3. Variable Cr values in porphyry 1 (200 to 300 ppm) are coincident with zones of alteration and mineralization (see Figure 38) and reflect at least local (within lithology) remobilization of the Cr.

Velvet GDD535

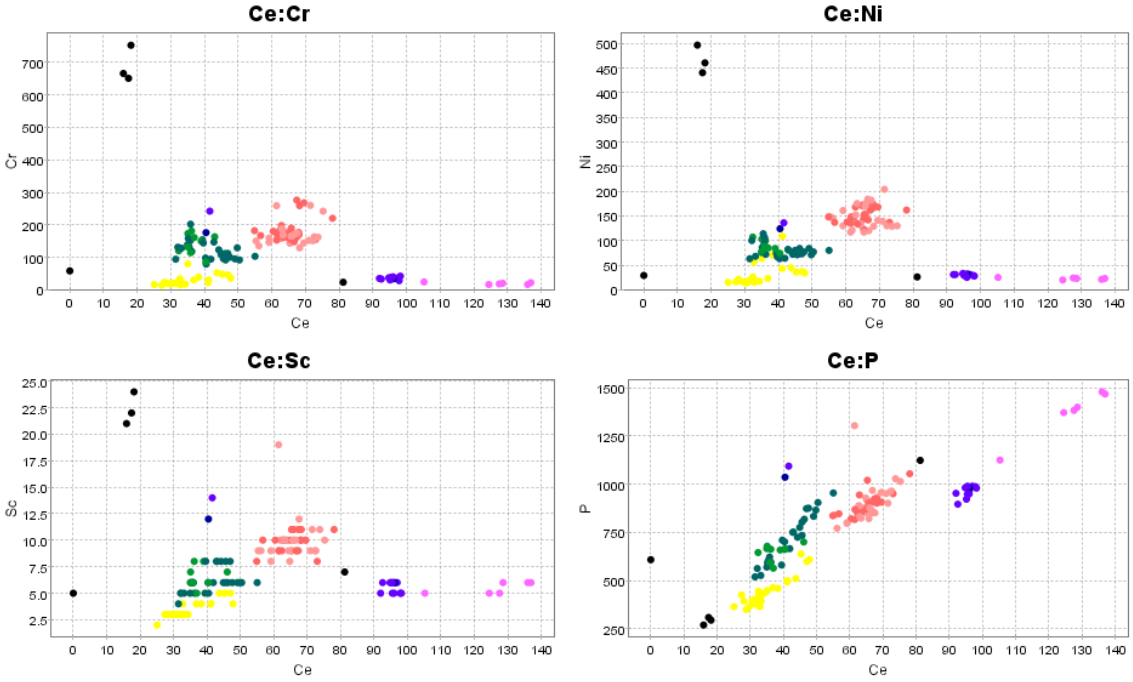

Fig. 37: Plots of Cr, Ni, Sc and P against Ce for Velvet hole GDD535 (west of Kanowna Belle) showing composition of Cr and Ni enriched porphyry 1 (pink) versus grits (yellow), polymict conglomerates with volcanic clasts (green), and LREE enriched porphyrys 2 (blue) and 3 (purple). The downhole distribution of these units is shown in Figure 36. Porphyry 1 is distinctly Cr and Ni enriched (100 to 200 ppm) compared with porphyrys 1 and 2 and equivalent LREE enriched and/or high-P porphyrys. The linear covariance of Ce with P indicates mobilization of the LREEs at least locally.

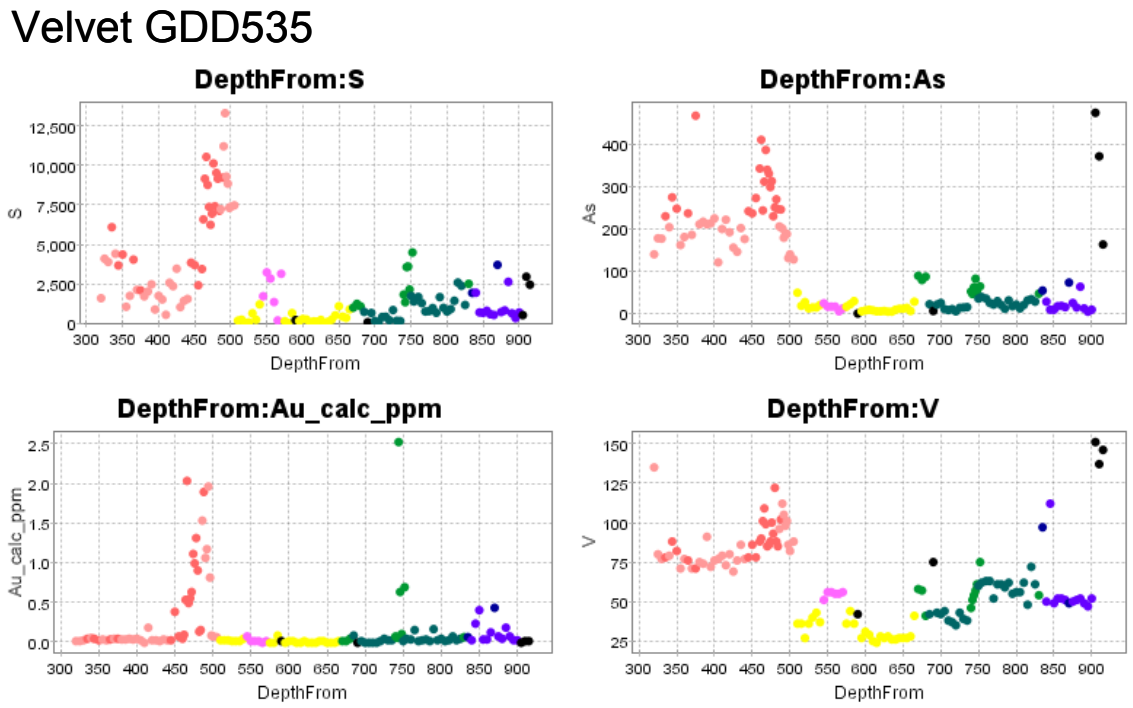

Fig. 38: Down-hole variation of S, As, Au and V for GDD535 illustrating the enrichments of these elements within porphyry 1, particularly in the contact zones with the grits (the upper contact zone is at 320 m).

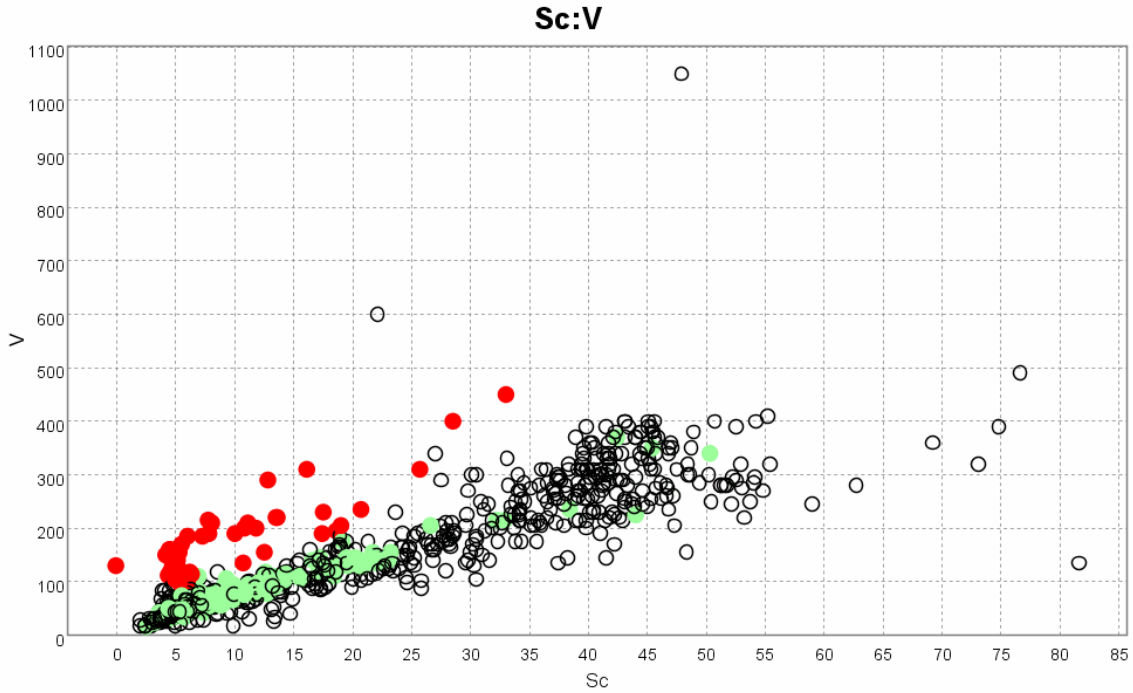

Fig. 39: V versus Sc plot illustrating both lithological as well as alteration controls on V abundance. The linear correlation of V with Sc (open circles) is a lithological control reflecting an increasing mafic component in the rocks. Samples that deviate from the linear V-Sc trend (red dots) indicate alteration by an oxidised fluid (the high-grade signal at Kanowna Belle and the Golden Mile). V is immobile in the common 3+ oxidation state. Sc also has a 3+ oxidation state and both these elements substitute for Fe. In unaltered rocks, they have a very linear correlation. However, under oxidised conditions, the valency of V can change to 4+ or 5+, and in this state it is quite mobile. (GAS plot by Scott Halley)

Deposit-Scale Architecture, Flowpaths and Mixing Boxes in the Kanowna Belle System

Relative Timing

Two temporally and mineralogically distinct styles of gold mineralization have been recognised at Kanowna Belle, corresponding to stages III and IV of the vein emplacement history (Aaltonen, 1997). The first, volumetrically minor, style of gold mineralization is represented by a telluride-associated mineralogy and is restricted to crustiform carbonate (±quartz) veins and breccias (Type III) in the vicinity of the Fitzroy Fault. Veins show structural overprinting relationships consistent with emplacement synchronous with regional D_2. Telluride-gold mineralization occurs as microfracture and microvug infill. Free gold occurs in association with altaite, coloradoite and melonite with rare hessite. No gold tellurides have been noted.

The second style of gold mineralization, the Lowes Shoot style, comprises the bulk of economic mineralization and overprints the telluride-associated style. It is a telluride-absent mineralization phase that displays a strong D_2 control on lode geometry. Gold occurs within pyrite-sericite-quartz-carbonate 'stringers' (Type IV veins), which comprise stockwork geometries in close proximity to the Fitzroy Fault but become more regularly aligned with the regional S_2 fabric away from the shear zone. Gold occurs as inclusions and/or is located in arsenic-rich growth zones in pyrite. Subordinate free gold occupies D_2 extensional sites adjacent to pyrite crystals.

Relationship of Mineralization to Architecture

The upper levels of the Lowes Shoot, which is the major resource of the Kanowna Belle deposit, is located within the footwall of the Kanowna Belle Porphyry above the NE trending, south dipping Fitzroy Fault (Figs. 29 and 30). It has a strike length of about 200m but a depth extent of more than 800m. At depth, the Lowes Shoot extends into the footwall conglomerate (the Golden Valley Conglomerate; Fig.40).

Several mineralized ore shoots occur in the hanging wall of the Kanowna Belle Porphyry. The most significant of these being the Troy Shoot, which is aligned along NW trending cross-structures. Additionally, an E-W trending structure(s) occurs in the hangingwall of the Kanowna Belle Porphyry (Fig. 41). Informally, this is referred to as the "fuchsite shear" reflecting the abundance of fuchsite observed in this part of the mine. In the upper levels of the mine, the Fitzroy Fault, the hangingwall structures, and the Troy Shoot structures appear to delineate the Lowes Shoot.

Domains of highest gold grades and highest sulphur (i.e., pyrite) concentration are not coincident at the Kanowna Belle deposit. Zones of highest pyrite concentration flank the domains of high grade gold, both along strike and in the hangingwall of the Kanowna Belle Porphyry (Figs 42 & 43). The distribution of fuchsite tends to be coincident with domains of high sulphur rather than domains of high grade gold.

The high grade gold zones (Lowes Shoot and Troy Shoot) are characterised geochemically by anomalous V, W, As and Pb, but relatively low S. In contrast, mineralization hosted in the hangingwall shear correlates with Fe and S, with low V, W, As and Pb (Figs. 44, 45 & 46). Both styles of mineralization are anomalous in Sb, Te, Cu, Zn, Ag and Mo. The W halo around Lowes Shoot is approximately 150 m wide and W concentrations show a systematic increase towards gold mineralization.

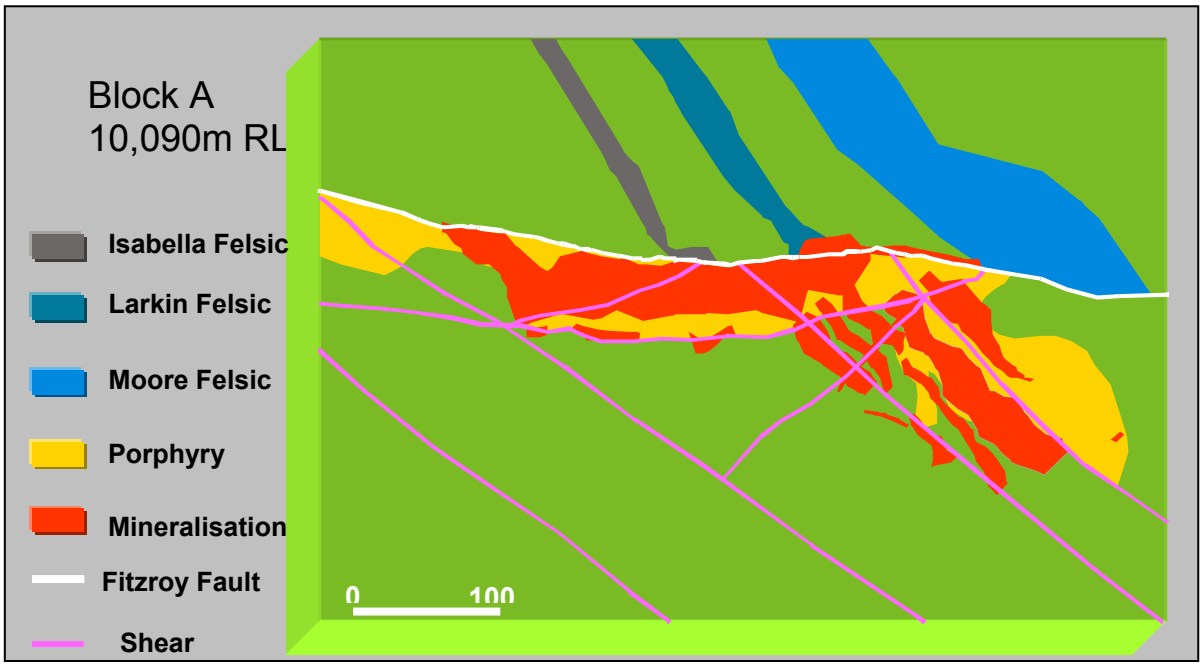

Fig. 40: Plan view of Block A, Kanowna Belle deposit showing the lithological and structural architecture of the upper mine. At this level the Lowes Shoot appears delineated by the Fitzroy Fault, the hangingwall structure to the Kanowna Belle Porphyry, and structures of Troy Shoot orientation.

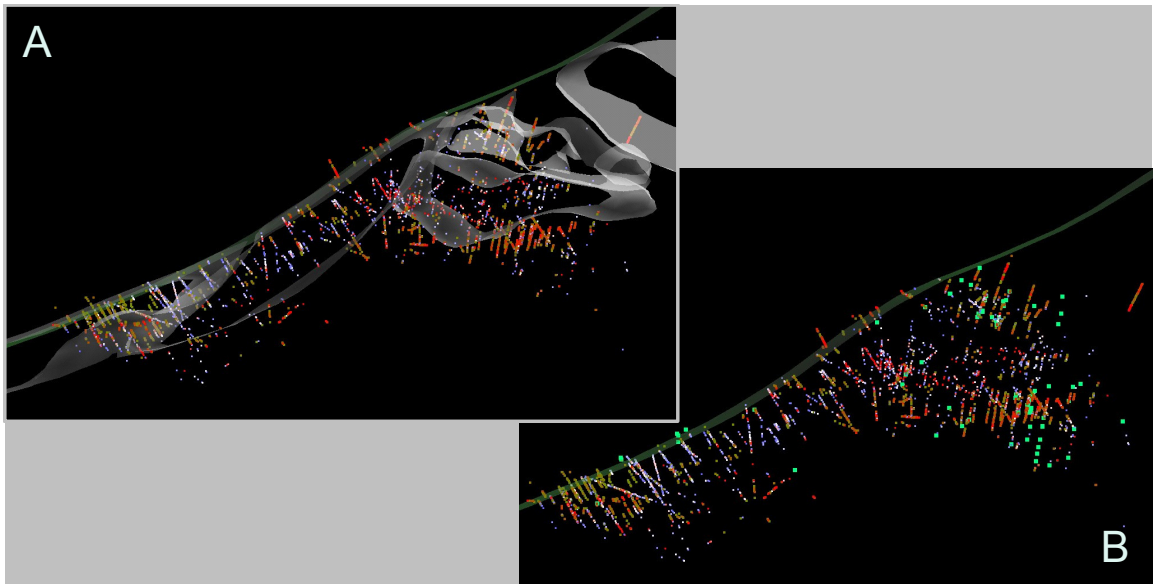

Fig. 41: A. plan view of Block A of Kanowna Belle deposit showing the distribution of high grade gold (white-blue dots) and high sulphur grades (red dots) with respect to Kanowna Belle Porphyry (white outlines) and the Fitzroy Fault (green outline). Domains of high sulfur (pyrite) flank the high grade gold domains, notably occurring in the hangingwall of the Kanowna Belle Porphyry while domains of high grade gold occur in the footwall of the porphyry. B. Same view as A showing the distribution of fuchsite (green dots).

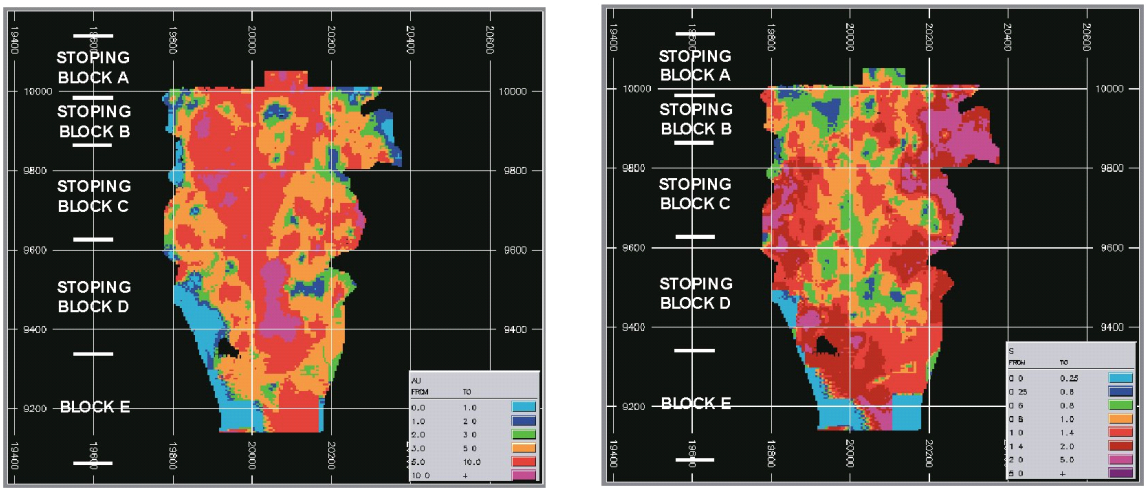

Fig. 42: Longsection of Lowes Shoot illustrating the distribution of Au (left) and sulfur (i.e. pyrite, right) illustrating that the highest sulphur concentrations are not coincident with but flank the domains of high grade gold.

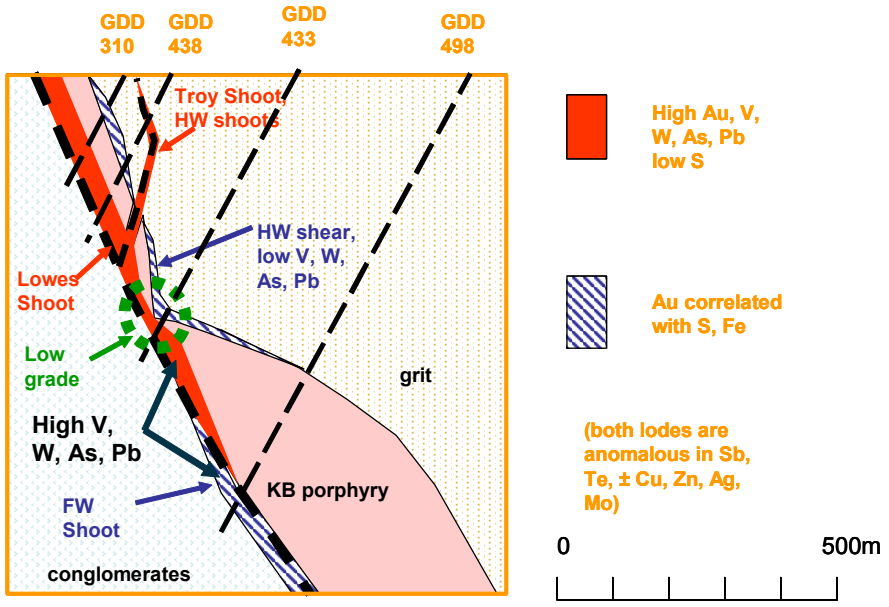

Fig. 43: Section through the Kanowna Belle deposit looking east showing the distribution of the high grade gold zones (Lowes Shoot and Troy Shoot) that are characterised geochemically by anomalous V,W, As and Pb but relatively low S. In the hangingwall shear, gold correlates with Fe and S, with low V, W, As and Pb. Both styles of mineralization are anomalous in Sb, Te, Cu, Zn, Ag and Mo.

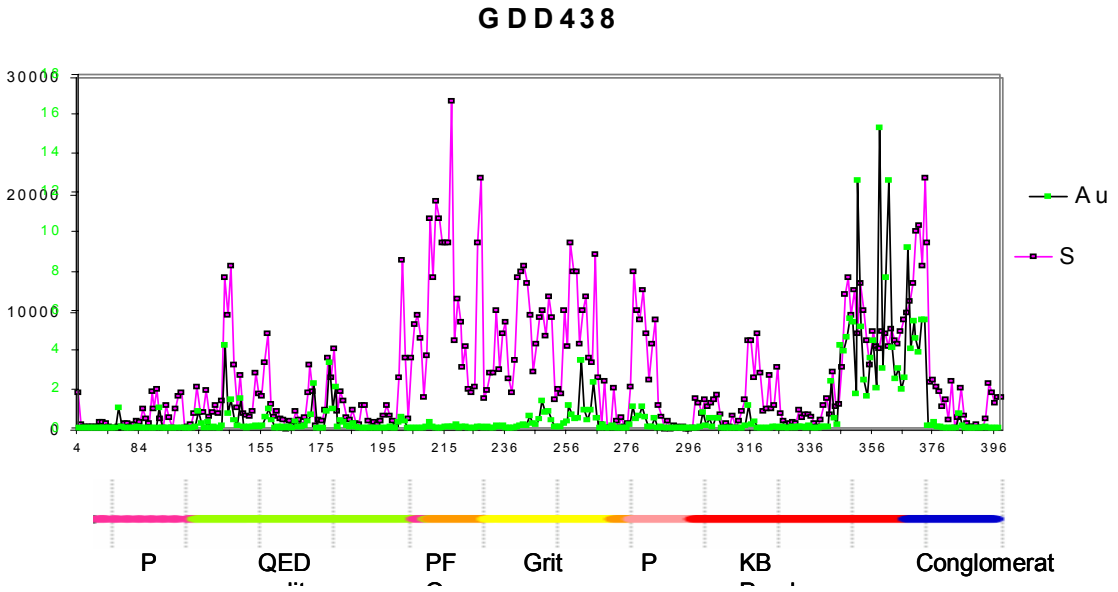

Fig. 44: Distribution of gold (green dots) and sulphur (pink dots) in GDD438 (Lowes Shoot) illustrating the relative enrichment of pyrite versus gold in the hangingwall of the Kannowna Belle Porphyry.

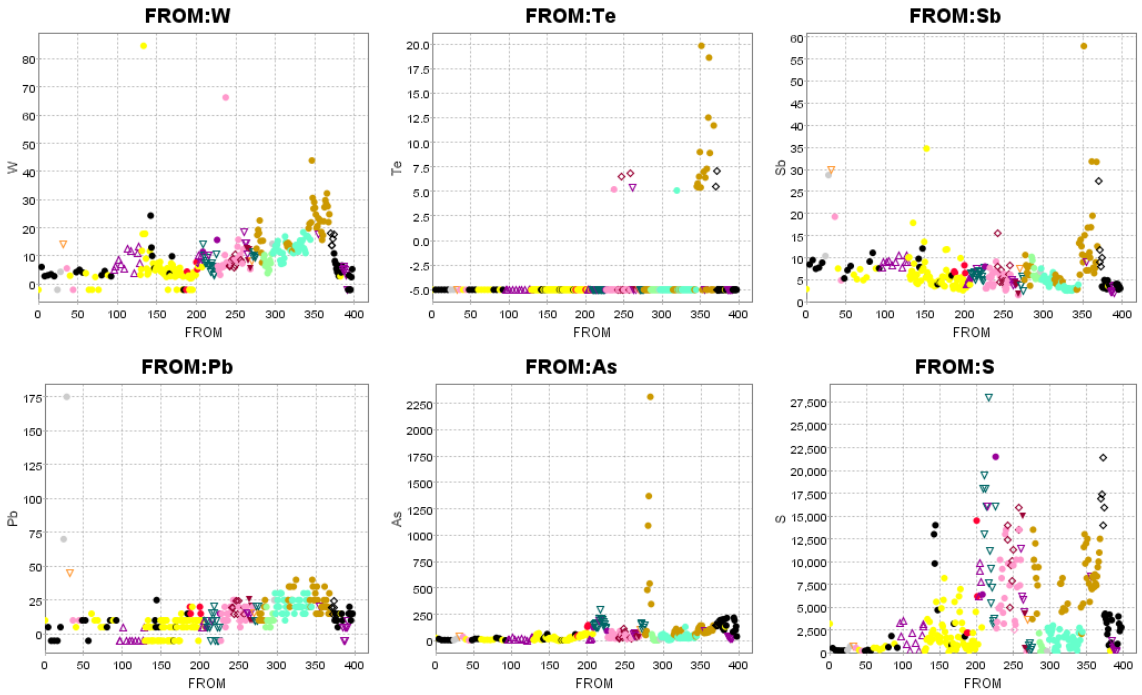

Fig. 45: Distribution of pathfinder elements in diamond drill hole GDD438 illustrating anomalous W, Te, Sb, As and Pb but relatively low S in Lowes Shoot compared with the hangingwall zone.

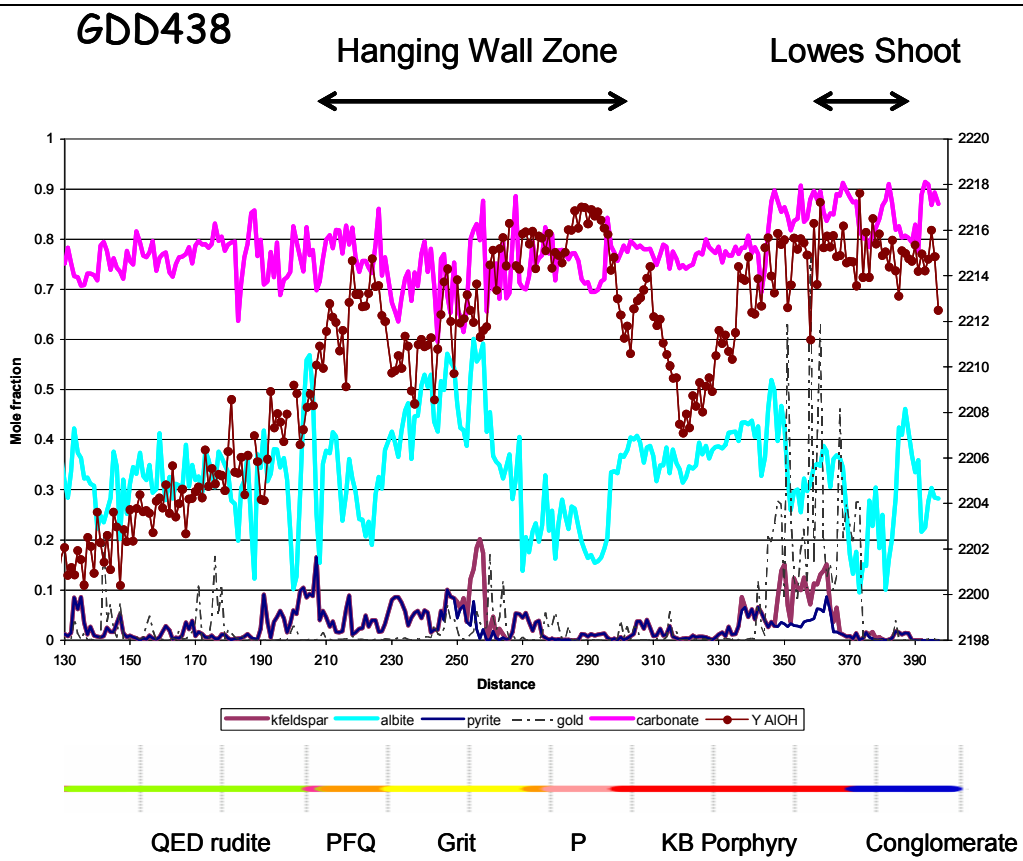

Fig. 46: Downhole mineralogical variation for GDD438, recalculated from multi-element data. The plot gives the mole fractions (mole proportions normalised) of pyrite, albite, K-feldspar, carbonate and white mica (muscovite – phengite solution). Gold abundances and the SWIR AlOH wavelength are shown for reference. Gold abundances are normalised. A summary of the calculation procedures is given in the Appendix. Notably the hangingwall zone is focused on a zone of albite alteration, with limited carbonate, fringed by zones of more intense carbonate alteration. The zones of intense carbonate alteration correspond with phengite peaks in the SWIR spectrum. By contrast, the Lowes Shoot interval shows more variable proportions of carbonate and albite with more limited white mica. Some K-feldspar occurs in the Hangingwall Zone but the best developed zone is within the Lowes Shoot.

Alteration/Geochemical Characteristics of Reduced and Oxidized Fluid Pathways

Major element data acquired by Placer Dome have been used to define the alteration mineralogy for selected diamond drill holes within the Kanowna Belle deposit. These data, together with trace element and PIMA data sets, are providing a basis for defining flow paths of chemically contrasting fluids and sites of fluid mixing in the Kanowna Belle system. Downhole changes in mineralogy and chemistry are illustrated in Figures 47 through 50. Additional details on the information contained within this section are provided in the Appendix and only a summary of the conclusions is given here.

The reduced fluid pathway in the hangingwall zone of Lowes Shoot is marked by:

- A pyritic zone with albite and little or no carbonate.
- Adjacent zones of well-developed carbonate and white mica. The carbonate may be calcitic or sideritic; the white mica is commonly phengitic with SWIR AlOH wavelengths greater than 2210 nm.

- Elements mobile and/or enriched in these zones include the first transition suite of elements Sc, Ti, V, Cr, Mn, Fe, Ni, Co, as well as Bi, As, S, Sb, Rb, Sr, Cs, Hf, Ta, Ce, Sm, and P.

These features are well developed in GDD310:50-90m (hangingwall grits) and GDD438: 200-290m (hangingwall of Kanowna Belle Porphyry). K-feldspar alteration is more strongly developed in the higher grade gold zones in GDD310 and GDD433. The element mobility appears to be correlated with the albite dominant to carbonate dominant parts of the reduced system and at depth.

Similar alteration zones with equivalent element mobility/enrichment patterns occur in the Velvet prospect, but notably the degree of albitization with respect to carbonate - white mica alteration is much weaker and there is an apparent element zonation with depth. The element mobility/enrichment patterns observed in the hangingwall of Lowe Shoot occur in the deeper drilling in KDU1618:825-840m, KDU1619:670-710m, and possibly KDU1648:440-500m. In the surface holes, GDD534, 535 and 537 these patterns are diminished. In the Velvet area, the strongest zones of albite to carbonate and white mica occur in GDD535, suggesting these intersections most closely approximate the reduced-fluid pathway conditions observed in the hangingwall of the Lowes Shoot. However, in contrast with the hangingwall zone of Lowes Shoot, minor element anomalies are subdued.

Oxidized fluid pathways are defined by zones depleted in albite with respect to carbonate and muscovite (AlOH wavelength between 2200 and 2205 nm). Pyrite abundance in these zones is low, carbonate is dolomitic, and most trace element concentrations are low, possibly depleted, except for Rb, Sr and Cs.

The gold zones tend to show oxidized geochemical signals (Te, V, Mo, W) or mixed oxidized-reduced geochemical signals (Te, V, Mo, W, Zn? Ag?), together with evidence of mobility of Cr, Ni, Fe, Sc, as well as Mn, Li, and in particular Bi.

While oxidized versus reduced fluid/alteration signatures can be inferred from the geochemical data, it is not yet possible to differentiate with confidence primary magmatic or clastic sedimentation influences on the distribution patterns of the first transition elements, HFSEs or REEs from metasomatic/hydrothermal influences. Much of the mobility appears to be within lithology as indicated by linear variation on scatter plots. However, in the hangingwall of Lowes Shoot, similar enrichment patterns for the first transition elements occur in both porphyries (GDD438) and grits (GDD310) in what is apparently the same style of alteration in the same structure implying more extensive mobility of these elements in parts of the reduced fluid pathway.

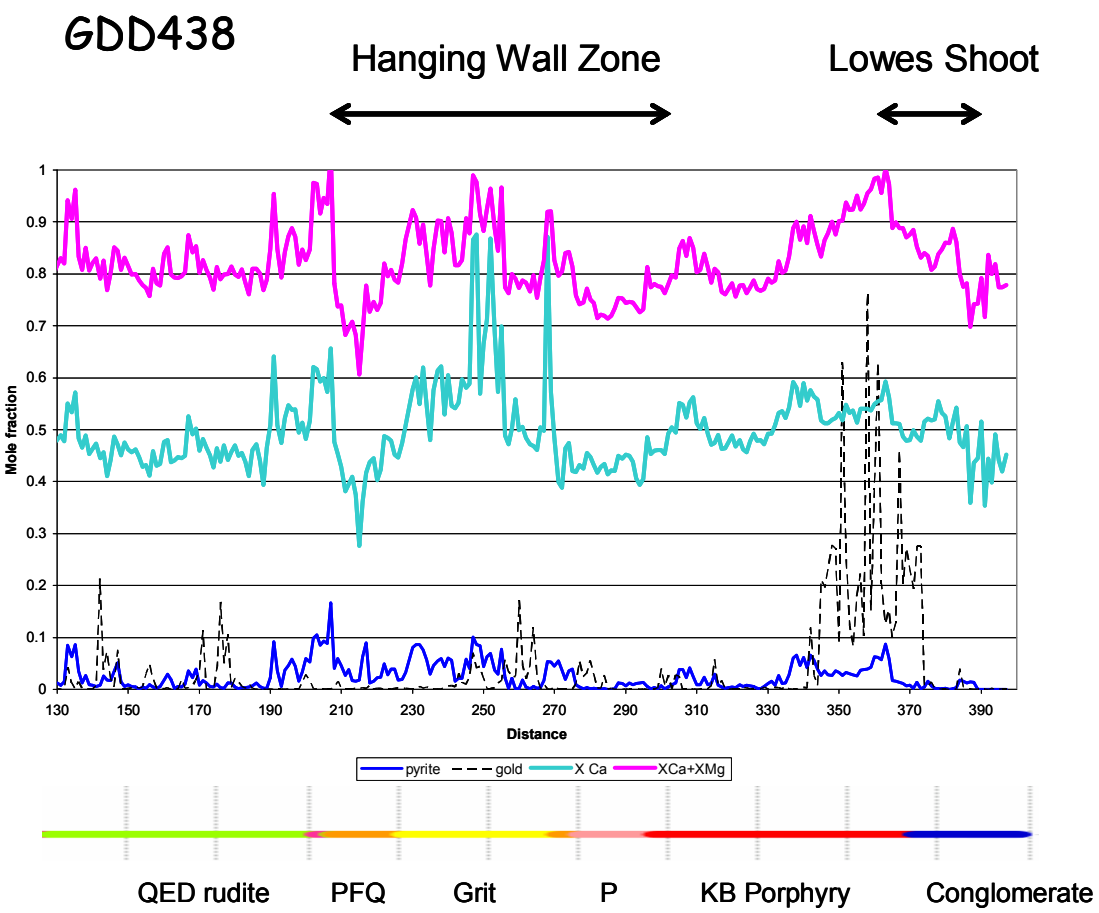

Fig. 47: Downhole variation in carbonate composition in GDD438, recalculated from multi-element data. Yellow: Mole fraction of Ca-carbonate (XCa); Pink: Mole fraction of XCa +XMg. Normalised gold and pyite abundances for reference. Notably the carbonate compositions tend to dolomite in the Lowes Shoot interval and are variably calcic and ferroan in the Hangingwall Zone.

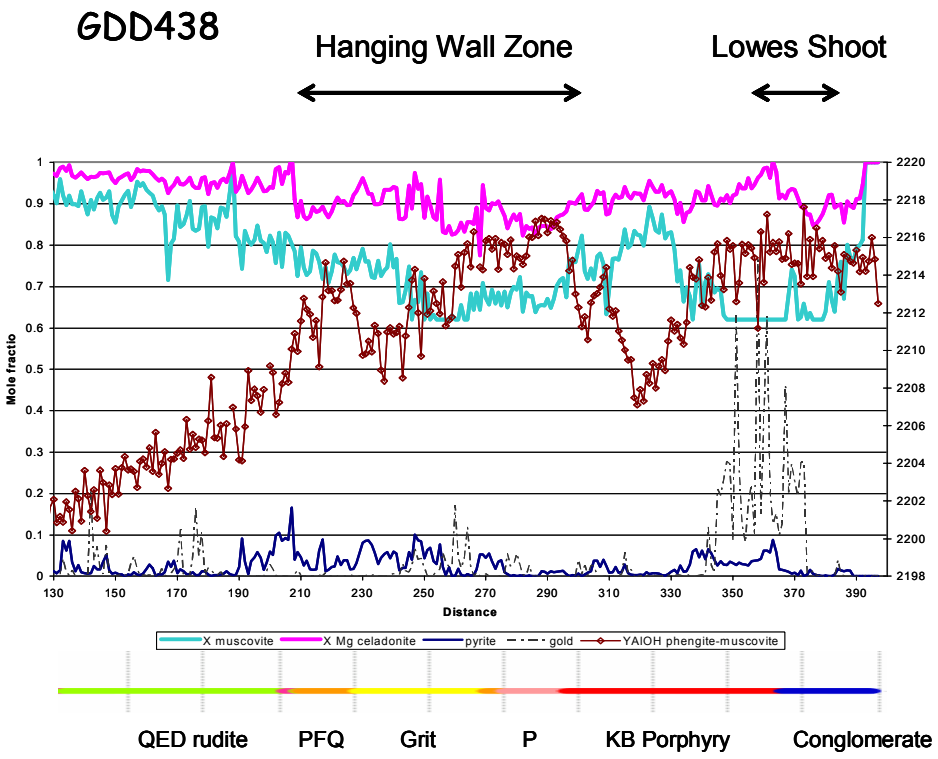

Fig. 48: Downhole variation in white composition in GDD438, recalculated from multi-element data. Blue-green: Mole fraction of muscovite ($KAl_3Si_3O_{10}(OH)_2$); Yellow: Mole fraction of celadonite ($K(Mg,Fe)AlSi_4O_{10}(OH)_2$). Normalised gold and pyite abundances and SWIR AlOH wavelengths are shown for reference. The calculated mole fraction of muscovite inversely correlates with the AlOH wavelength.

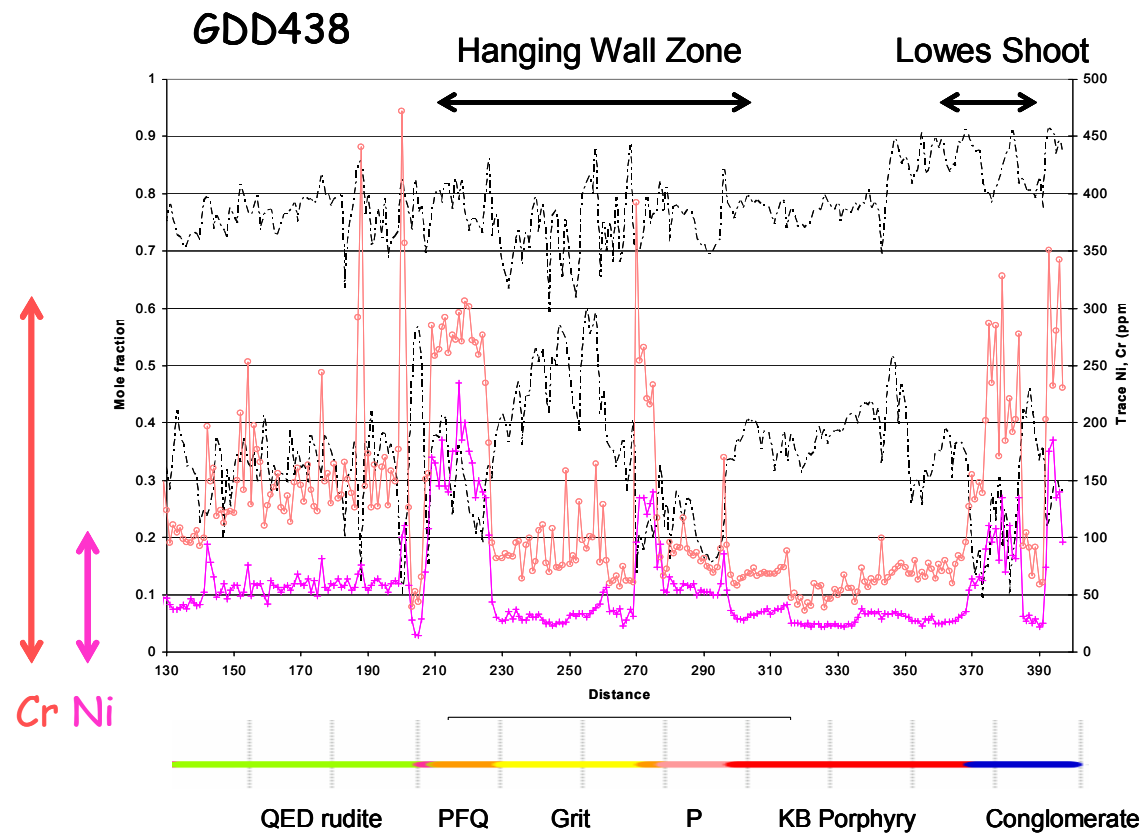

Fig. 49: Downhole variation in whole-rock Cr and Ni contents for GDD438 superimposed on mole fractions (mole proportions normalised) of albite, carbonate and white mica. The Ni and Cr enrichments in the Hangingwall Zone are best developed in the carbonate zones that flank the albite zone. In part, these enrichments are centred on particular lithologies.

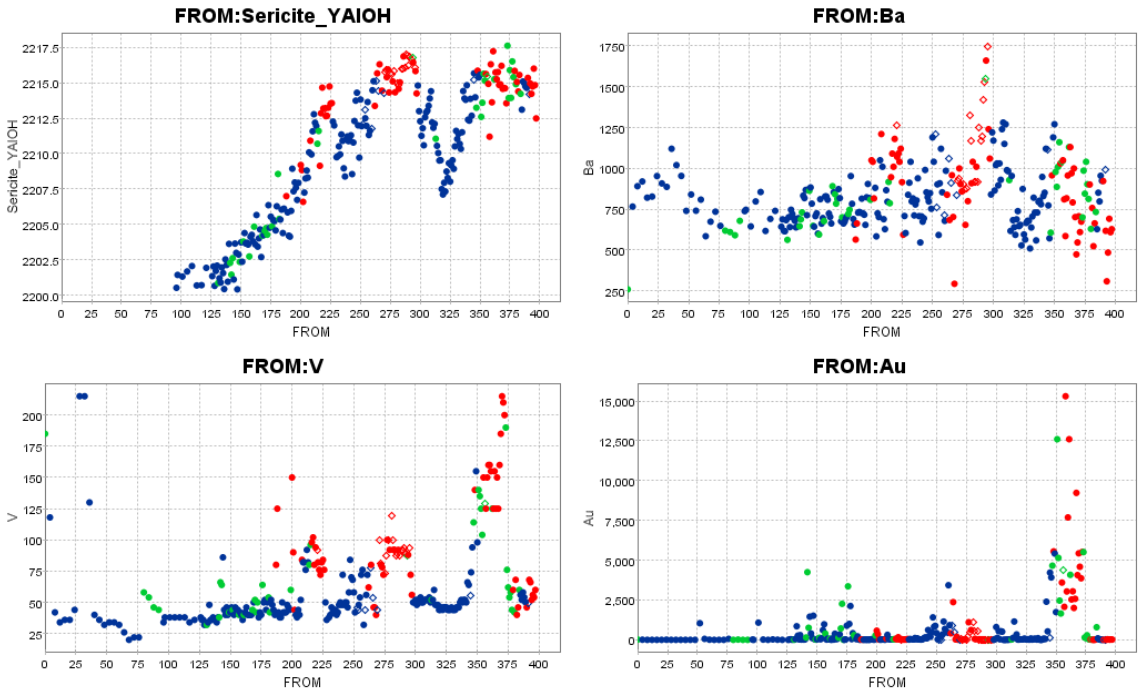

Fig. 50: Sericite infra-red absorption wavelength plotted against depth downhole, and gold grade plotted against depth downhole (GDD438). Also shown for comparison are the V and Ba enrichments. The V-enriched interval that is strongest in the Lowes Shoot may in part be controlled by mica compostion, being favoured by the presence of phengite (long wavelength AlOH). The Ba shows a broad pattern of enrichment across the mineralized zones in the hangingwall and footwall of the Kanowna Belle Porphyry.

Definition of Flowpaths and Mixing Boxes

Within the Kanowna Belle – Velvet area it is possible to define a set of approximately E-W trending structures that were reduced fluid pathways and a set of NW trending structures (Troy Shoot orientation) that were oxidized fluid pathways. In detail these pathways commonly occur along litholgical contacts or within porphyry dykes.

The distribution of the gold appears to reflect the intersections of these two structures (Fig. 51). The Lowes Shoot occurs where these structures intersect the Fitzroy Fault in the footwall of the Kanowna Belle Porphyry. Therefore, these elements of the architecture are interpreted to have created the mixing box for the reduced and oxidized fluids. The reduced fluid pathway defined in the hangingwall of Lowes Shoot and the Kanowna Belle Porphyry appears to cut into the footwall of the Fitzroy Fault at depth (Fig. 52) as does the Lowes Shoot. The distribution of pyrite and fuchsite (Fig. 52) reflects the architectural controls on fluid mixing and redox gradients. The highest sulphide concentrations occur where sulphate-rich fluids were reduced by methane or hydrogen-rich fluids at the intersections of the Troy Shoot orientation and the E-W reduced pathways. Drilling to date in the Velvet area allows definition of both reduced and oxidized pathways (Fig. 53). Integration of these observations with geological and geophysical constraints should permit the construction of a more robust targeting model for the Kanowna Belle – Velvet area.

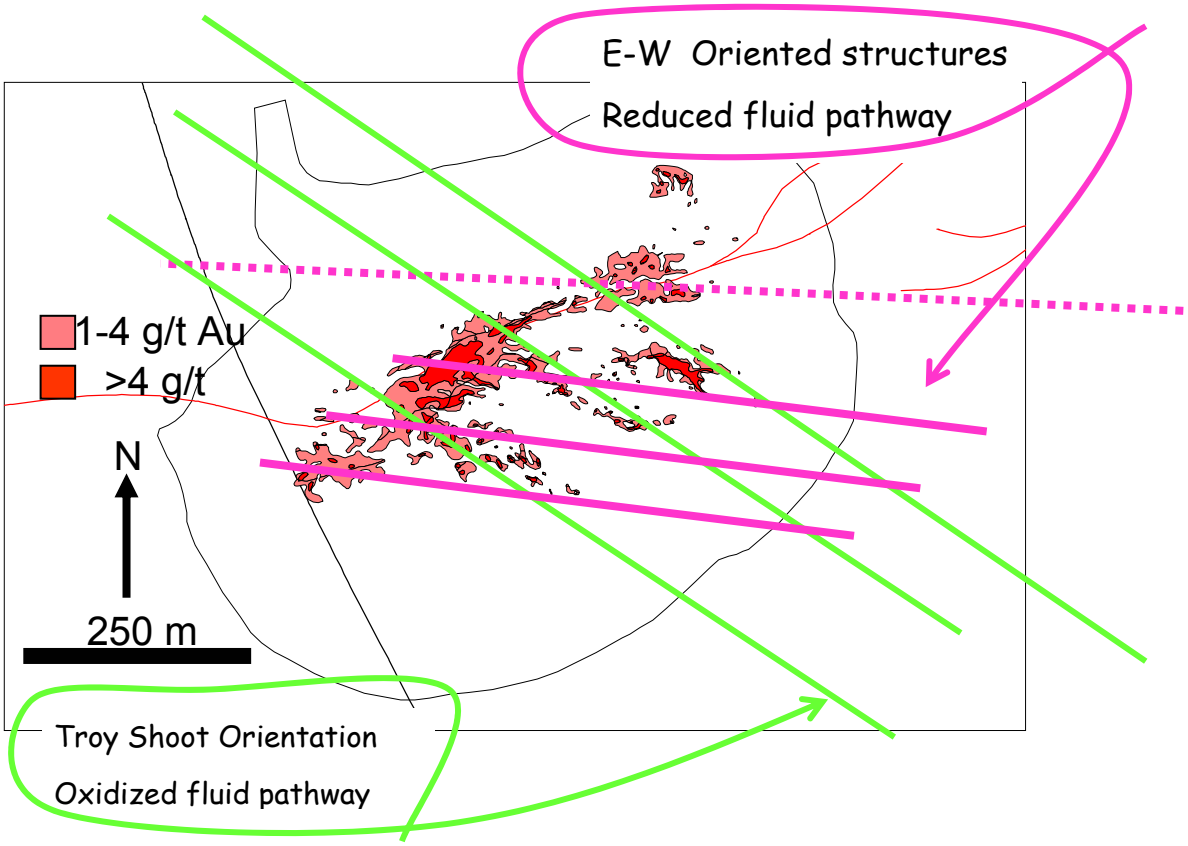

Fig. 51: Plan view of the Kanowna Belle deposit showing gold grades and schematic orientation of structures that were pathways for reduced and oxidized hydrothermal fluids.

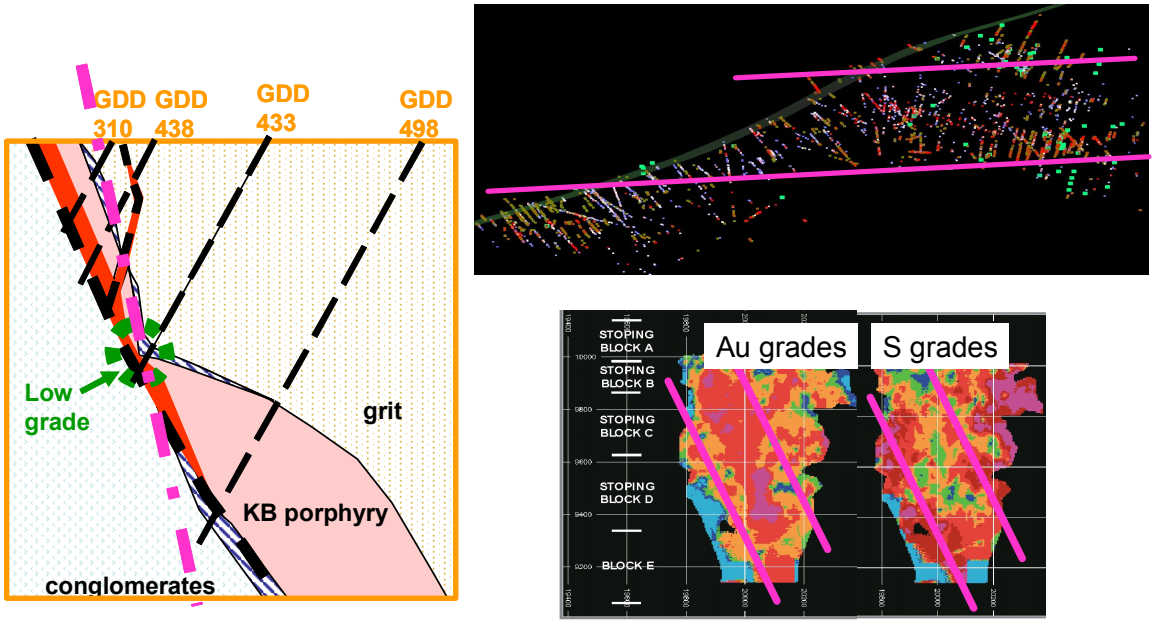

Fig. 52: Architectural controls on reduced fluid pathways. Domains of highest gold grades and highest sulphur (pyrite) concentration (lower right; long section of Lowes Shoot) are not coincident with the latter tending to flank the domains of high grade gold. The reduced fluid pathways are defined by the domains of highest

sulphide concentration (pink lines; lower right figure) and coincident domains of fuchsite (pinks lines; top right; plan view of Lowes Shoot). In cross-section the reduced fluid pathway is defined by albite-pyrite - minor calcite zones in the hanging-wall of the Kanowna Belle Porphyry (pink dashed line, left figure; see text for discussion). The reduced fluid pathway appears to cut into the footwall of the Fitzroy Fault at depth.

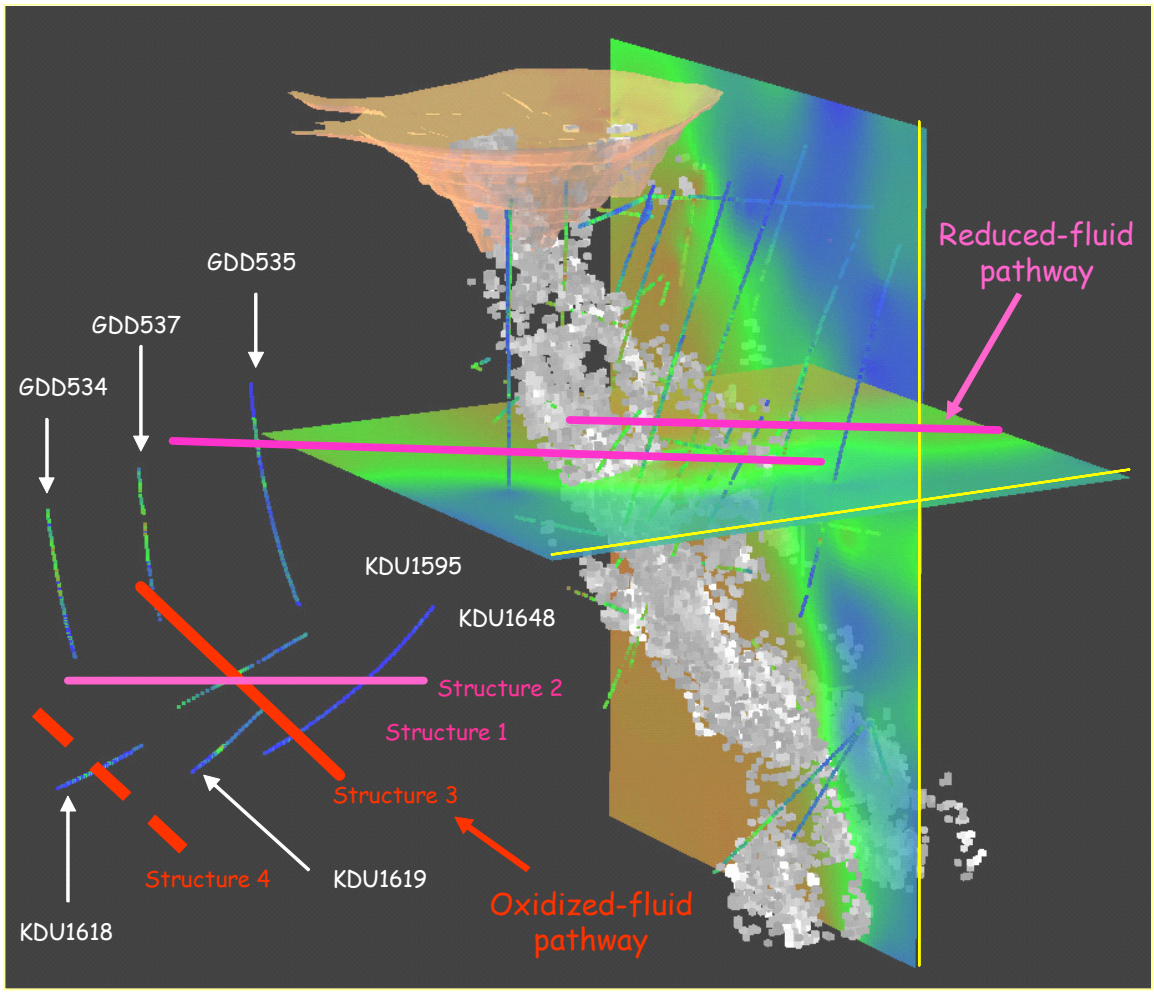

Fig. 53: Model of reduced and oxidized fluid pathways in the Kanowna Belle - Velvet area. Estimates of the location of major E-W structural pathways of reduced fluid are defined by relatively reduced alteration/element assemblages or by mixed oxidized/reduced element assemblages in gold zones. Intersections of oxidized fluid pathways are defined by relatively oxidized alteration/element assemblages or by mixed oxidized/reduced element assemblages in gold zones. See text and appendix for details.

Camp-Scale Alteration Zonation

Phengite – Muscovite Transition

Gold in Lowes Shoot occurs predominantly within high AlOH SWIR wavelength (V-bearing phengite) domains near the transition to low AlOH absorption wavelengths (Ba-rich muscovite) domains. The correlation between gold and white mica gradients is evident at all scales across Kanowna Belle (Fig. 54). The transition from V-rich phengite (oxidised) associated with ore to Ba-rich (reduced) muscovite implies that a redox gradient influenced

the composition of the white micas. This gradient is consistent with defined by the distribution of sulphur isotope values in ore-related and regional pyrite. The redox gradient observed at Kanowna Belle is interpreted to have resulted from multiple and contrasting fluid types that overlapped temporally and spatially during gold deposition.

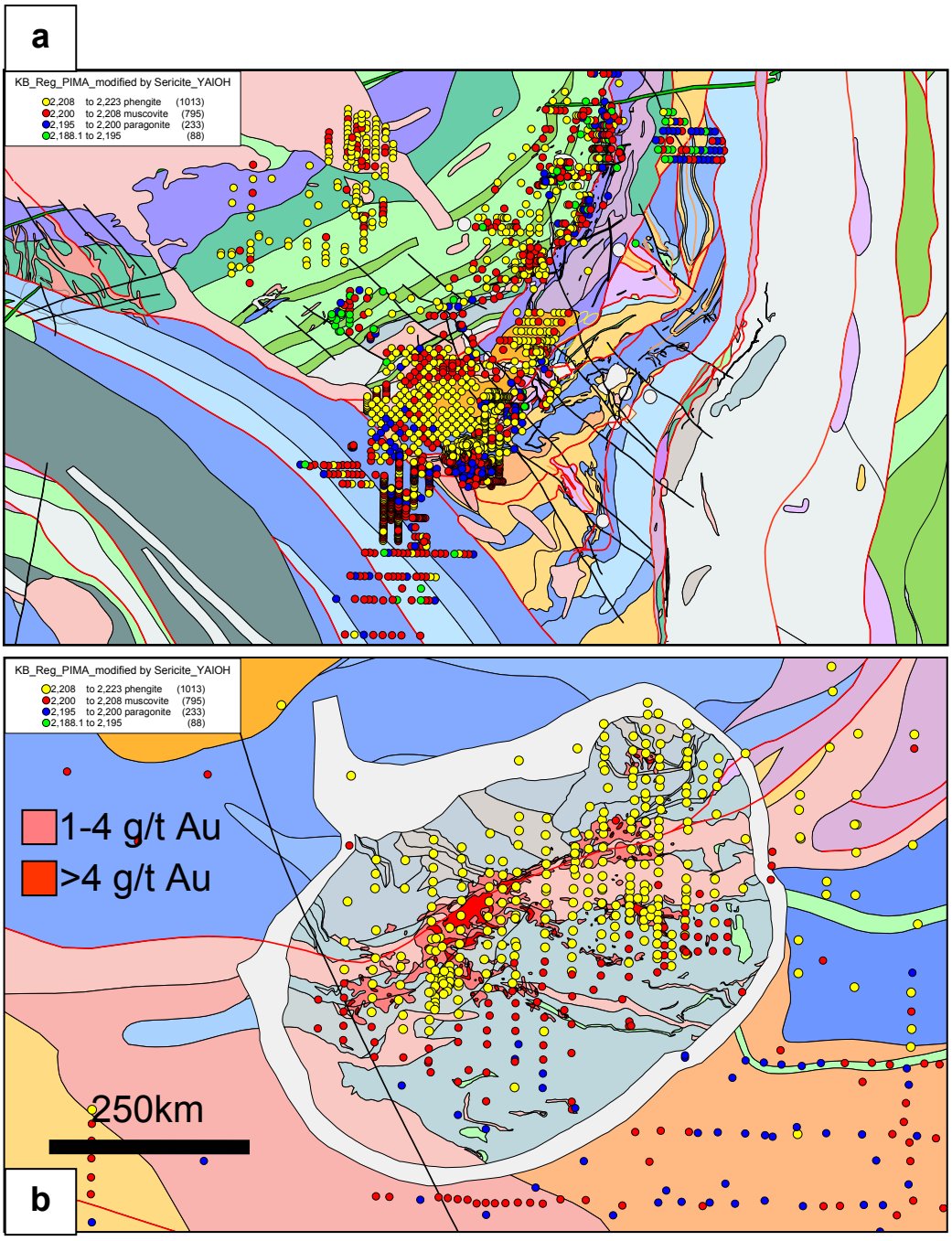

Fig. 54: Results of PIMA survey of SWIR white mica compositions: (a) across the Kanowna Belle district and (b) across the Kanowna Belle deposit. At the district scale the deposit lies at the transition of phengite (yellow) to muscovite (red). At the deposit scale the high grade gold zones lie within the phengite domain.

.

Regional Extent of Muscovite/Paragonite Alteration

A zone of paragonite, pyrite and carbonate occurs in KDU1648 with AlOH wavelengths of ~2190 to 2195 nm. The lack of Te, presence of Bi, Fe-rich carbonate, Fe-rich chlorite, and relatively abundant pyrite suggests the fluids were reduced as well as acidic. Gold grades are poor in this zone. The significant systematic enrichment in W, up to 60-70 ppm, suggests strong W anomalies may reflect acidic conditions rather than oxidized conditions.

The paragonite zone in KDU1648 is potentially equivalent to the low AlOH wavelength domains (2190 -2200 nm) that occur in the Velvet - Slimes Dam area along the Kanowna Shear, south of Kanowna Belle. Tungsten values in the regional mutielement data set are typically elevated in these domains, again implying W anomalies may reflect district-scale reduced-acidic conditions.

Wallaby

Introduction

The Wallaby gold deposit, located 25km southwest of Laverton, sits on the western margin of the Laverton Tectonic Zone of the Eastern Goldfields Province, Yilgarn Craton, Western Australia (Fig. 55). Gold mineralization is hosted in a >1,500m thick matrix-supported mafic conglomerate that has been intruded by a suite of fractionated alkaline dykes.

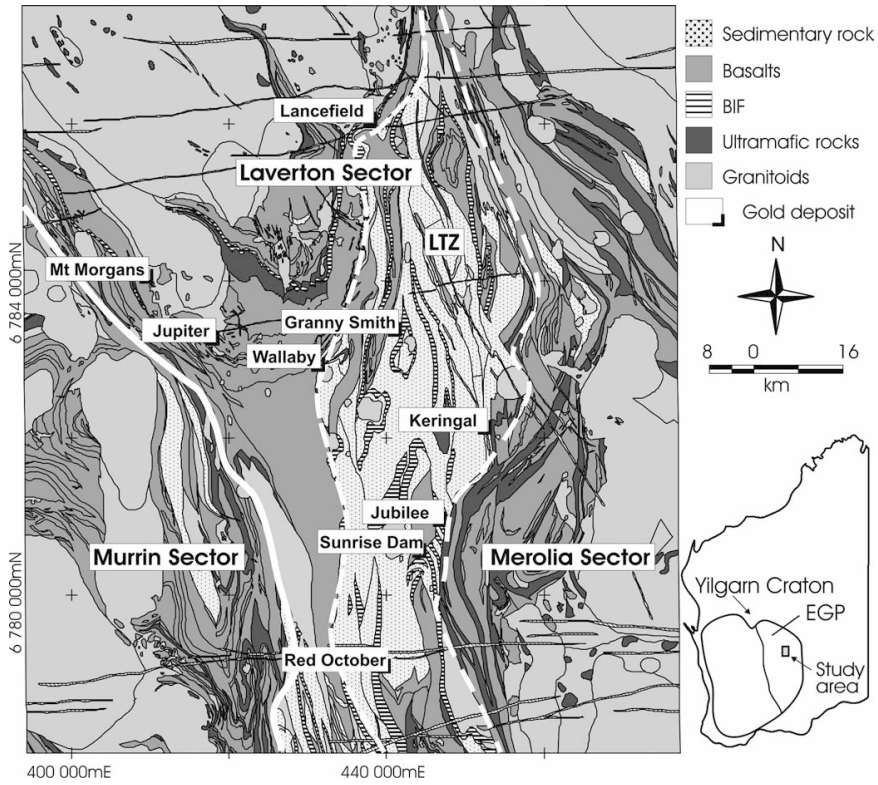

Fig. 55: Interpreted solid geology map of the Laverton greenstone belt (modified from Fitton, unpublished map, 1998) subdivided into sectors following Cassidy et al. (2002). Solid white line marks boundary between Murrin and Laverton Sectors. Dashed white line marks boundaries of the Laverton Tectonic Zone (LTZ). [From Salier et al., 2004]

The Wallaby conglomerate is mainly comprised of mafic volcanic clasts together with minor komatiitic and high MgO basalt, felsic porphyry, limestone, BIF, and chert clasts. The alkaline dyke suite, displaying increasing fractionation from early-stage mafic monzonite through monzonite, syenite, syenite porphyry, and late-stage carbonatite, has intruded the conglomerate in the core of the Wallaby gold deposit. The bulk of the intrusions form two main dykes, concave in profile and stacked one above the other, which plunge 50º to the south and extend to >1 km in depth.

A zone, tens of meters wide, of actinolite-magnetite-calcite±epidote±pyrite alteration mantles the two main dykes to form a broadly pipe-shaped body dipping approximately 50º→185º (Coggon, 2000). This zone of actinolite-magnetite alteration produces the distinctive bulls-eye anomaly that characterizes the magnetic signature of the Wallaby gold deposit (Fig. 56).

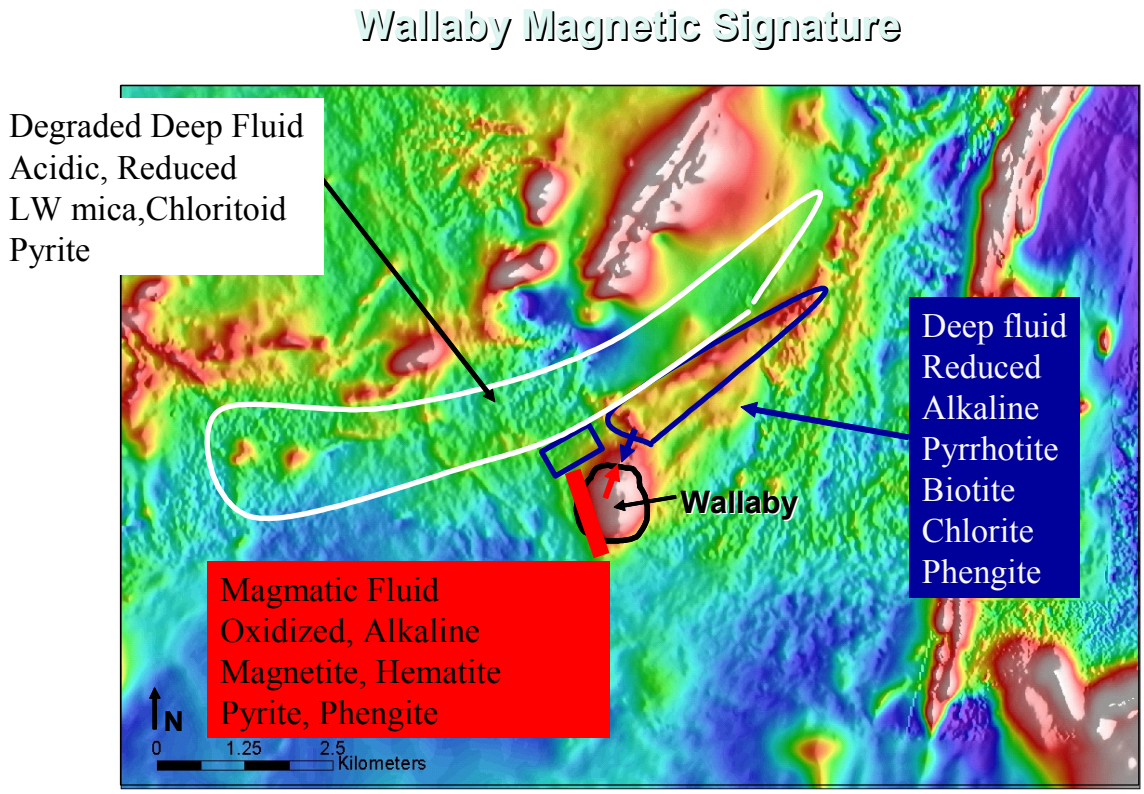

Fig. 56: Aeromagnetic image of the Wallaby deposit and surrounds and interpreted chemical composition of hydrothermal fluids based on alteration mineralogy.

Gold mineralization is hosted in a series of moderately dipping to subhorizontal structurally-controlled zones that are largely confined within the actinolite-magnetite pipe. Proximal gold-related alteration is characterized by the assemblage of dolomite-albite-pyrite-quartz-sericite±fuchsite±hematite. The transition from gold-related dolomite-albite-pyrite alteration to the actinolite-magnetite pipe alteration is sharp and commonly spans <1m. Gold typically forms 1 to 10µm grains included in pyrite and also forms rare grains of free gold.

Camp-Scale Architecture

The Wallaby gold deposit is located in the southern portion of the Lancefield-Wallaby Basin, a fault bound basin within the Rega Corridor of the Laverton Tectonic Zone (Fig. 57, Standing, 2002). The lower stratigraphy of the Rega Corridor consists of the Defiant Well Basalt and the Gladiator BIF Unit. Overlying the Gladiator BIF, the White Hill Felsic Sequence is a variably thick sequence of felsic sediments and volcaniclastics. The Bulldog Basalt, a sequence comprised mainly of high Mg and tholeiitic flood basalts, conformably overlies the White Hill Felsic Sequence (Standing, 2002). Together, this sequence of rocks defines the eastern limb of the Margaret Anticline, the core of which is the Mt Margaret granitoid dome that lies to the northwest of the Wallaby gold deposit.

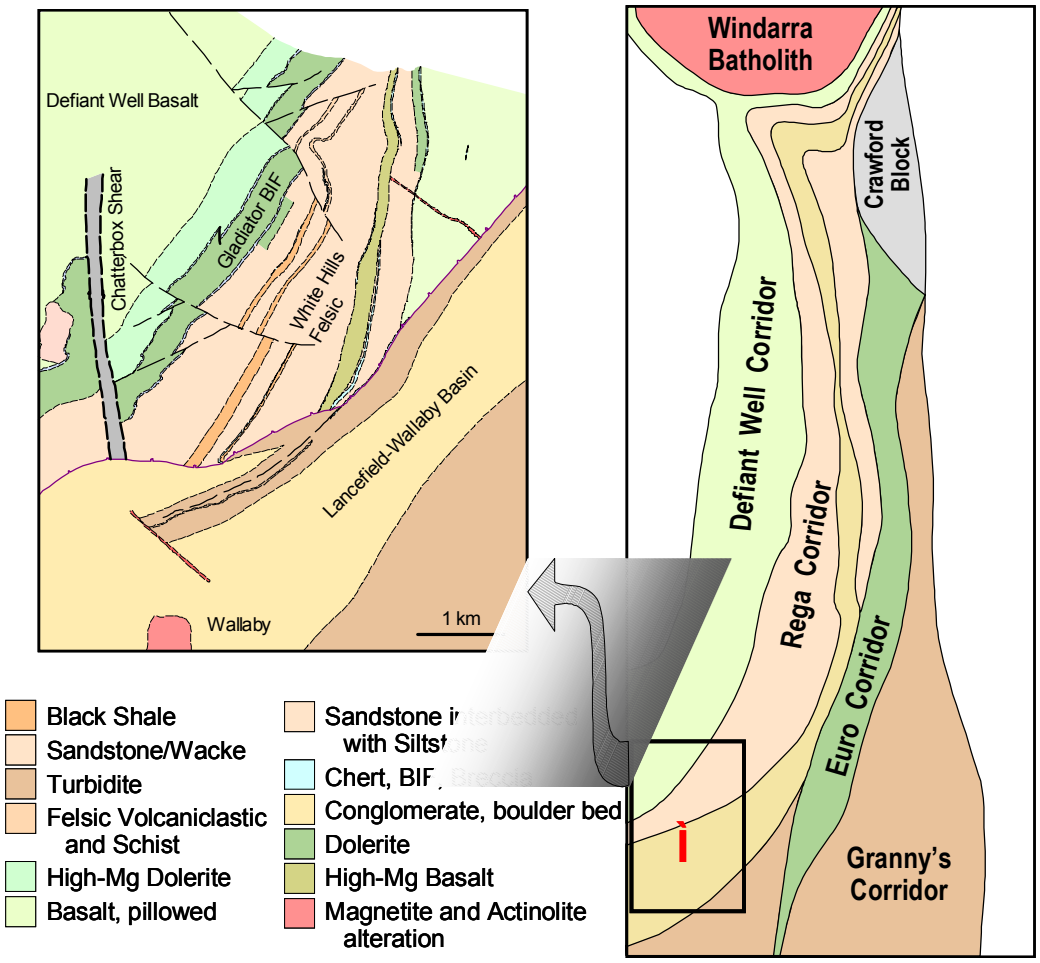

Fig. 57: Rega corridor. Schematic plan showing revised tectonic subdivisions of the Laverton Tectonic Zone and the position of the Lancefield-Wallaby basin. The left hand map shows solid geology interpretation of the Wallaby area (after Standing 2002).

The tectonically late Lancefield-Wallaby Basin unconformably overlies both the White Hill Felsic and the Bulldog Basalt Sequences (Fig. 58). The lower stratigraphy in the basin is a

350-600m thick sequence of conglomerate, wackes, chert, and sandstone. This sequence is conformably overlain by the 1,500-1,800m thick Wallaby Conglomerate, the host to the Wallaby gold deposit. The stratigraphic top to the basin is comprised of a 1,500-2,000m thick package of interbedded siltstone, sandstone, and wacke (Standing, 2002). The youngest Achaean rocks in the Laverton Greenstone Belt are these late supracrustal sedimentary successions. The upper age limit of sedimentation is constrained to <2675±4 Ma (SHRIMP U-Pb analysis of detrital zircon) for the Alabama sandstone that overlies the Wallaby conglomerate (Cassidy et al., 2002). A similar age of 2673±5 Ma has been determined for detrital zircon from the matrix of the Wallaby conglomerate itself (unpublished data reported in Purdie, 2000).

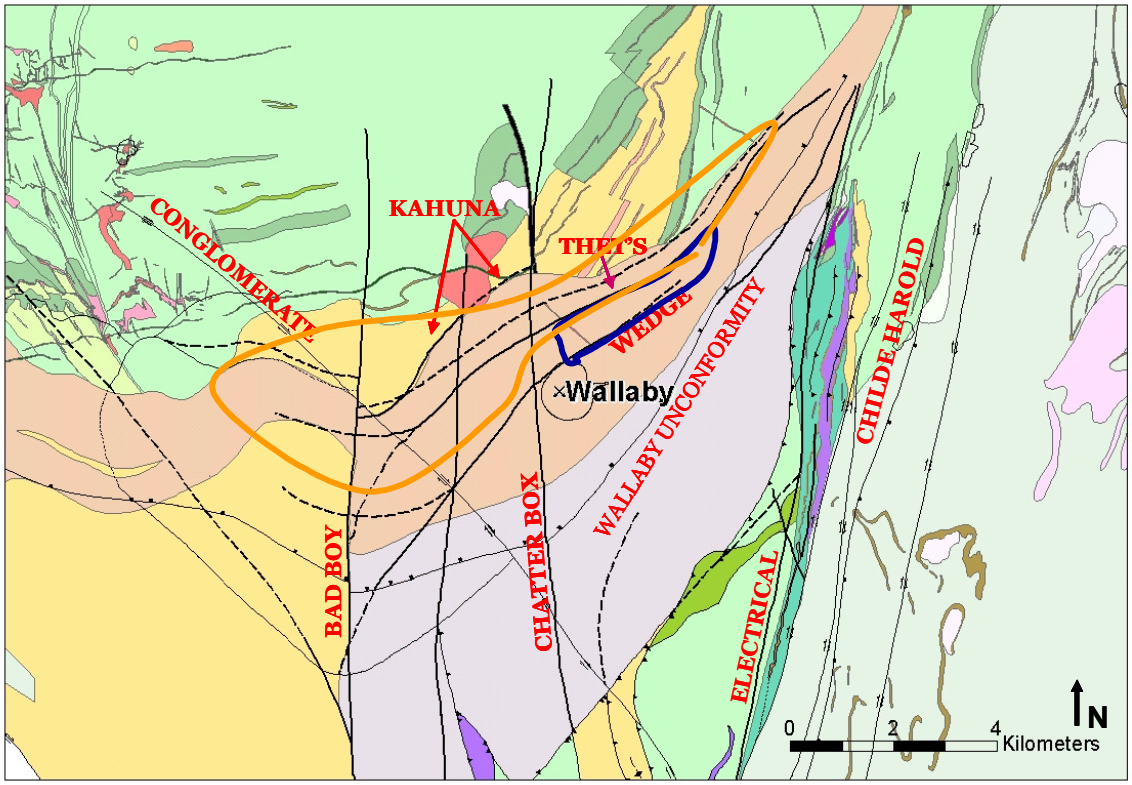

Fig. 58: Geological and stuctural map of the Wallaby district.

The Wallaby conglomerate is typically unbedded, however, where observed, rare graded bedding indicates the rocks are right-way-up and dip moderately at 45º toward the southeast (Purdie, 2000). It has previously been claimed that bedding flattened toward the center of the Wallaby deposit due to flexure of bedding during structural deformation (Davis, 1999). However, recent access to better underground exposures in the center of the gold system has revealed there is no deflection in bedding across the deposit (Standing pers comm., 2004).

The Lancefield-Wallaby Basin is a tectonically late, fault-bound basin and consequently has not preserved many of the deformation events recorded elsewhere in the Laverton Greenstone Belt. There are two main orientations for regional-scale structures in the vicinity of the deposit: (1) dominant N-S trending, near vertical fault systems such as the Chatterbox

Fault and (2) ENE-WSW trending extensional faults, dipping moderately to steeply to the south, restricted to the late basin. The Chatterbox Fault, a strike-extensive and variably mineralized structure, is one of the more significant fault zones in the Laverton Region (Standing, 2002). This shear zone has been hypothesized to be one of the main structures that control the location of the Wallaby deposit (Beeson pers comm., 2004). However, while the trace of the Chatterbox Fault can be mapped north of the Lancefield-Wallaby Basin (Fig. 58) and its position beneath the basin has been inferred from seismic data, there is no expression of the Chatterbox Fault within the Lancefield-Wallaby Basin itself. (Standing, 2002). In addition, the basin margin does not appear to be offset by the 1.5km dextral displacement along the southern continuation of the Chatterbox Fault (Standing, 2002).

The ENE-WSW faults parallel the basin margins and are interpreted to be extensional faults that developed during basin growth and were later reactivated during compression (Halley pers comm., 2004). One of the largest of these faults is Thet's Fault (Figure 58), which has been both mapped on the surface over a strike length of >2.5km (Standing, 2002) as well as intersected in the deepest core holes drilled under the Wallaby deposit. In diamond core, Thet's Fault is a massive 250m thick zone of intense alteration and ductile deformation.

The pipe-like geometry of both the actinolite-magnetite alteration system and the alkaline dykes that form the core architecture of the Wallaby gold deposit suggests the features controlling the location of Wallaby are the intersection of N-S and NE-SW trending structures.

Camp-Scale Chemistry

The least altered Wallaby conglomerates have a lower greenschist facies mineral assemblage of chlorite + calcite + zoisite + albite. A comparable lower greenschist facies assemblage of sericite + chlorite is observed in meta-pelitic 'Wallaby cap rock' (Mason, 2001a). Mason (2001b) suggests that some of the chloritoid zones within Thet's Fault (and the lower basin stratigraphy) had an earlier composition of chlorite-carbonate altered conglomerate, but now have a new lower greenschist foliated assemblage dominated by muscovite + carbonate + chloritoid porphyroblasts.

There is a gradation from this to chlorite + calcite alteration to chlorite + calcite + magnetite alteration with increasing proximity to the Wallaby mineralized system. This gradation occurs over a distance of several hundred metres.

Actinolite + pyrite + magnetite alteration overprints the chlorite-carbonate lower greenschist alteration assemblage. This alteration is pervasive in the matrix of the conglomerate, and fracture controlled in the clasts. It also affects the intrusive rocks, suggesting the intrusive rocks predate or are synchronous with this alteration event.

Anhydrite locally forms part of this alteration assemblage. Other minerals associated with this event are garnet and clinopyroxene. Garnet is seen as ragged grains within the matrix which are partially consumed by very fine grained calcsilicate phases including clinopyroxene. At depth calcsilicate veins comprising garnet + calcite + pyrite ± pyroxene occur associated with this alteration event. This mineral assemblage suggests a high temperature (between 450 and 600°C) oxidised fluid source, most likely magmatic in origin. Rare hematite and greenish pleochroism seen in biotite support the oxidised nature of this fluid.

Geochemistry shows minor chemical affects associated with this event, with the addition of minor S, SiO_2, and maybe 1 or 2% Fe. The proportion of magnetite to pyrite seen in conglomerate affected by this event is relatively constant. Assuming a fluid of mostly $SO_4/H_2S + H_2O$, the precipitation of magnetite would reduce the fluid and cause precipitation of pyrite in a constant ratio (Vic Wall pers. comm, 2001).

As magnetite is intimately associated with this event, and the surrounding chlorite altered conglomerate is effectively nonmagnetic, the extent of the actinolite-magnetite-pyrite alteration can be modelled using magnetic susceptibility. The gross geometry of this alteration is a 500m-600m diameter pipe plunging at 50° to 190°. Magnetite alteration within this pipe is inhomogeneous, and there is a low magnetic area in the centre of the pipe that coincides closely with the syenite dykes. The location of the dykes and the magnetite alteration suggests they are related. However, it is more likely that both events have utilised the same structures as the volume of magmatic intrusions seen at Wallaby is insufficient to create the amount of alteration seen in the actinolite event. It is assumed that this fluid has entered via the same structure as the dykes. The outer limit of the alteration is gradual – there does not appear to be any bounding structure. Extent of alteration is more likely related to distance from the source structure.

Deposit-Scale Architecture

The current interpretation is that the magmatic intrusions form two main dykes, one above the other, plunging at about 45-50 degrees to the south down the middle of the Wallaby mineralized system. The dykes are concave in profile. The different intrusive types have often utilized the same feeder pipe. The main intrusions are:

1. Mafic monzonite, monzonite, and early carbonatite are NE trending, narrow vertical dykes.
2. Syenite and porphyry syenite are broadly circular plugs (in section) and form the two concave pipe dykes.
3. Second stage of carbonatite associated with margins of syenite porphyry, but structural relationships unclear and may have mutually crosscutting relationships.

Gold lodes at Wallaby form a stacked series of ore zones. There are two types of lodes: (1) thick (average 7m) sub-horizontal to gently NE-dipping lodes, and (2) narrower, moderately NE-dipping lodes. The majority of ore is contained in sub-horizontal lodes. Gently dipping shear zones are interpreted as being linking structures (Davis, 1999), which, in turn, are important as auriferous fluid conduits.

Large-scale shear zones, which may have acted as fluid conduits, are absent in association with ore zones. Marginal shearing is common to many ore zones, with shear strain accommodated by phyllosilicate-rich zones external to lodes (Davis, 1999). Given that the broad orientation of lodes is consistent with ENE-WSW compression, such marginal shearing is consistent with formation of gold lodes syn-D2.

Deposit-Scale Chemistry

Gold mineralization is associated with strong metal enrichments in Mo and W and moderate enrichments in Sb, As, Pb, and Ba. Additionally, ore zones show significant enrichment in

S, CO_2, K_2O, and LILE over unaltered conglomerate (Mason, 2001). Analysis of Doug Mason's geochemistry data shows that at grades >5g/t Au there is subtle V-enrichment, indicating a redox control on gold precipitation, and also a shift from K-mica to K-feldspar (Halley, 2003).

Garnet (gt-an-ab-chl-ep-tn) in skarn is interpreted as metamorphism due to heat only. Fluid flow out from syenite destroys this garnet but produces the overall Wallaby pipe at high temperatures (an-ab-chl-bi-act-ep-tn-mt-cc). Therefore, heating of "wet" Wallaby conglomerate to 550 deg C causes skarn-type mineral assemblages (garnet-pyroxene). The H_2O-CO_2-Cl fluid from the syenite brine causes the proximal high temperature alteration of actinolite-magnetite-chlorite-epidote-calcite. It also destroys the previously-formed "skarn". (Cleverley, 2004).

Preliminary geochemical modeling indicates all alteration at Wallaby can be explained solely with a syenitic fluid source. However, it is impossible to carry both Au and S together in this fluid; therefore, an outside fluid source is required for gold precipitation.

Relative Timing/Paragenesis/Genetic Model

Alteration distal to the Wallaby deposit comprises a pre-ore regional chlorite-calcite-pyrite±pyrrhotite±chloritoid alteration formed under lower greenschist facies metamorphism (Wall and Mason, 2001). Proximal alteration is composed of actinolite-magnetite±epidote±pyrite that forms a pipe-like body mantling the syenite dyke suite (Wall and Mason, 2001). The actinolite-magnetite alteration event was accompanied by the formation of calc-silicate veins and abundant carbonate-rich veins with variable amounts of biotite, magnetite, and garnet implying a relatively high temperature of formation. Early magmatic intrusions such as monzonite and carbonatite are overprinted by the actinolite-magnetite alteration while younger syenite and porphyritic syenite intrusions are not overprinted. Gold mineralization is wholly contained within the actinolite-magnetite alteration pipe and occurs as a series of flat-lying ore lodes linked by small, steep, high-grade ore lenses. Gold-related alteration is composed of albite-ferroan dolomite-pyrite with abundant quartz-carbonate veins, and is hosted in structures that have previously undergone biotite-carbonate±pyrite alteration. The gold ore event crosscuts the conglomerate and the majority of magmatic intrusions, and overprints both actinolite-magnetite and biotite alteration (Drieberg, 2004).

While gold-related alteration post-dates the majority of intrusive activity and its associated actinolite-magnetite alteration, it is not known for certain whether the gold ore event and magmatism are directly related or whether there was a significant hiatus between these two events. Recent detailed mapping and reinvestigation of diamond drill core has identified a close spatial and paragenetic link between gold mineralization and syenite magmatism. The presence of pegmatite bodies, miarolitic cavities, and extensive magmatic-hydrothermal breccia pipes provide evidence that the syenite and porphyritic syenite dykes, the youngest intrusive phases, exsolved a CO_2-rich volatile phase. In addition, syenite dykes intrude along the same flat-lying structures that host gold mineralization and rare post-ore syenite dykes have been documented. Geochronological studies currently in progress will help to constrain this close spatial and temporal link between gold mineralization and syenite magmatism (Drieberg, 2004).

Integration of Common Camp-Scale Geological and Chemical Components

Introduction

The emphasis on "where is the deposit" has led inevitably to a restating of the "source" "transport" and "trap" paradigm of mineral systems. The "5 Question" description of the mineral system explicitly highlights the problem of understanding the system in time and space. The "where" question is inherently scale independent. As part of the scientific drive to build scale-integrated models we are developing camp-scale comparative studies. The work is focused on properties of Placer Dome Asia Pacific in the Kalgoorlie and Laverton districts and the St Ives property of Gold Fields Ltd. and supported by MERIWA within the framework of the ***pmd****CRC* Yilgarn terranes (Y) project.

The comparative study of camps is designed in part to understand the influence of district-scale factors, such as bulk composition of host sequences, regional metamorphic grade, proximity to granites and porphyries on the types of alteration assemblages and the compositions of the fluids that produced these alteration assemblages. Another goal is to establish the diversity of processes leading to the formation of high grade gold deposits. Inter-camp comparisons may help to elucidate lithological and structural controls on seals, aquicludes and aquifers in the system and the size and geometry of large-scale hydrothermal cells.

This section summarizes progress in correlating mineralizing patterns across camps, mapping alteration systems at the district scale utilizing geophysical and geochemical surveys (aeromagnetic, SAM, PIMA, multi-element) and integration with deposit-scale data sets to develop robust scale-integrated models of the gold mineralizing systems. The aim is to understand the architectural controls on fluid pathways, map the geochemical gradients in the system (redox, pH, sulphur activity, etc) that control gold transport and deposition and identify likely domains of gold deposition.

Of the intensive variables of interest (T, P, redox, pH, sulphur activity, water activity, salinity) we have focused on redox and pH and sulphur activity.

Camp-Scale Litho-Stratigraphic Controls

Gold deposits occur within 100s of metres stratigraphically of the:

- footwall of the Black Flag Beds in St Ives Camp
- footwall of the late basins (Wallaby and Kanowna Belle deposits; Agnew Camp)

This suggests that these units acted as regional aquicludes at the time of gold mineralization, sustaining fluid pressures in compartments beneath these units.

The occurrence of ultramafic units subjacent to deposits (e.g., Kanowna Belle, Central Corridor St Ives camp) indicates that more component rocks such as the porphyries and mafic intrusions were the aquifers and the ultra-mafic rocks were aquicludes. The andesitic volcaniclastic rocks and fine-grained sandstone-shale units ("BIF") of the Edjudina domain are also potential regional-scale aquicudes.

All of the major rock types are host to mineral deposits (Fig. 59) so there is no specific chemical control by a particular rock-type on the process(es) of gold deposition.

Competency contrasts between units appears to be important in developing sites of dilation and focusing fluid flow.

AGNEW
LITHOSTRATIGRAPHY

ST IVES
LITHOSTRATIGRAPHY

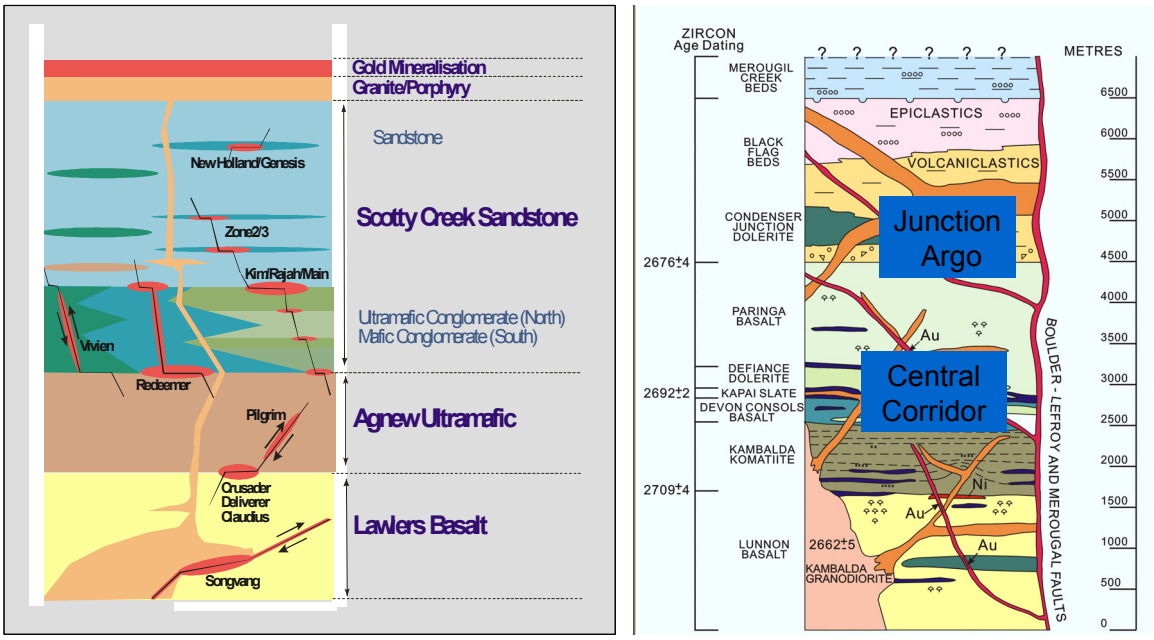

Fig. 59: Stratigraphic columns for the St. Ives and Agnew Camps.

All of the major rock types are host to mineral deposits. In the St Ives Camp this includes the Kambalda Komatiite, Kapai Slate, Paringa Basalt, Defiance, Argo, Junction Dolerites and Paringa Basalt. The Kanowna Belle Porphyry is the major host rock of the Kanowna Belle deposit and at the Wallaby deposit is hosted by the Wallaby Conglomerates and porphyries.

In the Agnew Camp, the host lithologies are the Lawlers Basalt, Agnew Ultramafic and Scotty Creek Sandstone (late basin).

Comparative Camp-scale Alteration and Geochemical Gradients

All camps appear to show evidence of significant geochemical gradients at least at the district-scale (Fig. 60) as defined by variations in mineralogy as well as stable isotopes of S and C (see Figure 61 and later discussion of the isotopes). The S isotope constraints suggest much of the variation is due to changes in redox, acidity and sulphur activity and not simply a function of temperature.

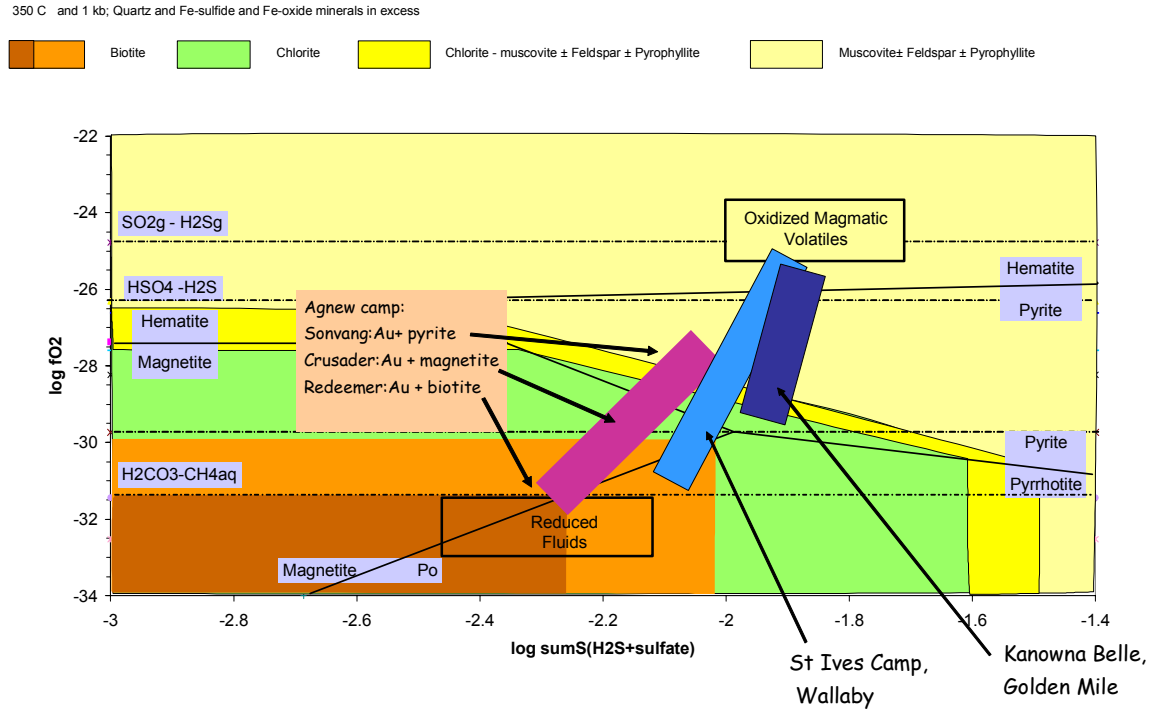

Fig. 60: Redox- sumS plot summarising the range in redox and sum S (H2S+sulfate) conditions in the St Ives and Agnew Camps and the Wallaby, Kanowna Belle and Golden Mile deposits. Conditions are inferred from the alteration mineralogy together with S and C isotope data. Broadly camps and deposits formed in more reduced environs will be dominated by pyrite/pyrrhotite assemblages with Fe - rich silicates (biotite/chlorite) although the stability of these assemblages will be influenced by host-rock composition, temperature, pH and sulfur content of the fluids. The assemblages of the Crusader and Redeemer deposits of the Agnew Camp indicate mineralizing fluids that extremely reduced /sulfur poor fluids and/or higher temperatures of formation cf other deposits of the Eastern Goldfields.

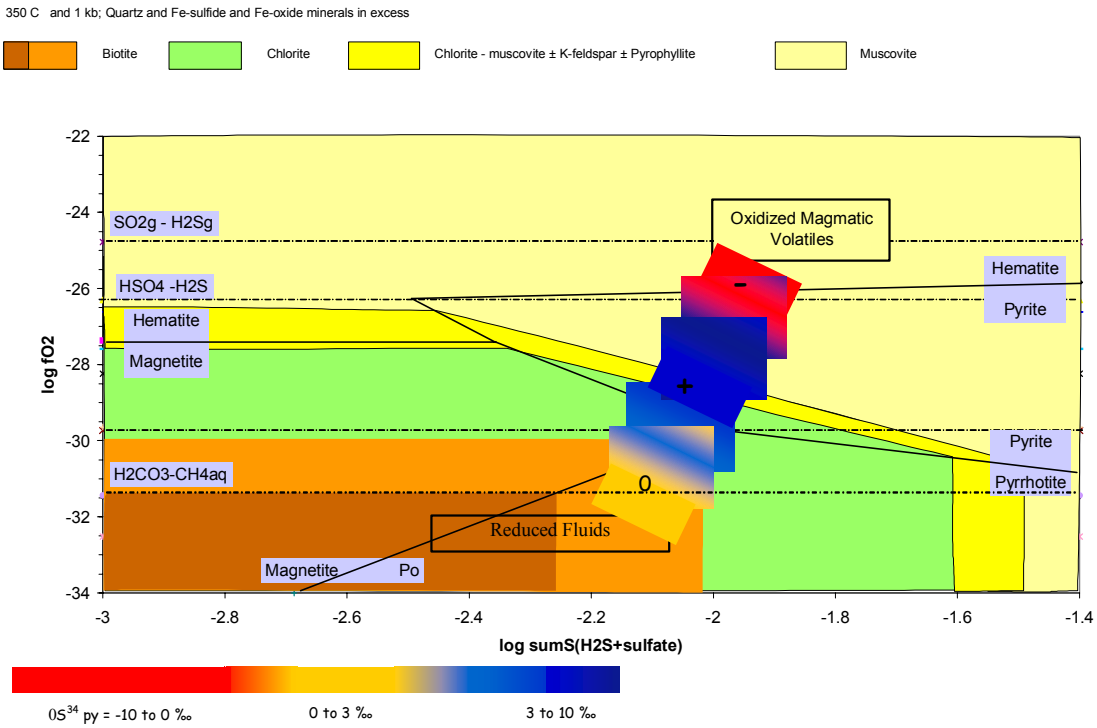

Fig. 61: Redox- sumS plot summarising the range in redox and sum S (H2S+sulfate) conditions illustrating the variation in S isotope values as a function of redox state.

The St Ives camp and Kanowna Belle deposit and environs show similar ranges in sulfur isotope values indicating similar ranges of redox – S conditions. Mineralogy differences (Kanowna Belle is dominated by pyrite cf St Ives camp pyrrhotite-magnetite-pyrite) reflect different host-rock compositions and different temperatures of formation.

Redox – Sulphur Activity Gradients

In the St Ives gold camp high-grade gold mineralization is localized in zones where reduced, pyrrhotite-bearing assemblages overlap with oxidized, magnetite-bearing assemblages. In contrast in the Kanowna Belle deposit and environs pyrite is the dominant phase with little known magnetite or pyrrhotite. However, the sulphur isotope variations in pyrite at the deposit- to district-scale at Kanowna Belle are similar to those documented in the St Ives camp (see below) indicating similar ranges of redox – sulphur activity conditions. Mineralogy differences reflect different host-rock compositions and different temperatures of formation.

The Agnew Camp shows systematic S-N variations in sulphide-oxide-silicate mineralogy over about 8 km from:

- Au-pyrite mineralization (Sonvang deposit) with marginal magnetite and distal pyrrhotite (features typical of deposits in the Central Corridor of the St Ives gold camp), to
- Au-magnetite mineralization (Crusader deposit) with no sulphide, to

- Au-biotite-amphibole mineralization (Redeemer deposit), lacking in sulphide or magnetite.

These deposits occur in an equivalent stratigraphic setting to deposits in the Central Corridor, St Ives and in the Kanowna district so clearly the mineralogical differences do not reflect a host-rock control. The assemblages of the Crusader and Redeemer deposits indicate mineralizing fluids that were extremely reduced /sulphur poor fluids (Figure 60) and/or higher temperatures of formation cf other deposits of the Eastern Goldfields. These deposits are of interest because they potentially can provide insight into an "end-member" fluid(s).

pH Gradients

Deposit and district-scale PIMA data sets from the Kanowna Belle deposit and environs and the Wallaby deposit and environs reveal systematic variations in distribution of muscovite and phengite as defined by λ AlOH wavelengths (Figs 62 and 63). These patterns are interpreted in terms of pH changes within the system with the low λ AlOH wavelengths (2190 -2200) taken to imply acid conditions and the high λ AlOH wavelengths (2210-2225) neutral to alkaline conditions. The domains of low λ AlOH wavelengths may also include paragonite based on the observations from Velvet Hole KDU1648, west of Kanowna Belle (Fig. 64). A zone of paragonite, pyrite and carbonate occurs in KDU1648 with λ AlOH wavelengths of around 2190 to 2195. The lack of Te, presence of Bi, Fe-rich carbonate, Fe-rich chlorite and relatively abundant pyrite suggests the fluids were reduced as well as acidic. Gold grades are poor in this zone but significant systematic enrichment in W, up to 60-70 ppm, occurs.

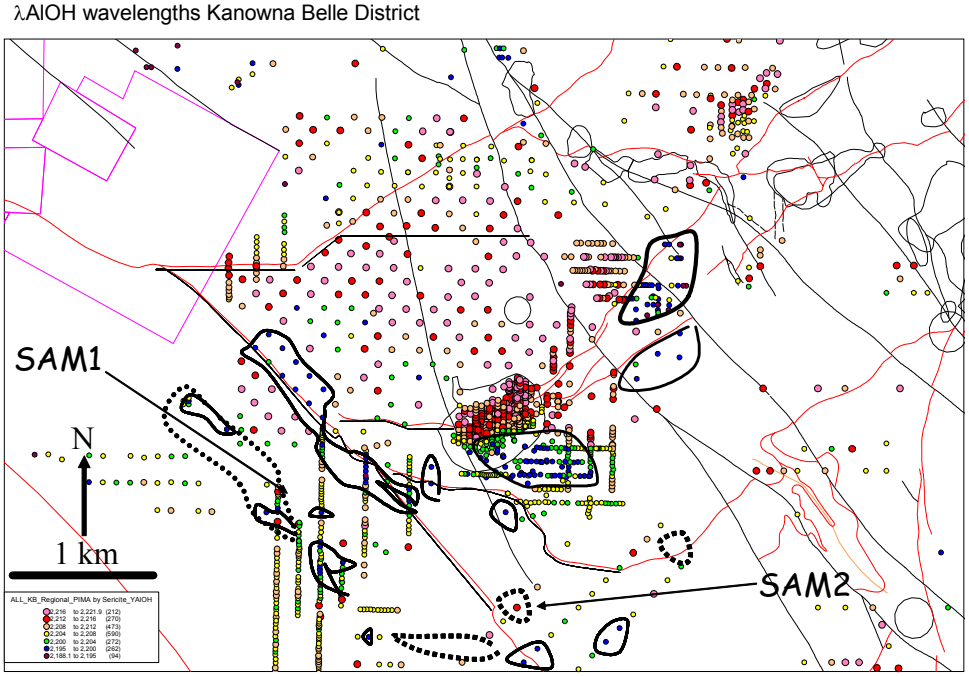

Fig. 62: Map of λAlOH for the Kanowna Belle district. Note the strong gradient in wavelengths across the Kanowna Belle deposit from footwall (long wavelength) to hangingwall (short wavelength). The Lowes Shoot

occurs within the long wavelength domain. Black contour shows λAlOH less than 2200; taken to reflect acidic alteration conditions with muscovite and possible paragonite based on the observations from Velvet Hole KDU1648; 300-350m'just west of Kanowna belle. Black dotted contours are W highs (greater than 10 ppm) some of which correspond to the low wavelength domains.

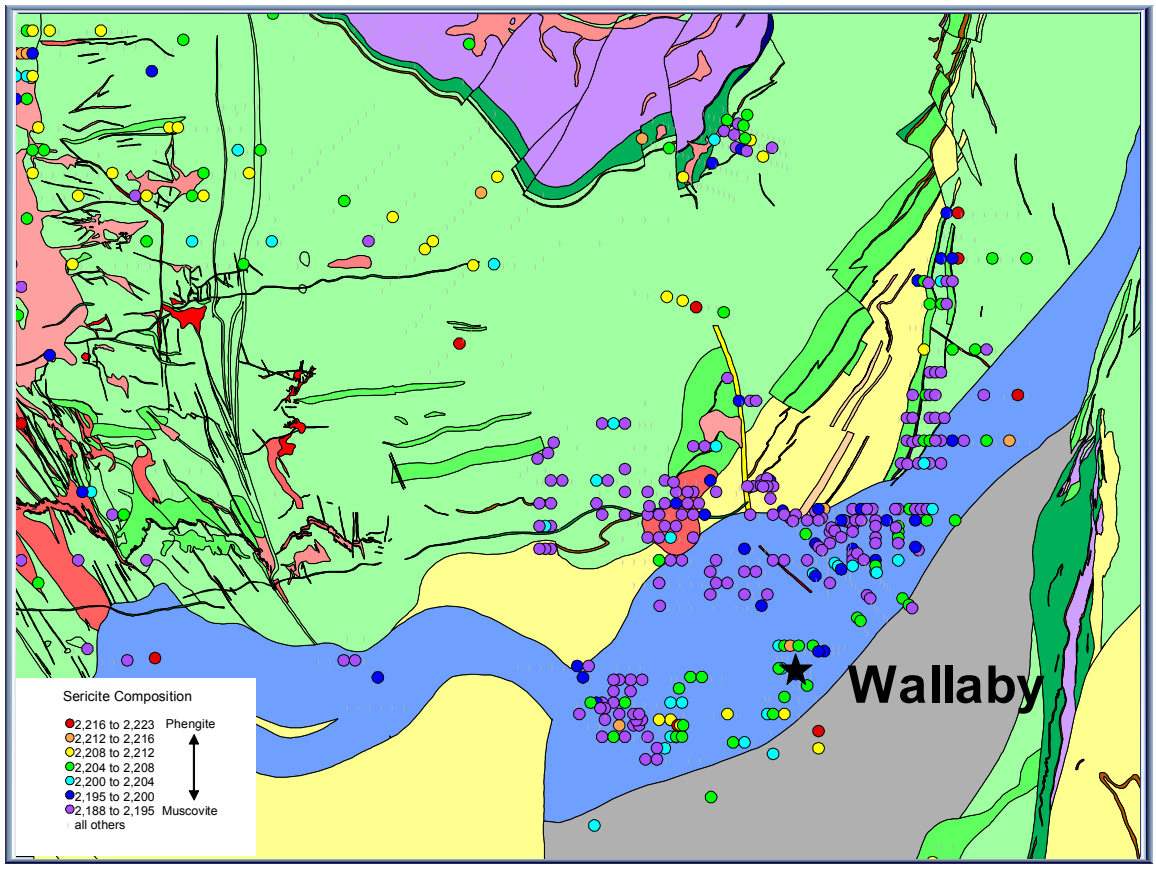

Fig. 63: Map of λAlOH for the Wallaby district. λAlOH less than 2200 (purple and blue dots) taken to reflect acidic alteration conditions with muscovite. Zone is coincident with mapped chloritoid, taken to indicate reduced and acid conditions.

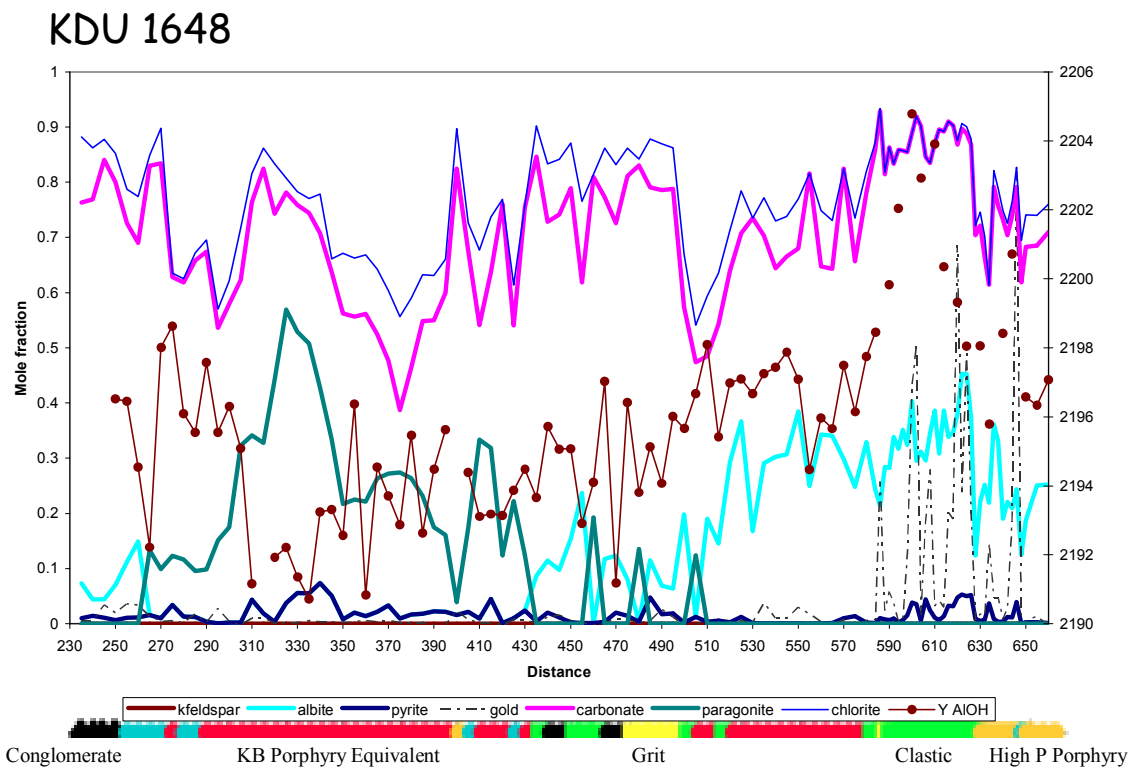

Fig. 64: Down-hole mineralogical variation for KDU1648, Velvet area, west of Kanowna belle, calculated from multi-element data, following procedures outlined in the appendix 3b. The plot gives the mole fractions (mole proportions normalised) of pyrite, albite, paragonite, carbonate and white mica (muscovite – phengite solution) and chlorite. Normalised gold abundances and the λ AlOH (SWIR) are shown for reference.

A zone of paragonite occurs from 300 to 350 m with bounding zones of muscovite ± chlorite (270-300 and 350-400). The paragonite zone corresponds with λ AlOH wavelengths of around 2190 to 2195 and is depeted in carbonate. Strong carbonate alteration with relatively little albite from 230-300 and 400-500 probably represents an outer carbonate halo to the paragonite zone. The mineralogical zonation suggests an overall fluid/rock reaction sequence of paragonite to white mica ± carbonate to albite ± carbonate. Pyrite occurs from 230 to 500 m with the best pyrite associated with paragonite.

Gold deposition is favoured by neutral to alkaline conditions. Gold in Lowes Shoot occurs predominantly within high AlOH SWIR wavelengths (V-bearing phengite domains) near the transition to low AlOH absorption wavelengths (to Ba-rich muscovite). The correlation between gold and white mica gradients at Kanowna Belle is evident at the pit-scale (Fig. 62). A strong gradient in wavelengths occurs across in the Kanowna Belle deposit from footwall (long wavelength) to hangingwall (short wavelength) with the Lowes Shoot located within the long wavelength domain.

In the Wallaby district, broad areas of low λ AlOH wavelength mica occur (Figure 63), implying widespread acid conditions, but again the deposit occurs with a domain of longer wavelength mica. The coexistence of chloritoid with short wavelength mica is consistent with reduced-acid conditions (Fig. 65).

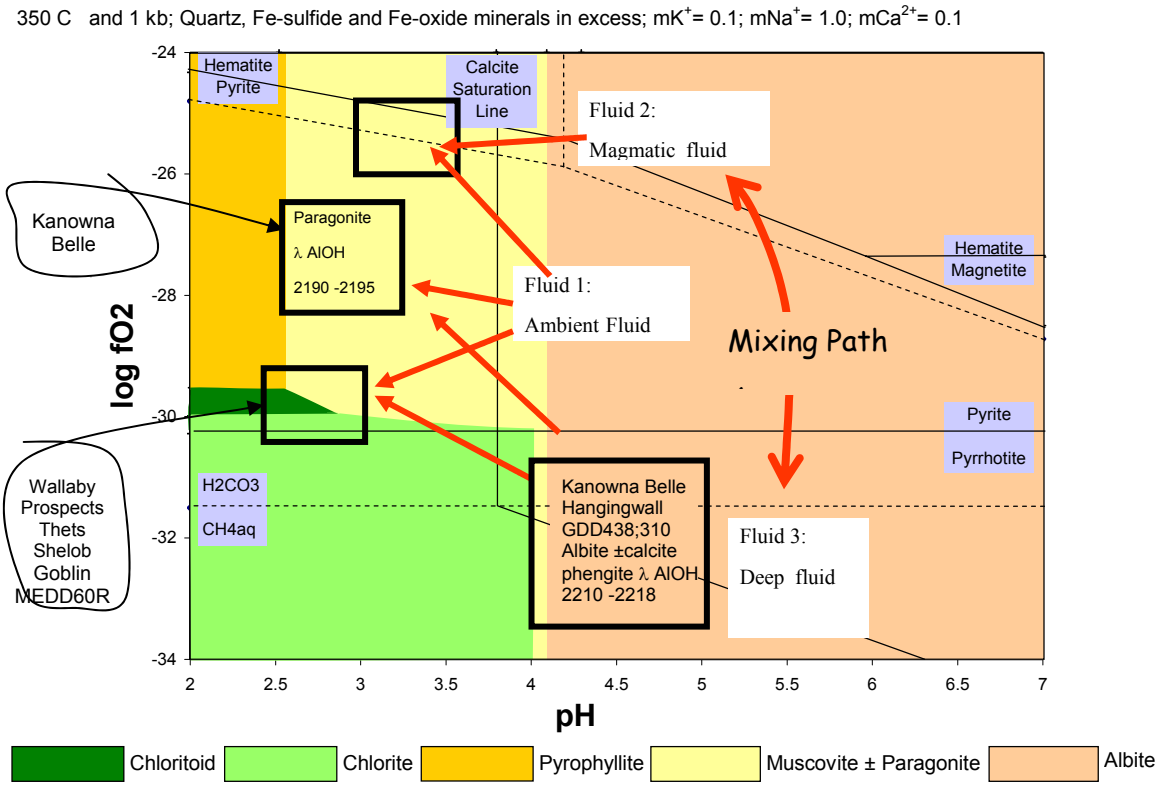

Fig. 65: Redox- pH plot illustrating the range in redox-pH conditions derived from interaction of the three different classes of fluids and fluid-rock reaction. Gold deposition processes appear not to generate acid, based on the λAlOH wavelengths observed in gold zones. Acid conditions occur subjacent to gold zones at the deposit scale and also the district scale.

The mechanisms of acid generation are not understood but spatial correlations hint that the generation of acid is in some way related to degradation of the fluids "with outlet zones" (pH scale is relative only. The absolute pH depends on the assumed K+ in solution).

Sulphide and Gold Precipitation on the Chemical Gradients

In theory, zones of pyrite, pyrrhotite, magnetite as well as Au zones will precipitate along the chemical gradients. Identification of domains of sulphide deposition on the gradients should help to identify domains of gold precipitation. In the Wallaby district, a domain of pyrrhotite precipitation occurs across a pH gradient from acid (short wavelength mica) to neutral-alkaline (long wavelength mica) to the northeast of the Wallaby pipe. The domain of pyrrhotite can be identified in the aeromagnetics and is strongly controlled by the architecture (Fig. 66). Similarly, a SAM survey west and south of Kanowna Belle (Fig. 67) may identify zones of pyrite (directly/indirectly) precipitated on redox-sulphur activity- pH gradients. The SAM responses occur subjacent to the domains of low wavelength mica and anomalous W indicative of acid/reduced fluids.

The long wavelength mica signal and the high W value centred on the SAM2 "doughnut" suggests a focused upflow zone of oxidized magmatic fluid surrounded by zones of reduced fluid with sulphide precipitation occurring on the redox gradient. The gold should occur within the W and phengite mica zone.

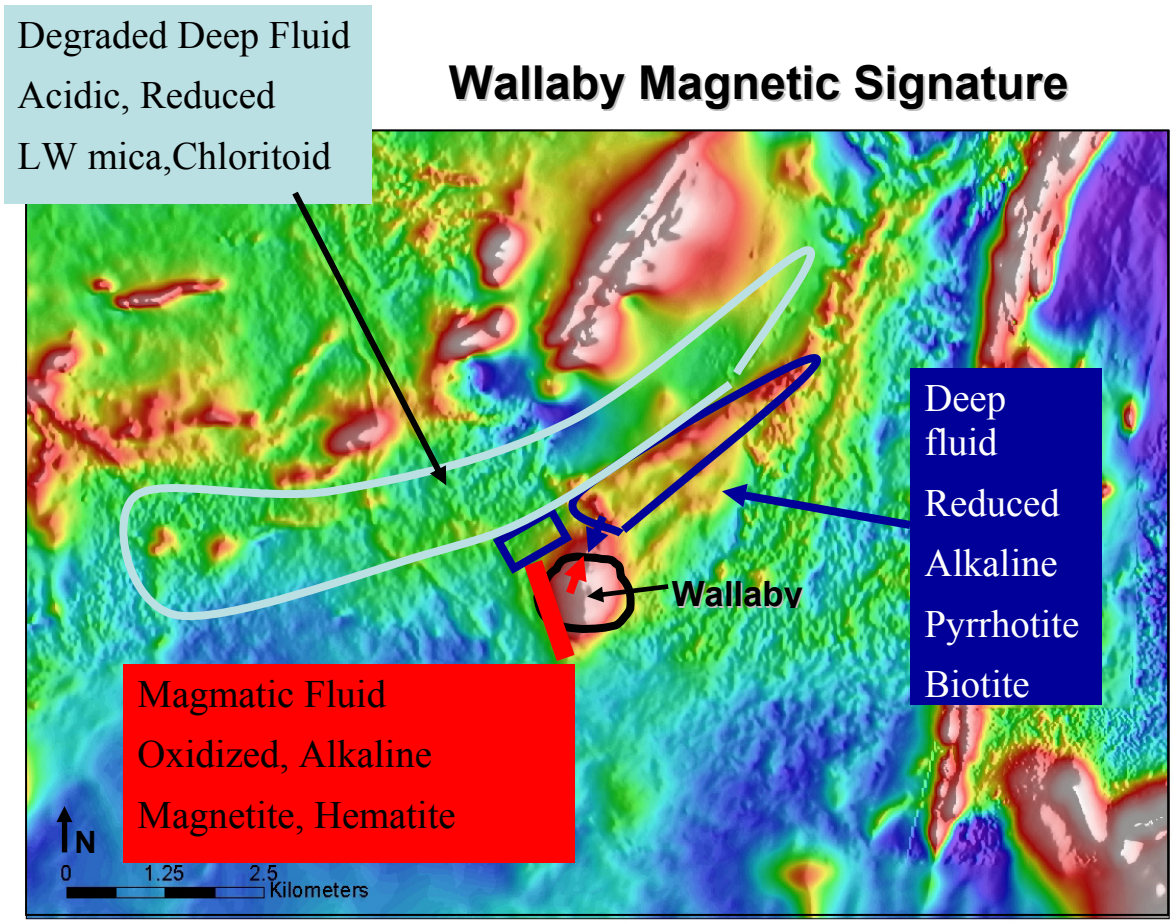

Fig. 66: Aeromagnetic map of the Wallaby district showing interpreted district-scale domains of reduced-acidic fluids (muscovite and chloritoid stable) and reduced-alkaline domains (pyrrhotite-phengite stable). The Wallaby pipe – magnetite stable - occurs subjacent to both domains.

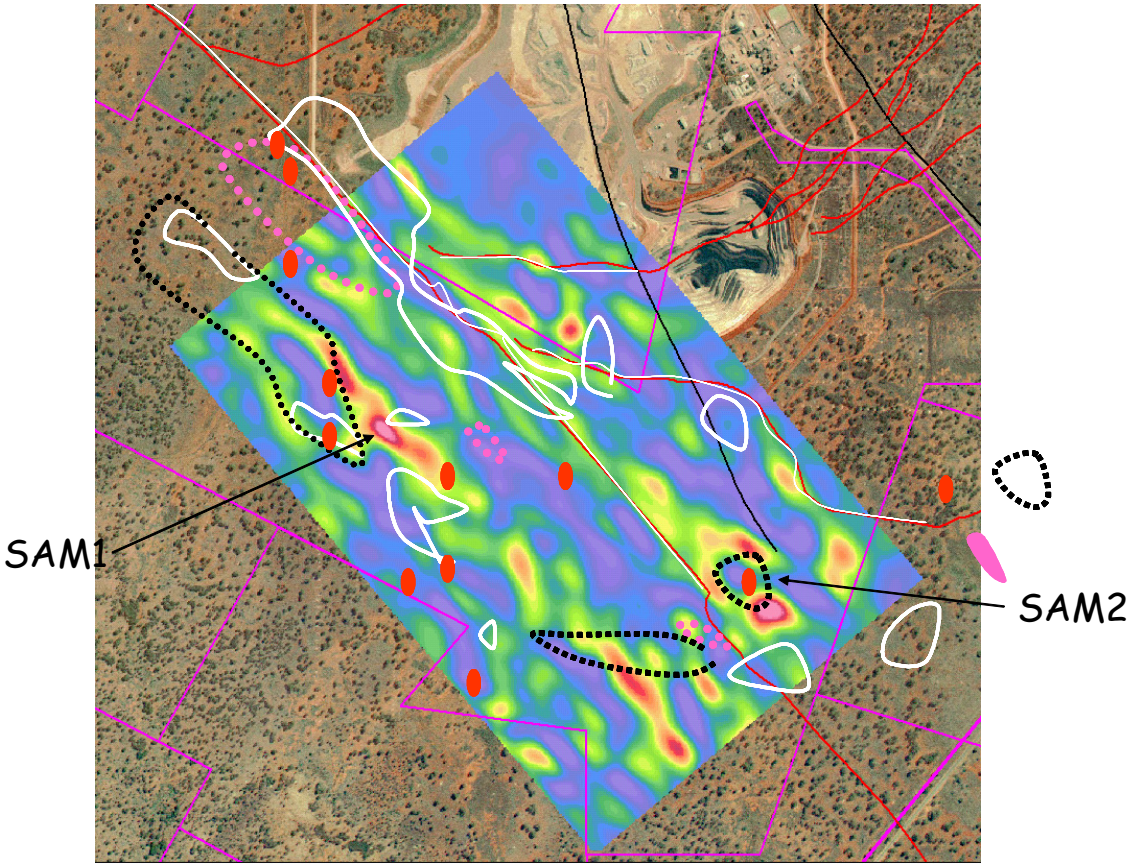

Fig. 67: Map of SAM survey south and west of Kanowna Belle with an overlay of PIMA data and W geochemistry. The SAM survey may be identifying (directly/indirectly) zones of pyrite and the overlays are an attempt to identify the chemical gradients that controlled pyrite deposition. In theory Au zones will be subjacent to the sulfide zones on the same chemical gradients.

Sulphur Isotopic Constraints on the Redox States of Fluids at Deposit to District-Scale

Sulphur isotope values in pyrite ($\delta^{34}S$) observed in Eastern Goldfields range from about -10 to +15 ‰. The range associated with high grade gold (greater than 10 ppm) mineralization is more limited; from -8 to +5 ‰ (Figs 68 and 69).

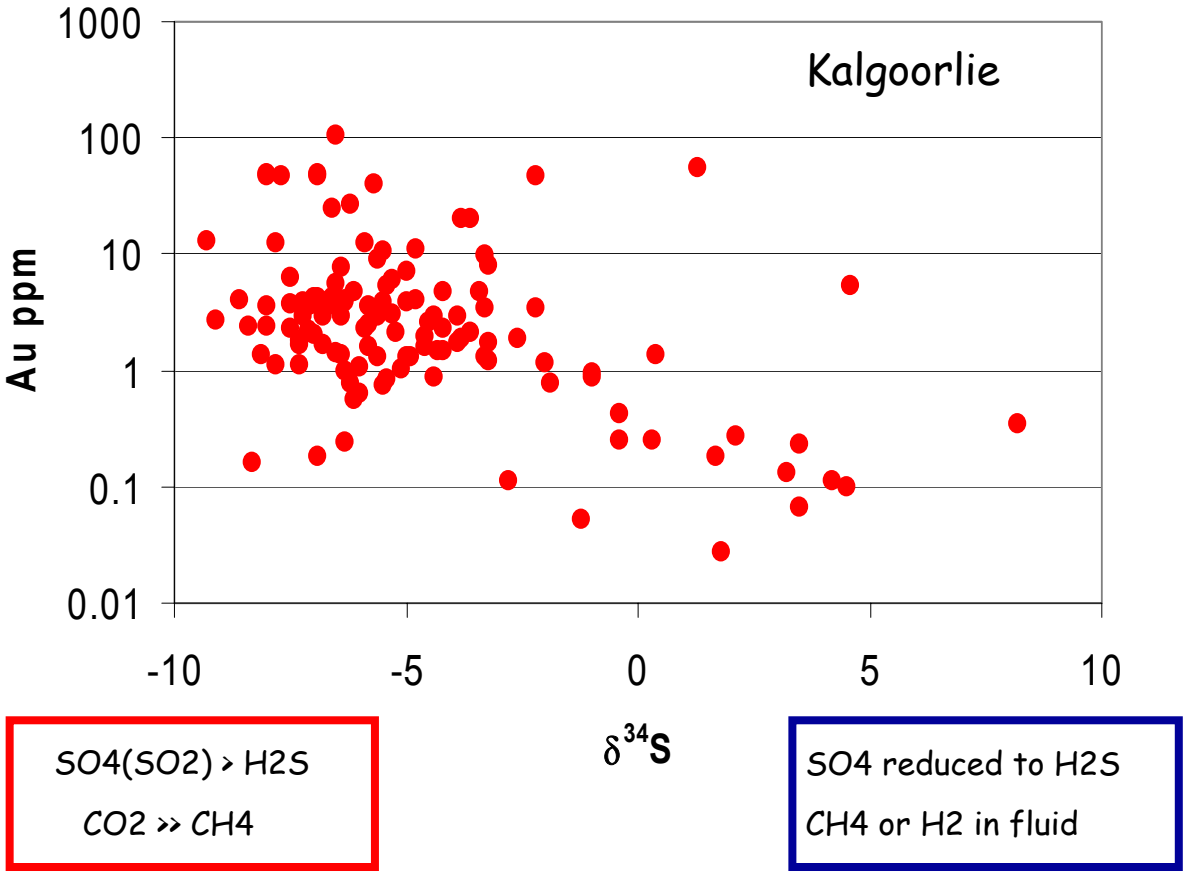

Fig. 68: The Golden Mile has a wide range of $\delta^{34}S$ values in pyrite, from –9 to +9 per mil. Clout (1989) demonstrated a strong correlation between gold grade and $\delta^{34}S$ values. High gold grades occur where there are negative $\delta^{34}S$ values, and positive $\delta^{34}S$ values occur in distal parts of the lode system. The Au - $\delta^{34}S$ correlation indicates that there was a shift from oxidation of H_2S to SO_4^{2-} within the gold zones to reduction of SO_4^{2-} to H_2S in proximal zones.

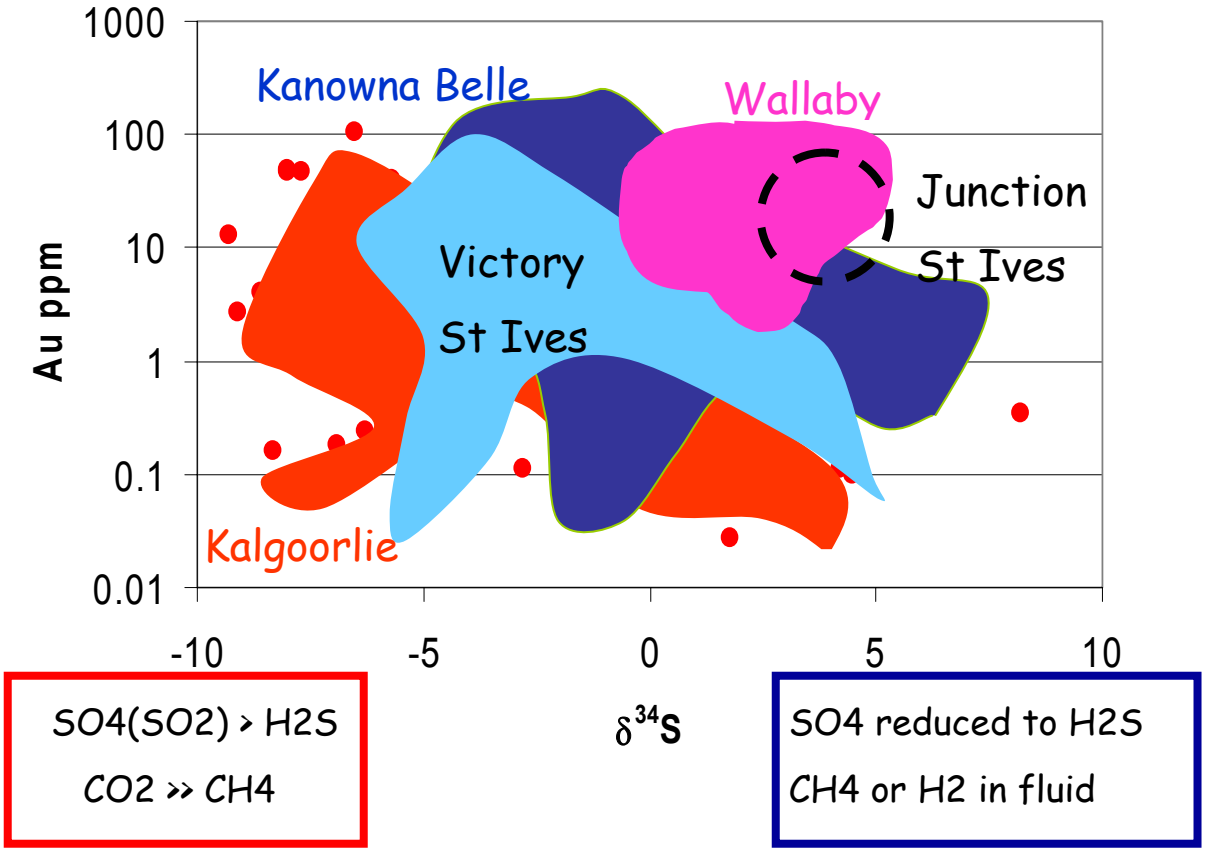

Fig. 69: The Kanowna Belle and Victory-Defiance deposits show a strong correlation between gold grade and δ34S values; comparable with the Golden Mile but without the strong negative signal in the high grade gold zones. By contrast high grade zones in the Wallaby deposit and Junction, St Ives, show more limited and positive δ34S values.

The most negative sulphur isotope signals in pyrite associated with high grade gold ($\delta^{34}S$ of 0 to -10 ‰) occur in the Golden Mile (Figures 68 and 69). These values, together with the mineralogical evidence, indicate that the gold deposited in highly oxidized conditions ($SO_4^{2-} \geq H_2S$). Low grade gold (< 1ppm) tends to be associated with more positive sulphur isotope values in pyrite (from about -3 to +8 ‰). The strongly positive values (> +3 ‰) are taken as evidence of reduction of sulphate or sulphur dioxide; the only known source of heavy sulphur in the system (Fig. 70). The reduction requires significant amounts of CH_4 or H_2 to be present in the fluids and implies that highly oxidized fluids ($SO_4^{2-} > H_2S$; $CO_2 >> CH_4$) mixed with highly reduced fluids ($H_2S >> SO_4^{2-}$; $CH_4 \geq CO_2$).

$\delta^{34}S$ values of pyrite from high grade gold zones in the Kanowna Belle deposit and Victory, St Ives, range from -5 to +5 ‰ (Fig. 69, Ren et al., 1994). As with the Golden Mile, the highest gold grades tend to occur with the lightest sulphur isotope values in the Kanowna Belle and Victory-Defiance deposits, athough the inverse does not hold. In contrast with the Golden Mile, pyrite from high grade zones in deposits such as Wallaby and Junction, St Ives, have positive $\delta^{34}S$ values (0 to +5 ‰). However, there is a limited data set for the Junction deposit.

The spread of sulphur isotope values associated with high grade gold indicates that gold deposited over a range of redox conditions from close to the SO_4^{2-} / H_2S buffer, in the case of the Golden Mile, to at or below the pyrite/pyrrhotite and CH_4/CO_2 buffers in the case of the Junction deposit. Other geochemical indicators are consistent with this conclusion both for the Golden Mile and the Junction deposit where pyrrhotite is a dominant phase and methane fluid inclusions are documented (Polito, 1999; Polito et al., 2001). The negative correlation between gold grade and $\delta^{34}S$ values of pyrite seen in the Golden Mile as well as the Kanowna Belle and Victory-Defiance deposits indicates oxidized fluids were dominant in the zones of maximum gold deposition, but reduced fluids were sufficiently abundant in some proximal zones to cause reduction of sulphate. The heavier sulphur isotope values of pyrite from the gold stage in the Wallaby deposit suggest redox conditions dominated by the reduced fluid and close to the stability conditions of pyrrhotite. While the Wallaby pipe is dominated by pyrite and magnetite, pyrrhotite is a common phase in the immediate environs and minor pyrrhotite is documented in the deposit associated with biotite shears.

Within the greater Victory area, St Ives camp, $\delta^{34}S$ values of pyrite correlate spatially with the camp-scale zonation from secondary magnetite, centred on the intrusive complex to subjacent domains of pyrrhotite (Fig. 71). This correlation of $\delta^{34}S$ pyrite with alteration mineralogy links the mechanisms that generated the range in $\delta^{34}S$ values with the mechanisms that generated the camp-scale alteration patterns.

In detail, $\delta^{34}S$ values of pyrite correlate with particular structures (Fig. 72). The negative signal is focused on the Repulse Fault which was a significant conduit for oxidized fluids. In contrast structures such as 32, Britannia and Sirius Shears yield the positive signal and can be interpreted as flow paths for reduced fluids and/or structures within which significant mixing and reduction occurred.

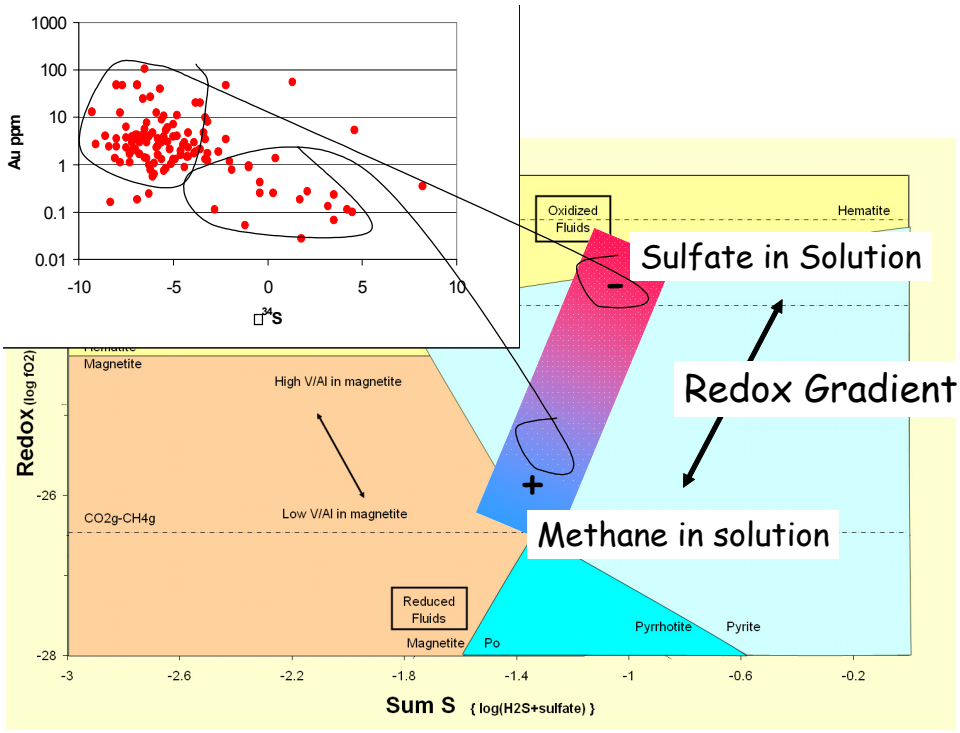

Fig. 70: Redox – sum S (in fluid) illustrating the range in redox conditions defined by the $\delta^{34}S$ of pyrite.

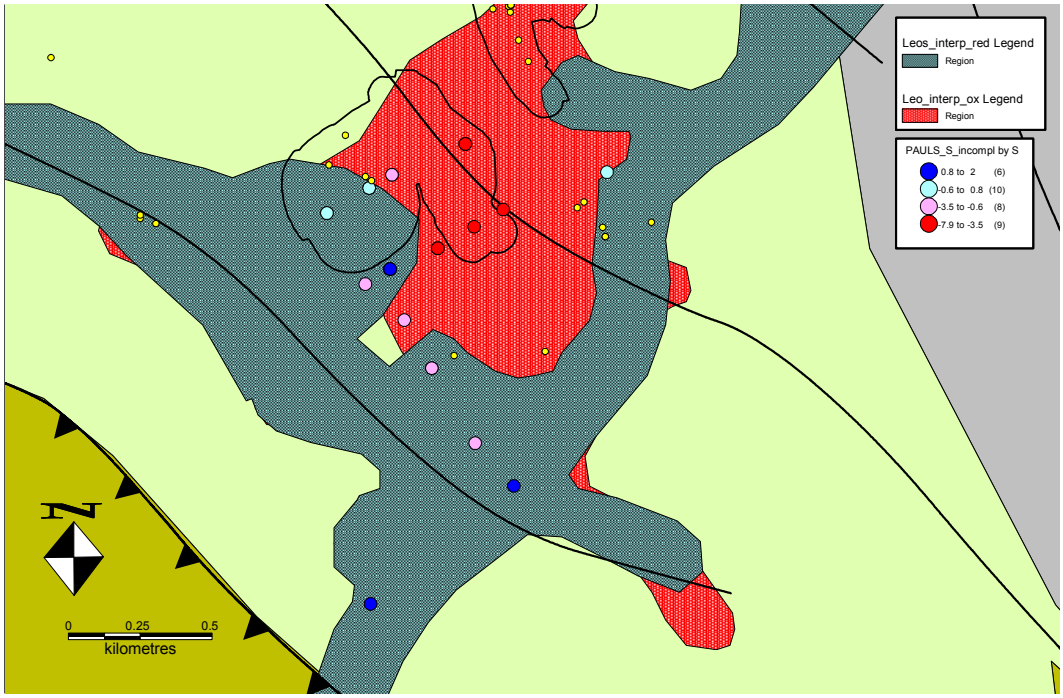

Fig. 71: Correlation of $^{\delta 3}$4S pyrite values with zones of secondary magnetite and pyrrhotite alteration in the Greater Victory Area, Central Corridor of the St Ives Camp.

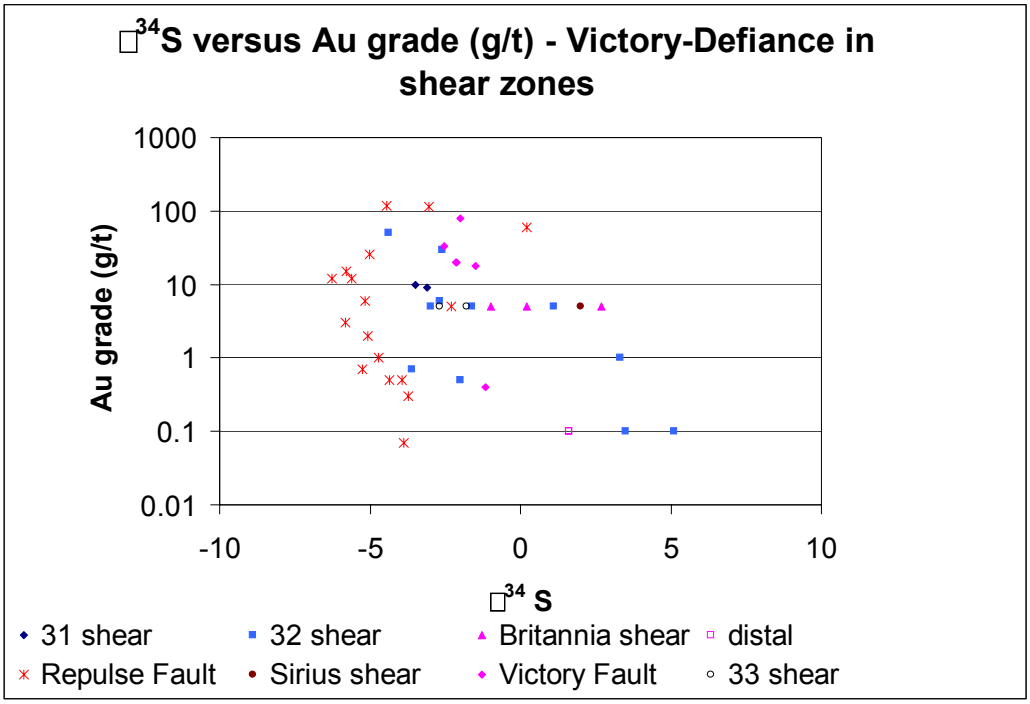

Fig. 72: Plot of gold grades vs δ34S pyrite for the Victory- Defiance area, illustrating that different structures show different S isotope values. The focus of the negative signal is on the Repulse Fault while the 32, Britannia and Sirius Shears yield the positive signal.

Gold Transport and Deposition (Q5)

Introduction

A number of physical and chemical processes can lead to the precipitation of gold mineralization. Whilst some processes have been extensively documented and discussed in literature for Archaean gold deposits (e.g., wallrock sulphidation, phase separation of the hydrothermal fluid), others have not been considered extensively in Archaean deposits (e.g., fluid mixing). The main processes which potentially lead to the precipitation of gold mineralization are:

- Wallrock sulphidation,
- Phase separation,
- Fluid unmixing,
- Fluid mixing.

This section provides first constraints on the chemistry of the main fluid types in the system using alteration mineral assemblages and stable isotopes and then discusses the different precipitation mechanisms. There is no doubt that in a typical Archaean gold deposit many of these processes operate sequentially or even simultaneously in different parts of the system.

For exploration purposes, however, it is critical to determine which of the processes precipitated the bulk of gold mineralization and provides the best guide to ore.

Isotopic and Mineral Constraints on Fluid Chemistry

The fluid chemistry can be read using the alteration mineralogy and stable isotopes as well as whole-rock, multielement chemistry. In the St. Ives gold camp, sulphide-oxide mineral assemblages provide an easy to read guide to the redox state of the hydrothermal fluids. The mineralogy can be determined in hand-sample using a hand lense, or with fine-grained minerals using a polished thin section. Pyrrhotite-arsenopyrite and pyrrhotite-pyrite assemblages indicate quite reduced hydrothermal fluids. Loellingite would indicate even more reduced fluids, but has not been documented in the camp. Magnetite-pyrite assemblages indicate moderately oxidized fluids, and hematite-pyrite assemblages indicate oxidized fluids. The presence of anhydrite in the alteration assemblages would indicate extremely oxidized hydrothermal fluids. This comparison provides only a rough guide, because it assumes that the minerals formed approximately at the same temperature.

The composition of alteration mineralogy can also be read in PIMA short wave infrared (SWIR) spectra such as that developed for Kanowna Belle. White mica AlOH absorption wavelengths across Lowes Shoot are zoned from phengitic compositions (2212-2216 nm) to muscovitic compositions (2200-2204 nm). Gold in Lowes Shoot occurs predominantly within phengititc white mica domains near the gradient to muscovitic AlOH wavelengths. Electron microprobe analyses show that ore-related phengites have elevated V (650 ppm), Mg (2 wt. %) and high K/Al ratios (0.38 - 0.40) relative to muscovite (V = 250 ppm, Mg = 0.5 wt. %, K/Al = 0.33) in the distal envelope. Muscovite Ba contents (2800 ppm) are higher in than in the V-rich phengite (1500 ppm) proximal to ore.

The regional Kanowna Belle spectral map is dominated by a cell of phengitic white micas, surrounded by a muscovite envelope. The asymmetry in white mica compositions at the mine can be explained in terms of being on the edge of a regional plume of white mica alteration. The northern edge of the plume is defined by the Slimes Dam Fault, the southern edge is defined by the Fitzroy Fault. A map of the mica crystallinty index (defined by the depth of the AlOH absorption feature relative to that of H_2O abortion) shows that highly crystalline micas occur in the core of the phengite cell, whereas less crystalline white micas occur around the edges.

We interpret variations in white mica crystallinity to reflect a temperature gradient from high in the core of the plume to low around the edges. Lower temperatures on the margins possibly caused pH to decrease below phengite stability to muscovite. The transition from V-rich phengite (oxidised) associated with ore to Ba-rich (reduced) muscovite implies that a redox gradient controlled the composition of white micas.

Fluid Inclusion Constraints on Fluid Chemistry

St. Ives Camp

The hydrothermal fluid composition varied significantly between the different stages of hydrothermal alteration. The diversity of fluids was described earlier in this report and this section focuses only at the intermediate fluid stage which is related to gold mineralization. Detailed petrographic observations on growth zones in gold-related dolomite indicate that

the cycle starts with aqueous fluids of high salinity (< 23 wt% NaCl equiv.). The origin of this high salinity fluid is unclear at present. However, the subsequent fluid changed rapidly to a low salinity H_2O-CO_2 and CO_2-H_2O fluid indicating the influx of a new, high-temperature (> 280º C) fluid and/or dilution of the original high-salinity aqueous fluid. Importantly, the change in fluid composition is characterized by sudden increase in fluid inclusion size and a rapid decrease in the Fe content and increase in Mn content of the hosting dolomite mineral. Together this is taken as evidence of rapid mineral growth, whereas outer zones of the dolomite indicate slow growth. The rapid change is also accompanied by precipitation of scheelite. Laser ICP-MS data indicate that the fluid contained Na, K, Zn, As, V, Rb and Pb at elevated levels. Importantly, fluid densities of the earlier aqueous and the later aqueous-carbonic inclusions can only be interpreted with either a pressure drop or a combined pressure drop and temperature increase during this stage. At present, it is interpreted that the timing of the rapid fluid change and rapid dolomite growth coincides with the onset of pyrite and gold deposition.

New Celebration

1. The earliest observed $CH_4 \pm CO_2$ fluid inclusions possibly represent a background, regional scale fault zone fluid. The source of this fluid is unknown; it may be mantle derived or could be a deep-crustal metamorphic fluid.
2. At or near peak metamorphism the fault experienced a localised burst of hot fluid of unknown origin (possibly magmatic?) overwhelmed the background fluids and formed early aqueous-carbonic inclusions in calcite. As this fluid cooled at approximately constant pressure it interacted with iron-rich wall rocks, which triggered the early mineralizing event, precipitating Porphyry and Mylonite (and possibly Contact?) style gold due to desulphidation reactions.
3. Early mineralization was overprinted by aqueous fluid
4. At post-peak metamorphic conditions (late D3 or early D4?) a second, localised burst of fluid, slightly cooler than the first, was injected into the fault. This formed the second, late mineralizing event, possibly by phase separation, although further data are required to confirm this scenario.
5. This was followed by a cool dense brine, which formed the late secondary, highly saline inclusions.
6. As the localised mineralizing fluids dissipated, the fault returned to steady state with background, regional scale methane-dominated fluids returning.

Exploration Significance

Introduction

Within the previous sections in this synthesis, it was attempted to demonstrate that two main geological features control the location of gold mineralization: 1) structural architecture, and 2) chemistry of hydrothermal fluids (which result in spatial distribution patterns of

hydrothermal alteration at a camp scale). Taking one of the features in isolation as a guide to gold mineralization may work sufficiently, but will also result in a number of failed targets. The key to success appears to be the combination of the architecture of both structures and geochemical alteration at least at camp scale and most likely at regional scale. Whilst this project made some inroads to define both architectures (structural and chemical) in the same camps, different camps have reached different maturity in the structural and alteration data sets and, therefore, a fully coupled chemical and structural architecture for single camps will be part of the Y-new project.

Both the structural and alteration evolution in large gold deposits and camps is typically complex. For the effective use of structural and spatial alteration data sets as a guide to gold mineralization, detailed timing of structures and alteration types needs to be determined in the camp.

The purpose of this section is to demonstrate how the research results on the structural evolution and the timing and spatial distribution of hydrothermal alteration can be used for targeting new gold ore bodies. As demonstrated in previous sections the critical observation is that multiple fluids of different chemistry were present in the gold camps at different stages of evolution and also, most likely, at the same time during gold precipitation. The key assumptions for the discussion below are that:

1. Different fluids were in the system and have some significance during gold precipitation.
2. Different structures potentially contain different hydrothermal fluids.
3. Interaction (mixing) of contemporaneous fluids is a powerful gold precipitation mechanism, but is most likely not the only precipitation mechanism.
4. Interaction (wallrock reaction) of hydrothermal fluids with previously precipitated alteration from a fluid with different chemistry (e.g., redox, pH) is also a powerful gold precipitation mechanism.

Structural implications for exploration

The exploration significance of the Golden Mile field based study contained in this report is multiple and relate to a wide range of scales.

The Golden Mile is a giant gold deposit hosting in excess of 60 Moz of gold. The deposit is approximately 4km in strike length and 500m in width. The deposit occurs within a mineralization envelope approximately 10km in strike length extending from the Golden Mile deposit at the southern end to the Mt-Percy deposit at the northern end. This mineralization envelope is contained within a broader carbonate alteration halo, the extent of which is not well constrained because it extends outside of the effective diamond drill hole coverage available.

Fimiston lodes, which host gold mineralization at the Golden Mile deposit, are spatially and temporally associated with feldspar porphyry dykes and later mafic alkaline hornblende porphyry dykes. The dykes and lodes share a common set of orientations and a clear spatial association. The feldspar porphyry dykes are associated with early stages of the Fimiston paragenesis consisting of carbonate-magnetite-hematite veins and breccias. The hornblende

porphyry dykes are syn-mineralization and associated with the later stages of the Fimiston paragenesis.

Fimiston lodes are overprinted by a penetrative NW, steeply W-dipping cleavage associated with NE-SW shortening. The Fimiston lodes typically display buckling consistent with bulk shortening.

The Mt-Charlotte deposit occurs only a few kilometres to the north-northeast of the Golden Mile deposit and is a multi-million ounce gold deposit. Mt-Charlotte is a late tectonic quartz-carbonate vein stockwork hosted in the granophyric portion of the Golden Mile Dolerite. The Mt-Charlotte quartz-carbonate veins clearly post-date the penetrative NW steeply W-dipping cleavage.

The presence of the Mt-Charlotte deposit in close proximity to the Golden Mile deposit has important exploration significance. Both deposits have completely different mineralogical associations, structural controls and timing of emplacement. Nonetheless both deposits are highly attractive exploration targets. The Mt-Charlotte deposit has a small surface footprint (a few hundred meters in strike length) and no geophysical signature. It is therefore quite conceivable that other Mt-Charlotte style deposits remain undiscovered to this day.

The implication is that from an early stage of exploration there should be a recognition of the style of gold mineralization present and of the appropriate geological characteristics.

The exploration guidelines for the Golden Mile listed below should be viewed in context. These guidelines will be of variable applicability elsewhere depending on data density and there will also be a large degree of variability related to the local geological context.

Some of the important exploration guidelines for the Golden Mile deposit derived from the present field study are as follows:

1. Large scale gold anomaly associated with As, Sb, Hg, Te and Ag. No significant Cu and Zn association. The pathfinder elements may display zonation patterns, which would likely vary according to the nature of host rocks and the erosional level.
2. Early fault jog, marked by a change in orientation of feldspar porphyry dykes and a change in the thickness and overall abundance of the feldspar porphyry dykes. Also a change in the orientation and geometry of the upright Kalgoorlie syncline-anticline fold pair.
3. The presence of early carbonate-magnetite veins and breccias extend quite far outside of the Golden Mile mineralization envelope and constitute an important exploration vector.
4. The presence of a favourable host lithology with a favourable geometric setting. The Golden Mile Dolerite forms an ideal host lithology by its competency, thickness and composition. In particular, the structural repetition by folding of the Golden Mile Dolerite and the shallow dipping eastern limb of the Kalgoorlie synclines allows the formation of a funnel shaped array of lodes, which is an ideal geometry to form a large deposit.
5. The presence of feldspar porphyry dykes, particularly those with high level textures. The significance of these dykes is as an indicator of the erosional level, and they also indicate the presence of early structures.

6. The presence of mafic alkaline dykes, altered and spatially and temporally related to gold bearing structures. These dykes may not be volumetrically important but they reflect an important magmatic evolution, which may have an important link to gold mineralization.
7. The presence of conglomerates along linear structures spatially associated with feldspar porphyry dykes. These conglomerates contain clasts of feldspar porphyry and are themselves cut by feldspar porphyry, which indicates the close temporal association of sedimentation and porphyry emplacement. The conglomerates are an important marker of early structure and potentially mark a favourable erosional level.
8. The Golden Mile presents a clear vertical zonation of gold grades. The whole deposit and individual lodes present clear vertical zonations of gold grades. Most of the high grade lodes are concentrated in the top 400m of the deposit both in the Western and Eastern Lode Domains. Nonetheless, some high grade lodes, such as the Phantom group of lodes, occur at depth and have no surface expression. Therefore, vertical gradients have to be taken into account.

Find the chemical gradients

What are the main geological features to assist with targeting

In the St. Ives camp, two different types of gold deposits are distinguished with respect to redox state of the hydrothermal fluids: 1) reduced deposits (e.g., Argo, Junction), and 2) oxidized deposits (e.g., all deposits in the Central Corridor, Bahama, Santa Anna). Whilst this project had some detailed studies on the reduced deposits, critical spatial data sets still need to be collected. Therefore, the discussion below focuses on the oxidized deposit group in the Central Corridor where most data sets which are necessary for interpretation are available. Further, despite a long and multistage alteration history in the camp which was described earlier, the discussion focuses directly on alteration types which have a direct link, or provide a vector, to gold mineralization.

There is a range of geological features that have a spatial relationship and in some cases a demonstrated genetic relationship, to gold mineralization. These are:

- Gravity lows, interpreted to represent felsic and intermediate intrusions at depth (>500m – 950m below present surface).
- Abundance of felsic and intermediate porphyries.
- Distinct magnetite alteration (with locally hematite, oxidized alteration assemblage) halo centred on gravity low and abundance of porphyry intrusions.
- Pyrrhotite alteration (reduced alteration assemblage) outboard to the SW and NE of the oxidized alteration assemblage.
- Strong magnetic response indicating presence of magnetite.
- Weak magnetic response coincides spatially with pyrrhotite (reduced) domain.
- S isotope zonation with strongly negative signals in oxidized zones and zero to positive signals in the reduced zones.

Although all these geological features are straight forward to read in the various data sets, it has to be understood that some of these features are more complex and need to be read more detailed to be useful for exploration. For example, the magnetite halo is readily detected using magnetic data sets either on a camp or drill core scale. However, there are at least two, probably more generation of magnetite in the rock record. Preliminary data sets on magnetite chemistry using laser ICP-MS analytical techniques suggest, however, that magnetites which immediately predate gold, form a disseminated halo around gold-bearing structures and are the best guide to gold mineralization, are distinct in their chemical composition (e.g., high V/Al ratios, high Zn and Mn content). Similar identification criteria have also been established in the whole-rock multielement data sets. For example, the early epidote alteration, which contains significant magnetite veins and disseminated magnetite, is chemically distinct in whole-rock analyses with high Te, Bi and Ge concentrations. There is also a clear link of specific alteration types (e.g., epidote alteration) and at least one generation with specific porphyry types. These relationships are currently investigated in greater detail and will be reported in Y-new.

The structural controls on the distribution of the reduced assemblage are less clear except that the structures appear to originate outboard of the Central Corridor. There is some evidence for this hypothesis to the SW of the Conqueror area where pyrrhotite is controlled by a gently SW dipping structure. High abundance of pyrrhotite, which spatially correlates with E-W trending structures in the Revenge area, may also indicate an E-W control on the reduced fluid flow.

How Do We Read the Chemical Gradients in the Rock

The key to use geochemical or mineralogical data sets as a guide to gold mineralization is to determine the spatial distribution of signals which indicate flow pathways of hydrothermal fluids with a particular chemistry. Hydrothermal alteration is the product of the chemical composition of the incoming hydrothermal fluid(s) and the chemical composition of the host rocks. Consequently, hydrothermal fluid compositions are best compared by documenting hydrothermal alteration within host rocks of similar chemical composition. However, calibration across host rocks allows reading the signals also in different host rocks.

Spatial data sets indicate that gold mineralization is not bound to a particular fluid type. It is located in zones where spatial data sets indicate a change in the chemistry of the fluid. For example, in the St. Ives camp, gold is located proximal to the boundary between oxidized and reduced domains (Figs 73, 74, 75, 76, 77). This indicates that at least one of the controls on the location of gold mineralization is the interaction of at least two different hydrothermal fluid systems. This interaction resulted in the drastic change of the chemical properties of both fluids and destabilized the gold complexes focusing gold precipitation into a small volume of rock. For this mechanism to operate effectively, it is not important to have the fluid at a specific redox state. The critical factor is to create a drastic change in redox conditions, i.e. a gradient. Whilst redox gradients appear to be the most important control on the location of gold mineralization in the St. Ives gold camp, there are a number of other chemical gradients which potentially are powerful gold precipitation mechanisms and are documented elsewhere (e.g., Kanowna Belle). These are:

- redox

- pH
- S

For exploration purposes, it is critical to collect data sets which allow to map flow pathways and the chemistry of the hydrothermal fluids and also determine the location of zones where fluid chemistry changed dramatically, i.e. the location of chemical gradients. The best data sets to track chemical domains and zones of drastic change in the fluid chemistry (gradients) are:

- sulphide-oxide mineralogy
- PIMA or other spectral technique
- Multielement, whole-rock geochemistry
- S-isotope data
- C-O isotope data on carbonates
- Magnetite chemistry

The sulphide-oxide mineralogy is best tracking the redox state of the hydrothermal fluid. Importantly, single minerals do not necessarily indicate a particular redox state and observation of assemblages is needed. For example, arsenopyrite-pyrrhotite assemblages indicate reduced conditions and from reduced to oxidized conditions pyrrhotite-pyrite, magnetite-pyrite, hematite-pyrite assemblages are observed. This classification is strictly only correct, if the minerals formed broadly at similar temperature and pressure conditions.

PIMA and multielement data sets can also be used to track fluid chemical compositions and have been described in detail above (e.g., for Kanowna Belle).

Sulphur isotope data sets are also tracking redox changes in the hydrothermal fluid. If for example an oxidized sulphate is reduced, then S isotopes fractionate as such that the oxidized assemblages have extremely negative values, whereas the reduced assemblages have zero or positive values. The interpretation of S-isotopes as redox pairs is strictly only valid, if there was no sulphur source with strong positive values in the system.

Carbon isotopes can be used to track whether there was a strong reductant in one of the hydrothermal fluids. Reduction would be indicated by quite negative $\delta^{13}C$ around -6 to -8 ‰. If the reduction was extreme, strongly positive values would be observed. The co-variation of S- and C-isotopes in cogenetic sulphides and carbonates is a powerful tool to determine zones where both extremely reduced and oxidized fluids were present, i.e. zones of maximum chemical gradient and best conditions for gold precipitation.

Grade versus Tonnage Controls

Grade controls

In the St. Ives gold camp, redox domain boundaries and high-grade gold intersections have a clear spatial relationship. This is particularly obvious in the Victory-Defiance, Britannia, Sirius, Conqueror and Orchin/North Orchin gold deposits. In the Greater Revenge group of deposits, reduced and oxidized zones are much more intricate and complex which might

mask some of the relationships. However, even there, high-grade gold intersections are located at redox domain boundaries.

In the Victory-Defiance group of deposits, the oxidized domain is focused and envelopes all the deposits. The reduced domain is located outboard of the oxidized domain. High-grade gold intersections (> 100 g/t) are located at the domain boundary within about 100 m in 2D, but always within the oxidized domain. This is also supported by drill core observations at the domain boundary, where gold grades always occur with magnetite halos and locally with specular hematite. The reduced fluid conduits and domains contain only low levels of gold if any (< 1 g/t, mostly around 0.1 g/t). In Figures 73, 74, 75, 76, and 77, gold grades were plotted as classes in 2D. Only really high-grade intersections are strongly focused at the domain boundary, but lower grades are more dispersed from the domain boundary. Importantly, even lower gold grades occur within the oxidized domain.

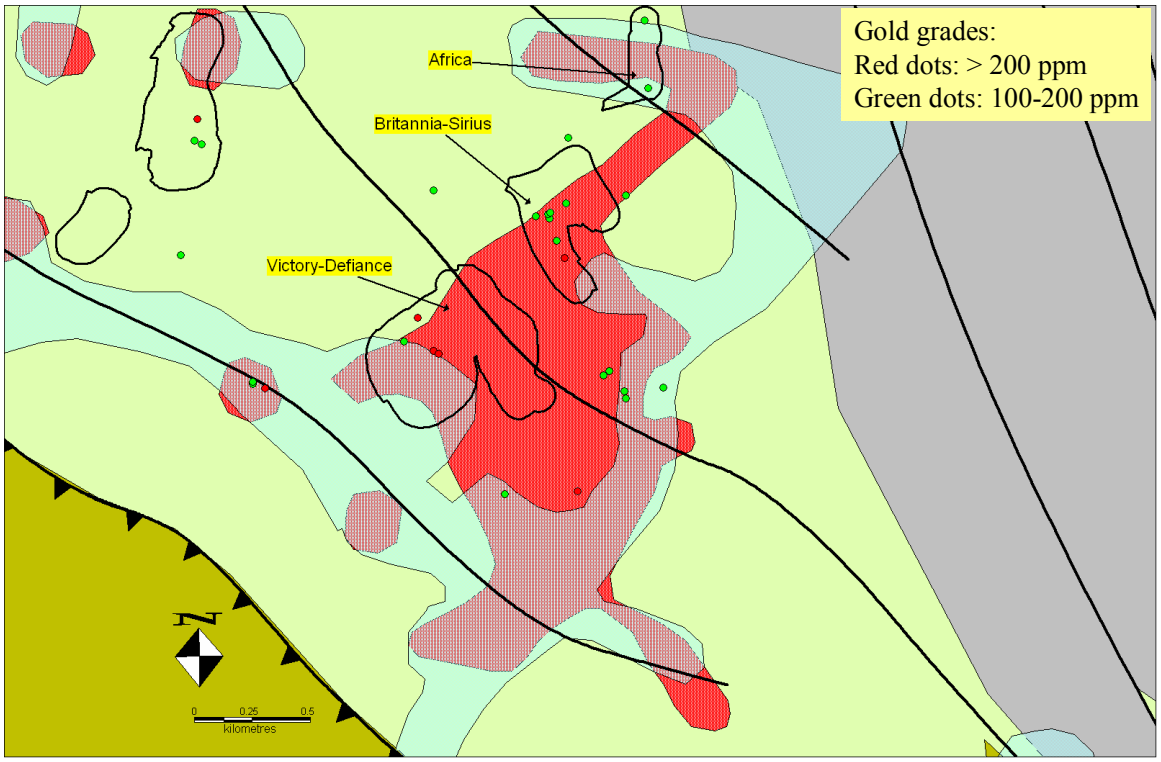

Fig. 73: Geological map of the Victory-Defiance area showing distribution of gold grades with respect to redox domains.

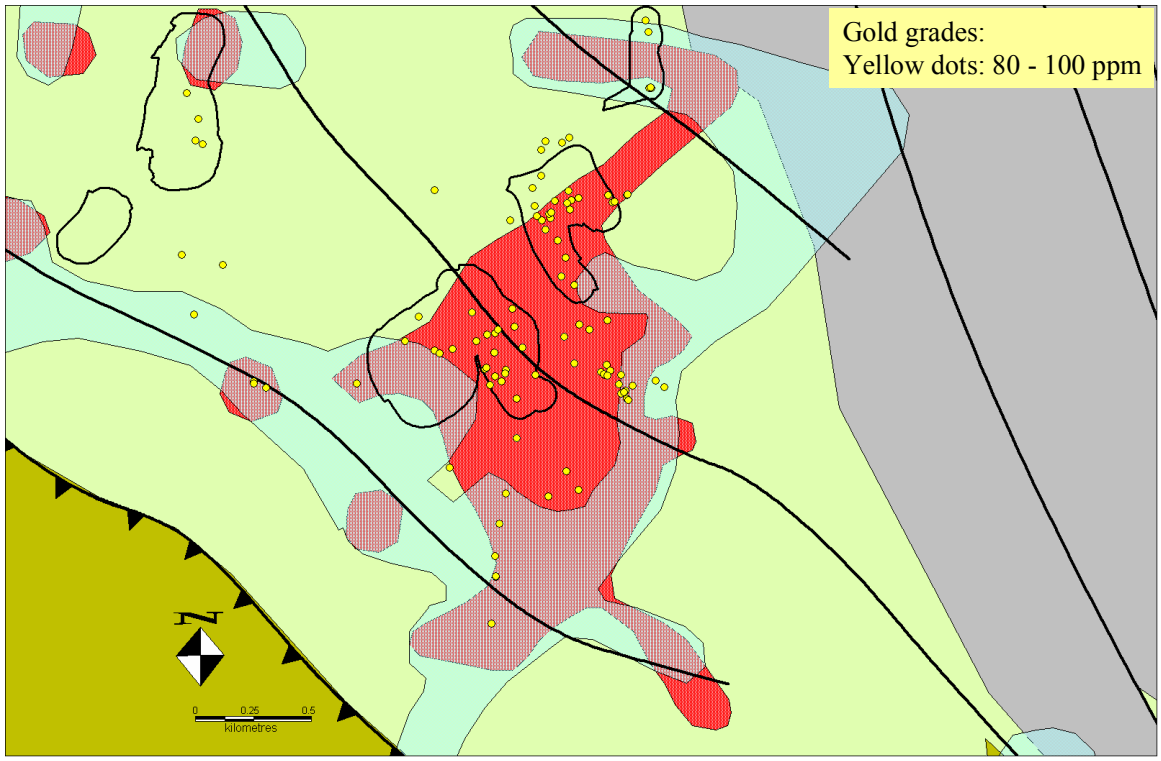

Fig. 74: Geological map of the Victory-Defiance area showing distribution of gold grades with respect to redox domains.

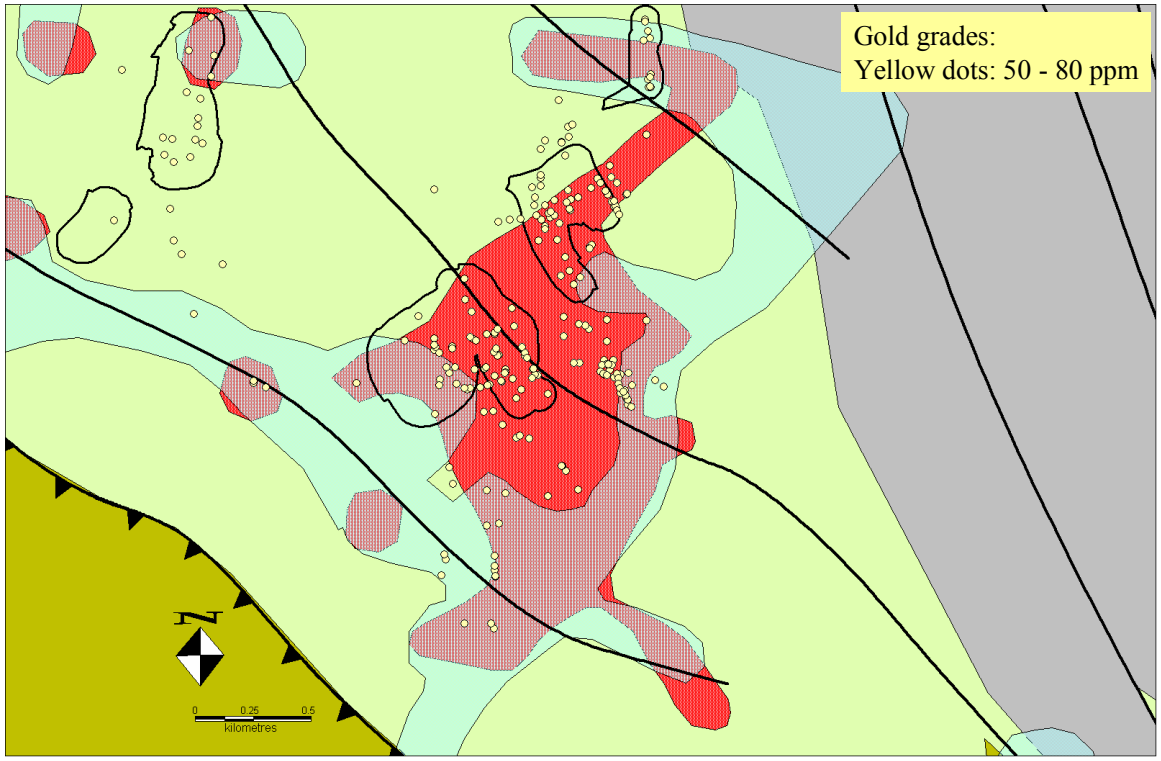

Fig. 75: Geological map of the Victory-Defiance area showing distribution of gold grades with respect to redox domains.

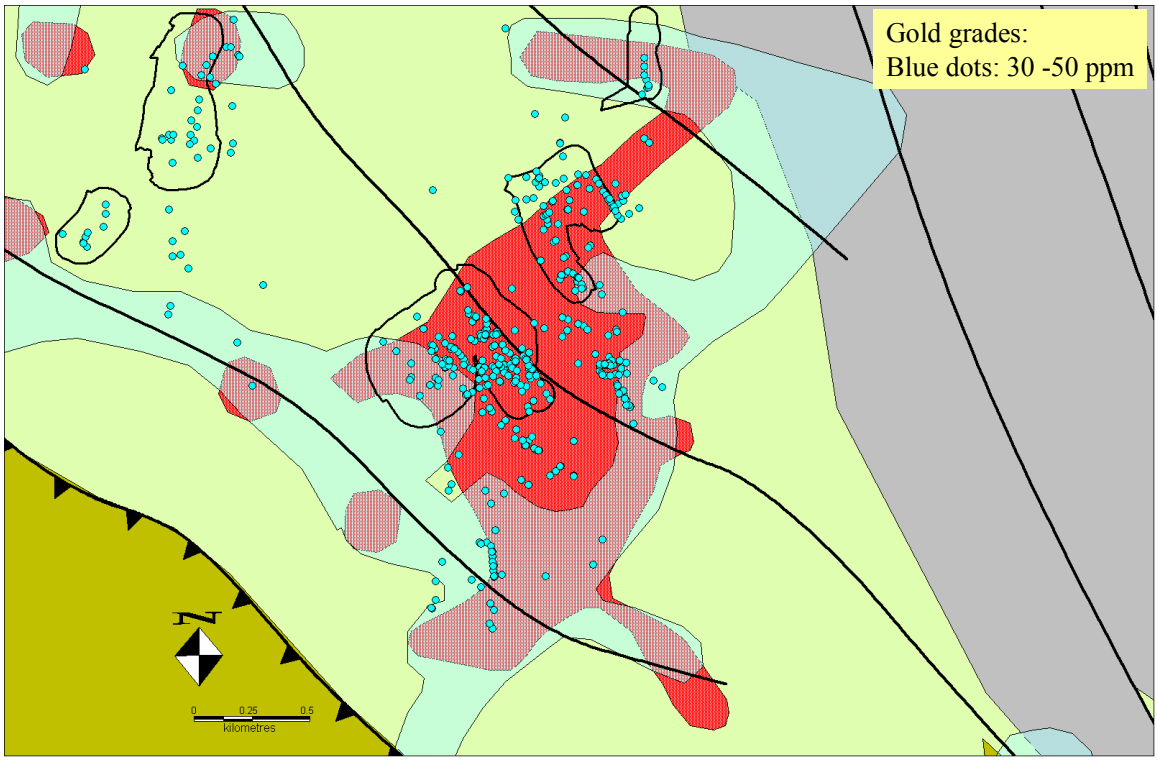

Fig. 76: Geological map of the Victory-Defiance area showing distribution of gold grades with respect to redox domains.

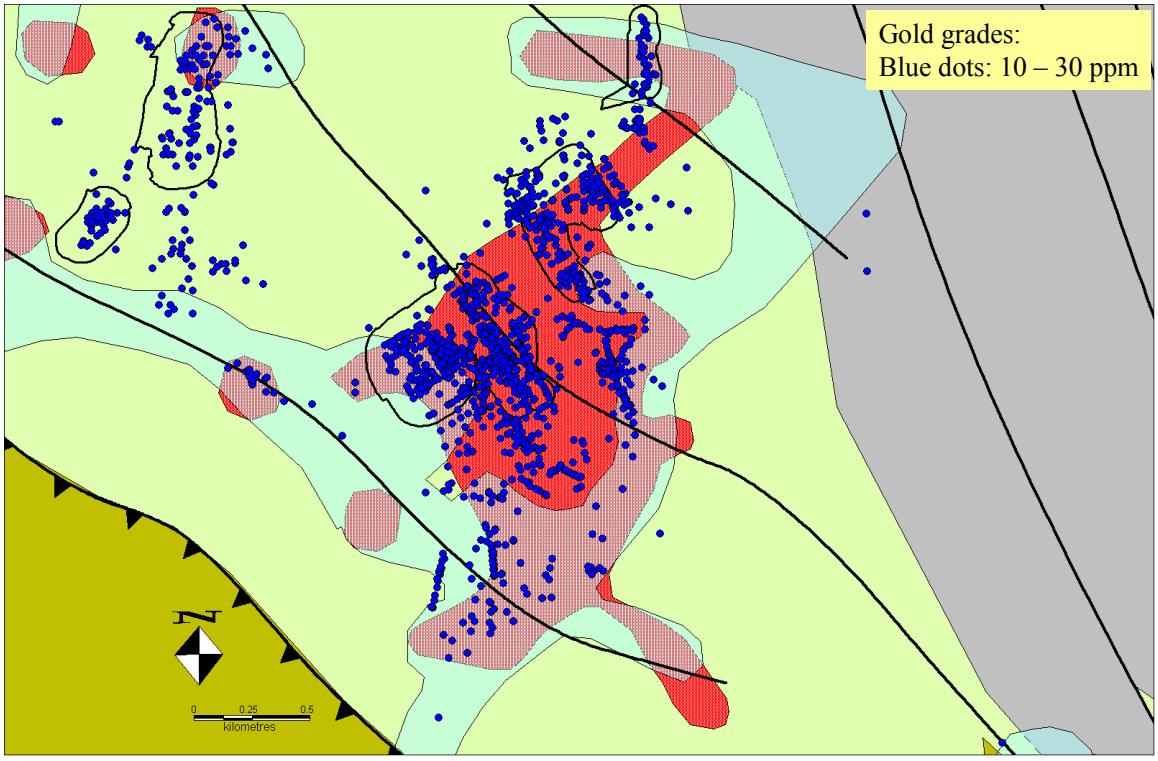

Fig. 77: Geological map of the Victory-Defiance area showing distribution of gold grades with respect to redox domains.

Tonnage Controls

As depicted in Figure 27, the main gold lodes occur also proximal to the domain boundary in 3D. Even though lower gold grades are dispersed more than high grade zones, the main lodes occur within the oxidized domain proximal to the domain boundary. This suggests that the domain boundary has a strong control on the tonnage as well as the grade.

Summary

In summary, an assessment for exploration targeting should follow these steps:

- Identify regional architecture (structural mapping, seismic, gravity, magnetics)
- Define local architecture (structural mapping, seismic, gravity, magnetics)
- Link architecture with chemistry (mineral mapping, PIMA, CCP, WRGC, magnetite chemistry)
- Identify structural traps which are located proximal to chemical domain boundaries indicating a strong chemical gradient.

References

Aaltonen, A., 1997, The significance of vein and breccia mineralization at the Kanowna Belle gold mine, Eastern Goldfields Province, Western Australia: Unpub. Honours thesis thesis, University of Western Australia.

Archibald, N. J., 1985, The stratigraphy and tectono-metamorphic history of the Kambalda-Tramway area, Western Australia, WMC.

Barley, M. E., Brown, S. J., Krapez, B., and Cas, R. A. F., 2002, Tectono-stratigraphic analysis of the Eastern Yilgarn Craton: an improved framework for exploration in Archaean terrains, Australian Mineral Industry Research Institute, p. 200.

Barton, P.B. Jr. and Skinner, B.J., 1979, Sulfide mineral stabilities: In: Geochemistry of Hydrothermal Ore Deposits, 2nd ed., H.L. Barnes (ed.). New York: Wiley, p. 278-403.

Bateman, R., 2001, Archaean gabbros and basalts (Kalgoorlie); geochemistry and tectonics in time, in Cassidy, K. F., Dunphy, J. M., and van-Kranendonk, M. J., eds., Fourth International Archaean Symposium; extended abstracts: Canberra, Australian Geological Survey Organisation, p. 124-126.

Blewett, R. S., Cassidy, K. F., Champion, D. C., Henson, P. A., Goleby, B. S., Jones, L., and Groenewald, P. B., in press, The Wangkathaa Orogeny: an example of episodic regional "D2" in the late Archaean Eastern Goldfields Province, Western Australia: Precambrian Research.

Cassidy, K. F., Champion, D. C., Fletcher, I. R., Dunphy, J. M., Black, L. P., and Claoue-Long, J. C., 2002, Geochronological constraints on the Leonora-Laverton transect area, north eastern Yilgarn Craton, in Cassidy, K. F., ed., The GA-GSWA North Eastern Yilgarn Workshop, Record 2002/18: Perth, Geoscience Australia, p. 31-50.

Claoue-Long, J. C., Compston, W., and Cowden, A. C., 1988, The age of the Kambalda greenstones resolved by ion-microprobe: implications for Archaean dating methods: Earth and Planetary Science Letters, v. 89, p. 239-259.

Clark, M. E., 1987, The geology of the Victory Gold Mine, Kambalda, Western Australia, Queens University.

Clout, J. M. F., 1989, Structural and isotopic studies of the Golden Mile gold-telluride deposit, Kalgoorlie, Western Australia: Unpub. Ph.D. thesis, Monash University, 352 p.

Clout, J. M. F., 1991, Geochronology of the Kambalda-Kalgoorlie area: A review: Kalgoorlie, Western Mining Corporation.

Compston, W., Williams, I. S., Campbell, I. H., and Gresham, J. J., 1986, Zircon xenocrysts from the Kambalda volcanics: age constraints and direct evidence for older continental crust below the Kambalda-Norseman greenstones: Earth and Planetary Science Letters, v. 76, p. 299-311.

Cooke, D. R., and McPhail, D. C., 2001, Epithermal Au-Ag-Te mineralization, Acupan, Baguio District, Philippines: Numerical simulations of mineral deposition: Economic Geology, v. 96, p. 109-131.

Davis, B. K., 1999, Structural analysis of the Wallaby deposit: Perth, Delta Gold NL.

Golding, S. D., 1984, Stable isotope and geochemical studies of the porphyry-related gold mineralization, Kambalda: Perth, Western Mining Coperation, p. 153.

Groves, D. I., 1993, The crustal continuum model for late Archean lode-gold deposits of the Yilgarn Block, Western Australia: Mineralium Deposita, v. 28, p. 36-374.

Hagemann, S. G., Gebre-Mariam, M., and Groves, D. I., 1994, Surface water influx in shallow-level Archean lode-gold deposits in Western Australia: Geology, v. 22, p. 1067-1070.

Ho, S. E., Bennet, M. A., Cassidy, K. F., Hronsky, J. M. A., Mikucki, E. J., and Sang, J. H., 1990, Nature of ore fluid and transportational and depositioonal conditions in sub-amphibolite facies deposits: fluid inclusion studies, in Ho, S. E., Groves, D. I., and Bennet, M. A., eds., 20, University of Western Australia Extension Publication, p. 198-211.

Krapez, B., Brown, S. J. A., Hand, J., Barley, M. E., and Cas, R. A. F., 2000, Age constraints on recycled crustal and supracrustal sources of Archaean metasedimentary sequences, Eastern Goldfields Province, Western Australia: evidence from SHRIMP zircon dating: Tectonophysics, v. 322, p. 89-133.

Mernagh, T. P., 1996, Gold mineralization at Mount Charlotte: Evidence for fluid oxidation from fluid inclusions: 13th Australian Geological Convention, Canberra, 1996, p. 292.

Mikucki, E. J., 1998, Hydrothermal transport and depositional processes in Archean lode-gold systems: A review: Ore Geology Reviews, v. 13, p. 307-321.

Neumayr, P., Hagemann, S. G., Walshe, J., and Morrison, R. S., 2003, Camp- to deposit-scale zonation of hydrothermal alteration in the St. Ives gold camp, Yilgarn Craton, Western Australia: evidence for two fluid systems?: Mineral Exploration and Sustainable Development, Seventh Biennial SGA Meeting, Athens, 2003, p. 799-802.

Nguyen, T. P., 1997, Structural controls on gold mineralization at the Revenge Mine and its tectonic setting in the Lake Lefroy area, Kambalda, Western Australia: Unpub. Ph.D. thesis, The University of Western Australia, 195 p.

Polito, P. A., 1999, Exploration implications predicted by the distribution of carbon - oxygen - hydrogen gases above and within the Junction gold deposit, Kambalda, Western Australia: Unpub. Ph.D. thesis, University of Adelaide, 260 p.

Polito, P. A., Bone, Y., Clarke, J. D. A., and Mernagh, T. P., 2001, Compositional zoning of fluid inclusions in the Archaean Junction gold deposit, Western Australia: a process of fluid-wall-rock interaction?: Australian Journal of Earth Sciences, v. 48, p. 833-855.

Purdie, R. P., 2000, Depositional history and provenance characteristics of the host rock succession, Wallaby Gold Deposit, Eastern Goldfields Western Australia: Unpub. Honours thesis, Monash University, 117 p.

Ren, S. K., Heithersay, P. S., and Ballinger, T. A., 1994, The Kanowna Belle gold deposit and implications to Archaean gold metallogeny of the Yilgarn Craton, Western Australia: Ninth Quadrennial IAGOD Symposium, Beijing, China, 1994, p. 12-18.

Ridley, J., and Hagemann, S. G., 1999, Interpretation of post-entrapment fluid-inclusion re-equilibration at the Three Mile Hill, Marvel Loch and Griffins Find high-temperature lode-gold deposits, Yilgarn Craton, Western Australia: Chemical Geology, v. 154, p. 257-278.

Salier, B.P., Groves, D.I., McNaughton, N.J., and Fletcher, I.R., 2004, The world-class Wallaby gold deposit, Laverton, Western Australia: An orogenic-style overprint on a magmatic-hydrothermal magnetite-calcite alteration pipe?: Mineralium Deposita, v. 39, p.473-393.

Smithies, R. H., and Champion, D. C., 1999, Late Archaean felsic alkaline igneous rocks in the Eastern Goldfields, Yilgarn Craton, Western Australia; a result of lower crustal delamination?: Journal of the Geological Society of London, v. 156, p. 561-576.

Standing, J., 2002, The geological setting of the hinterland and lake environs around the Wallaby gold deposit, Laverton: Perth, Placer Dome, p. 18.

Walshe, J. L., Halley, S. W., Hall, G. A., and Kitto, P., 2003, Contrasting fluid systems, chemical gradients and controls on large-tonnage, high-grade Au deposits, Eastern Goldfields Province, Yilgarn Craton, Western Australia: Mineral Exploration and Sustainable Development, 7th Biennial SGA meeting, Athens, 2003, p. 827-830.

Walshe, J. L., Hobbs, B. E., Ord, A., Regenauer-Lieb, K., Barnicoat, A. C., and Hall, G., 2004a, Hydrogen flux from the Earth's Core, the formation of giant ore deposits through earth history: Goldschmidt Conference, Copenhagen, Denmark, 2004a, p. A777.

Walshe, J. L., Ruiz, J., Chesley, J., Barnicoat, A. C., Phillips, G. M., Hobbs, B. E., Regenauer-Lieb, K., and Ord, A., 2004b, Hydrogen flux from the Earth's core: origin of the Witwatersrand gold deposits and

related phenomena through Earth history: SEG 2004: Predictive Mineral Discovery Under Cover, Perth, 2004b, p. 195-198.

Williams, P. R., and Whitaker, A., 1993, Gneiss domes and extensional deformation in the Archaean Eastern Goldfields Province, Western Australia: Ore Geology Reviews, v. 8, p. 141-162.

Williams, Q., and Henley, R., 2001, Hydrogen in the Deep Earth: Annual Reviews of Earth and Planetary Science Letters, v. 29, p. 365-418.

Part 2: Deposit- and Camp-Scale Results

See DVD's for complete reports.

Report 1: Structural and hydrothermal alteration evidence for early and late stages of gold mineralization at the New celebration gold deposits in Western Australia

Nichols et al.,

Report 2: The New Celebration gold deposits: characteristics and evolution of hydrothermal fluids

Hodge et al.,

Report 3: Architecture and timing of gold mineralization at the Golden Mile gold deposit, Kalgoorlie, Western Australia

Gauthier et al.,

Report 4: Hydrothermal alteration footprints and gold mineralization in the St. Ives gold camp

Neumayr et al.,

Report 5: The hydrothermal architecture of the St Ives gold deposits

Petersen et al.,

Report 6: Alteration of the Kambalda Komatiite Formation in the Hannan lake area near Kalgoorlie, Western Australia

Heydari et al.,

Part 3: Appendices

Appendix 1: Project Proposal, Research Approach and Personal

Appendix 2: Data base including data from St. Ives, Golden Mile, New Celebration and Hanons Lake

Appendix 3a: Additional reports, St. Ives Gold camp

Appendix3b : Additional reports, Kanowna Belle

Appendix 4: Annual reports

2002

2003

2004

Appendix 5: Powerpoint presentations

Abstracts

SGA 2003

Walshe

Neumayr

AGC 2004

Abstract

Pmd*CRC Barossa Valley Conference

S. Drieberg et al – Embedded insights into the Wallaby gold deposit, Western Australia

L. Gathier et al – Geochemical characterization of the Golden Mile stratigraphy and implications for the structural architecture

S. Hagemann – Y3 Project: Camp- to deposit-scale multiple alteration footprints

M. Heydari et al – Komatiite alteration assemblages in the Kambalda Domain, WA.

J. Hodge et al – The structural, hydrothermal alteration and fluid evolution of the New Celebration lode-gold deposits: multiple deformation events and stages of gold mineralization.

P. Neumayr et al – Hydrothermal alteration footprints and gold mineralization in the St Ives gold camp

K. Petersen – P-T-x-fO_2-t of hydrothermal end-member fluids and fluid evolution in the St. Ives gold camp

J.Walshe – Comparative camp-scale studies in the Eastern Yilgarn Craton

Presentations

AGC 2003

CRC 2nd year review July 2003

CRC 2nd year review November 2003

Goldfields presentation 2003

SGA 2003

Honours presentations 2003

CRC project review 2003

Barossa conference – combined Y3 team presentations 2004

Posters

Scale integrated alteration studies at Kanowna Belle (Masterson et al)

Scale integrated studies in the Eastern Goldfields Province: From Brownfields to Greenfields (Y3 team)

Paragenesis of Finiston Style lodes at the Golden Mile, Kalgoorlie, Western Australia (Gauthier et al)

Redox mapping in the Central Corridor of the St. Ives Camp – Redox domains and application to drilling (Horn et al)

Whole-rock and fluid chemistry for alteration mapping and fluid identification (Neumary et al)

Alteration of Komatiites in the Kalgoorlie-Kambalda area, Western Australia (Heydari et al)

Structural architecture, hydrothermal alteration and fluid characteristics in the Kalgoorlie-Kambalda area, Western Australia (Hodge et al)

Alteration mapping and fluid identification in the St. Ives Gold Camp (Petersen et al)